ABSTRACT

COULIBALY, KAPO MARTIN. Permeability Reduction and Emulsified Soybean Oil Distribution in Aquifer Sediments: Experimental and Modeling Results. (Under the direction of Robert C. Borden and David Genereux).

Chlorinated aliphatic hydrocarbons (CAH) are among the most common and difficult to treat contaminants in soil and groundwater. The available information suggests that edible oil permeable reactive barriers (PRBs) can be a very cost effective approach for plume control because of their low capital and O&M costs. However important issues need to be addressed to assure its efficiency.

This work will address permeability losses and oil retention along with oil distribution in the subsurface after injection. PRBs design issues will also be dealt with through the implementation of a model to predict soybean oil spatial distribution after injection.

First, pure soybean oil was injected in laboratory columns packed with different materials varying in grain size distribution and clay content. Water permeability was measured before and after oil injection followed by deaired water flush and sediment oil content assessed at the end of the experiment. This preliminary experiment revealed major difficulties related to the injection of pure NAPL soybean oil. Among others: higher residual saturation (more than 20% of the pore volume), high hydraulic gradient during injection (2 order of magnitude increase over initial gradient with water injection).

Because of these problems emulsified soybean oil was considered as an alternative to the injection of NAPL soybean oil. Using a mixture of surfactants (glycerol monooleate and polysorbate 80), a fine and stable soybean oil in water emulsion was prepared. Injection of the emulsion induced very low to moderate permeability losses and low oil retention.

to investigate emulsion transport in the subsurface, long 1-D columns (80 cm long 1 inch in diameter), packed with a fine clayey sand amended with kaolinite were flushed with emulsion while monitoring effluent concentration. The columns were then cut in 10 sections of 8 cm, with each section analyzed for oil content to characterize the oil spatial distribution. A colloidal transport model based on deep bed filtration was successfully fitted to the long columns data. This model was validated by conducting two 3-D sandbox experiments (1.2 m x 0.98 m x 0.98 m) filled with the same fine clayey sand used previously. The first sandbox experiment consisted of one layer. The second experiment contained three layers varying in clay content. Parameters independently estimated from the long columns experiments were used to predict emulsion transport in the sandbox. Experimental results indicate that emulsified soybean oil can be effectively distributed in the sandbox at least 1 m away from the injection well without any observation of buoyancy effect. The mathematical model calibrated using independently estimated parameters yielded a good fit with measured data. This implies that the colloids transport model can be used to model soybean oil emulsion transport in the subsurface.

Permeability Reduction and Emulsified Soybean Oil Distribution in Aquifer Sediments: Experimental and Modeling Results

By

KAPO MARTIN COULIBALY

A dissertation submitted to the Graduate Faculty of

North Carolina State University

in partial fulfillment of the

requirements for the Degree of

Doctor of Philosophy

MARINE, EARTH AND ATMOSPHERIC SCIENCES

Raleigh

2003

APPROVED BY:

_____	_____
Dr. Aziz Amoozegar	Dr. John Fountain
_____	_____
Dr. Robert Borden Chair of advisory committee	Dr. David Genereux Co-chair of advisory committee

BIOGRAPHY

Kapo Coulibaly was born on January 25, 1971 in M'Batto (Ivory Coast). He received his Bachelor of Science in geology from the National University of Ivory Coast in 1994. After teaching for one year he returned to the University to complete his Master degree in Environmental Sciences from University Of Abobo-Adjame in 1997 while doing research at the Institute of Tropical Ecology. He started his doctorate research in 1998 with the CURAT (Remote sensing research center at University of Cocody). In 1999 he was awarded a Fulbright Scholarship to study at North Carolina State University.

Since 2000 he has been working on his PhD in hydrogeology under the supervision of Dr. R. C. Borden and Dr. D. Genereux.

ACKNOWLEDGEMENTS

I would like to thank Dr. Robert Borden for his guidance throughout this research. His patience and understanding has been much appreciated as I was not always the easiest person to be around. My gratitude goes also to Dr. David Genereux for spontaneously accepting to be the co-chair of my advisory committee, to all my committee members, Dr. Aziz Amoozegar and Dr. John Fountain for their availability and priceless contribution to this work.

Special thanks to my lab mates Cameron Long, Nicholas Lindow and Yong Jung who have conducted significant amount of lab work for me, without them this could have never been done.

To all my family and friends I say thank you for the support they have provided me during these difficult times.

I would like to acknowledge the Strategic the Environmental Research and Development Program (SERDP) for providing the financial support for this research.

TABLE OF CONTENTS

LIST OF TABLES

LIST OF FIGURES

GENERAL INTRODUCTION

Chlorinated aliphatic hydrocarbons (CAH) are among the most common and difficult to treat contaminants in soil and groundwater at Superfund sites (EPA, 2000). Pump and treat methods have been implemented at hundreds of CAH impacted sites. However, success has been limited and costs for system installation and on-going operation and maintenance (O&M) are very high. EPA (2000) has estimated that costs for remediation of CAH contaminated sites will exceed $45 billion in the coming decades. New technologies that are less costly and more effective are needed to cleanup aquifers contaminated by CAH.

Permeable Reactive Barriers (PRBs) are being considered at many sites. These systems have tremendous advantages over traditional pump and treat including lower operation and maintenance costs, no waste extraction, and they are more publicly acceptable as they rely on natural processes for contaminant treatment (EPA, 2000), the most important one being reductive dechlorination.

Reductive dehalogenation has been known for more than 20 years. However environmental application of this process started with the work of Reynolds et al. (1990) who observed the reductive dehalogenation of chlorinated solvent that had come into contact with metal (steel and aluminum). Since this observation, Zero Valent Iron (ZVI) has been extensively used in permeable reactive barriers for chlorinated solvents remediation in the past decade. This technology is efficient and has been applied successfully at numerous sites. However, capital costs for PRBs designed using ZVI technology are high.

Many highly chlorinated organics, including tetrachloroethene (PCE) and trichloroethene (TCE) are resistant to aerobic biodegradation but can be biodegraded anaerobically (Sewell et al., 1990, Suflita and Sewell, 1991). Anaerobic biodegradation

occurs through reductive dehalogenation where the chlorinated organic serves as electron acceptor and the chlorine is replaced by hydrogen forming a less chlorinated and more reduced compound. Many different substrates have been used as electron donors for reductive dehalogenation with variable success. These substrates can be divided into two broad categories: (1) soluble, readily biodegradable donors, and (2) low solubility, slow release donors. Soluble substrates include methanol, molasses, ethanol and sodium lactate. Edible oils, cellulose, chitin, methyl cellulose and Hydrogen Release Compound (HRC) constitute the slow release group. Farone and Palmer (2001) used lactate, molasses and vegetable oil successfully for stimulating reductive dechlorination. Fam et al. (2000) applied acetate and lactate for CAH remediation. Hydrogen release compound (HRC), a commercially available source of lactate ester, has been used to stimulate reductive dechlorination at a number of different sites (Koenigsberg and Farone, 2000; Wu, 1999).

Harkness (2000) reported that material costs for soluble substrates are lower. However total costs for soluble substrates are higher because of the need to continuously supply the more rapidly degrading materials. Using less expensive slow release compound could be a better option. His work showed that edible oils are the least expensive of the slow release donors. Zenker et al. (2000) conducted a screening study to evaluate the use of edible oils (corn oil and variations of soybean oil) in biologically active barriers. Results from this work showed that soybean oil biodegrades more slowly than corn oil making it more suitable for use in a reactive barrier. Additional evidence of reductive dehalogenation as a result of soybean oil injection in the subsurface has been reported by Boulicault et al. (2000). Recently, Hunter (2001) reported on the use of soybean oil for controlling chromate and nitrate migration in the subsurface.

The available information suggests that edible oil permeable reactive barriers (PRBs) can be a very cost effective approach for plume control because of their low capital and O&M costs. However for good performance, the oil must be effectively distributed away from the injection points without excessive permeability loss (Wiedemeier et al., 2001).

This work will focus on designing effective methods of implementing this new technology on the field. It will consist of three parts, each addressing a specific problem related to the use of soybean oil as a PRB. The very first issue is permeability reduction and oil residual saturation induced by soybean oil injection and will be dealt with in the first part of the thesis. The second issue is quantifying and predicting oil spatial distribution in the subsurface for planning and design purposes. In the third section, the model developed will be validated in a 3-D sand box experiments.

REFERENCES

Boulicault, K. J., Hinchee, R. E., Wiedemeier, T. H., Hoxworth, S. W., Swingle, T. P., Carver, E. and Haas, P. E. 2000. Vegoil: A Novel Approach for Stimulating Reductive Dechlorination. Bioremediation and phytoremediation of Chlorinated and recalcitrant Compounds. 2nd International Conference on Remediation of Chlorinated and Recalcitrant Compounds. Monterey, California, May 22-25, 2000

EPA. 2000. Engineered Approaches to In Situ Bioremediation of Chlorinated Solvents: Fundamentals and Field Applications. U.S. Environmental Protection Agency Office of Solid Waste and Emergency Response. Washington, DC

Fam, S. A., Findlay, M., Fogel S., Pirelli, T. And Sullivan, T. 2000. Full Scale Anaerobic Bioremediation Using Acetate and Lactate Electron Donors. Bioremediation and phytoremediation of Chlorinated and recalcitrant Compounds. 2nd International Conference on Remediation of Chlorinated and Recalcitrant Compounds, Monterey, California. May 22-25, 2000

Farone, W. A. and Palmer, T. 2001. Comparison of Reducing Agents for Dechlorination in a Simulated Aquifer. Proceedings of Anaerobic degradation of chlorinated solvents, San Diego, California. June, 2001

Harkness MR, 2000. Economic Considerations in Enhanced Anaerobic Biodegradation. Bioremediation and Phytoremediation of Chlorinated and recalcitrant Compounds. 2nd Internat. Conference on Remediation of Chlorinated and Recalcitrant Compounds, Monterey, California. May, 22-25, 2000.

Hunter, W.J. 2001. Use of vegetable oil in a pilot-scale denitrifying barrier. J. Cont. Hydro., 53, pp 119-131.

Koenigsberg, S. S. and Farone, W. A. 2000. The Use of Hydrogen Release Compounds (HRC™) For CAH Bioremediation. Engineered approaches for In Situ Bioremediation of Chlorinated Solvents Contamination, Battelle Press, Columbus, Ohio, pp 67-72

Reynolds, G. W., Hoff J. T. and Gillham R. W. 1990. Sampling Bias Caused by Materials Used to Monitor Halocarbons in Groundwater. Environ. Sci. Technol., 24 : 135-142

Sewell, G. W, Gibson, S. A, Russell, H. H. 1990. Anaerobic in-situ treatment of chlorinated ethenes. Water Pollution Control Federation Annual Conference: In-situ Bioremediation of Groundwater and Contaminated Soil, 68–79.

Suflita, J. M, Sewell, G.W. 1991. Anaerobic Biotransformation of Contaminants in the Subsurface. EPA Environmental Research Brief, EPA/600/M-90/024, U.S. Environmental Protection Agency, Ada, Okla.

Wiedemeier ,T. H., Henry, M. B. and Haas, P. E. 2001. Technical Protocol for enhanced reductive dechlorination via vegetable oil injection. Proceedings of Anaerobic degradation of chlorinated solvents, San Diego, California. June 2001

Wu, M. 1999. A pilot Study Using HRC™ to Enhance Bioremediation of CAHs. Engineered approaches for In Situ Bioremediation of Chlorinated Solvents Contamination, Battelle Press, Colombus, Ohio, pp 177-180

Zenker, M. J., Borden, R. C., Barlaz, M. A., Lieberman, M. T. And Lee, M. D. 2000. Insoluble Substrate for reductive Dehalogenation in Permeable Reactive Barriers. Bioremediation and phytoremediation of Chlorinated and recalcitrant Compounds. 2nd International Conference on Remediation of Chlorinated and Recalcitrant Compounds. Monterey, California. May 22-25, 2000

CHAPTER 1: Permeability reduction and oil distribution in aquifer sands.

ABSTRACT

Recent laboratory and field studies have shown that food-grade edible oils can be injected into the subsurface for installation of in-situ permeable reactive barriers. However to be effective, the oil must be distributed out away from the oil injection points without excessive permeability loss. In this work, we examine the distribution of soybean oil in representative aquifer sediments as non-aqueous phase liquid oil (NAPL oil) or as an oil-in-water emulsion. Laboratory columns packed with sands or clayey sands were flushed with either NAPL oil or a soybean emulsion followed by plain water, while monitoring permeability loss and the final oil residual saturation. NAPL oil can be injected into coarse-grained sands. However NAPL injection into finer grained sediments requires high injection pressures which may not be feasible at some sites. In addition, NAPL injection results in high oil residual saturations and moderate permeability losses. In contrast, properly prepared emulsions can be distributed through sands with varying clay content without excessive pressure buildup, low oil retention and very low to moderate permeability loss. For effective transport, the emulsion must be stable, the oil droplets must be significantly smaller than the mean pore size of the sediment and the oil droplets should have a low to moderate tendency to stick to each other and the aquifer sediments. In our work, oil retention and associated permeability loss increased with sediment clay content and with the ratio of droplet size to pore size. For sandy sediments, the permeability loss is modest (0 to 40% loss) and is proportional to the oil residual saturation.

1.1. INTRODUCTION

Enhanced anaerobic bioremediation can be a cost-effective approach for treating a variety of groundwater contaminants including certain heavy metals, nitrate, perchlorate, acid mine drainage and chlorinated organics. Many highly chlorinated organics are resistant to aerobic biodegradation but are degradable under anaerobic conditions through a process termed reductive dehalogenation where the chlorinated organic compound serves as an electron acceptor and the chloride moiety is removed and replaced by hydrogen, forming a less chlorinated and more reduced intermediate (Sewell et al., 1990). This process has been demonstrated for a wide range of chlorinated organics including tetrachloroethene (PCE), trichloroethene (TCE), *cis*- and *trans*-1,2-dichloroethene (*cis*-DCE and *trans*-DCE) and vinyl chloride (VC) (Sewell and Gibson, 1991; Freedman and Gossett, 1989; de Bruin et al., 1992). A wide variety of substrates can be used as electron donors for reductive dehalogenation including acetate, butyrate, benzoate, glucose, lactate, methanol, toluene and hydrogen (Lee et al., 1998).

The most common approach for stimulating in-situ anaerobic biodegradation of contaminated groundwater has been to circulate water containing a dissolved, readily biodegradable organic substrate through the treatment zone. This approach has been very effective at some sites (Ellis et al., 2000; Martin et al., 2001; Major et al., 2002). However problems with clogging of process piping, injection, and pumping wells may increase operation and maintenance costs. An alternative approach employed at some sites has been to distribute a 'slow-release' organic substrate throughout the treatment zone that can support anaerobic biodegradation of the target contaminants for an extended time period. Slow-release substrates used include cellulose, chitin, Hydrogen Release Compound (HRC®) and certain edible oils. HRC is a polymerized ester that dissolves over time releasing lactate

which can support anaerobic biodegradation of chlorinated solvents and other contaminants (Koenigsberg et al., 2000; Wu, 1999). A variety of edible fats and oils has been shown to support reductive dehalogenation including corn oil, hydrogenated cottonseed oil beads, and solid food shortening (Dybas et al., 1997), beef tallow, melted corn oil margarine, and coconut oil (Lee et al., 1998). Zenker et al. (2000) screened a variety of organic substrates to identify materials that would slowly biodegrade over time. Subsequent studies showed that both liquid soybean oil and semi-solid hydrogenated soybean oil could support complete dehalogenation of TCE to ethene in microcosms containing sediment from a site contaminated with chlorinated solvent. Studies by Hunter (2001; 2002) demonstrated that soybean oil could be used to stimulate anaerobic degradation of other problem contaminants including nitrate and perchlorate.

The most common field-scale application of edible oils has been the installation of biologically active permeable reactive barriers. In this approach, edible oils are injected through a series of temporary or permanent wells installed along a line perpendicular to groundwater flow. As groundwater moves through the oil treated zone under the natural hydraulic gradient, a portion of the oil dissolves providing a carbon and energy source to accelerate the anaerobic biodegradation processes. Two different approaches have been used to distribute the oil: (1) injection of pure liquid oil as a non-aqueous phase liquid or NAPL (Boulicault et al., 2000); and (2) injection of an oil-in-water emulsion followed by a water flush to distribute emulsion throughout the treatment zone (Borden et al., 2001; Lee et al., 2001). In this work, laboratory column experiments were conducted to evaluate the effect of injection method on the final oil distribution and sediment permeability. Permeability loss is a critical parameter in the design of an edible oil barrier. If permeability loss is excessive, contaminated groundwater will flow around the barrier and will not be treated.

1.2. MATERIALS AND METHODS

1.2.1 Injection procedure

Injections tests were conducted on sediments with varying grain size distributions and clay contents (Table 1.1). The field sand (FS-7%) and concrete sand (CS-9%) used in this project were purchased from local suppliers (Raleigh, NC). The -_% designation is used to indicate the weight fraction finer than 75 μm (silt + clay fraction). For this work, clay content is defined as the fraction finer than 4 μm. Ottawa ASTM 20/30 sand was purchased from U.S. Silica Company (Ottawa, Illinois). Kaolinite (Thiele Kaolin Company, Sandersville, Georgia) was added to certain materials to evaluate the effect of increasing clay content. Kaolinite was added to FS-7% and CS-9% to produce FS-11% and CS-15%. Grain size distributions for each material are presented in Figure 1.1. All materials tested are classified as sands (D_{50} > 0.3mm) with less than 15% passing a #200 sieve (Table 1.1). The pore size distribution of each sediment (Figure 1.2) was calculated from the grain size distribution using the procedure presented by Barr (2001) with 20 separate size increments as recommended by Arya et al. (1999).

Table 1.1 Characteristics of sediments used in permeameter studies**.**

Material	D_{50} (mm)	D_{10} (mm)	Cu D_{60} / D_{10}	% Finer than 75 μm (#200 sieve)	% Clay	Hydraulic Conductivity (cm/s)
OS-1%	1.07	0.66	1.9	1.2	NM	0.41 ± 0.06
PS-1%	0.30	0.10	3.3	1.1	NM	0.024 ±0.004
CS-9%	0.82	0.15	8.2	9.0	1.9	0.053 ±0.027
CS-15%	0.74	0.03	35	14.7	7.2	0.041 ± 0.013
FS-7%	0.38	0.1	4.5	6.9	4.8	0.011 ± 0.003
FS-11%	0.37	0.07	6.7	10.5	5.6	0.006 ± 0.001

NM = Not Measured CU = Coefficient of Uniformity OS= Ottawa Sand PS = Play Sand
Hydraulic conductivity values are mean ± 1 standard deviation of replicate measurements.

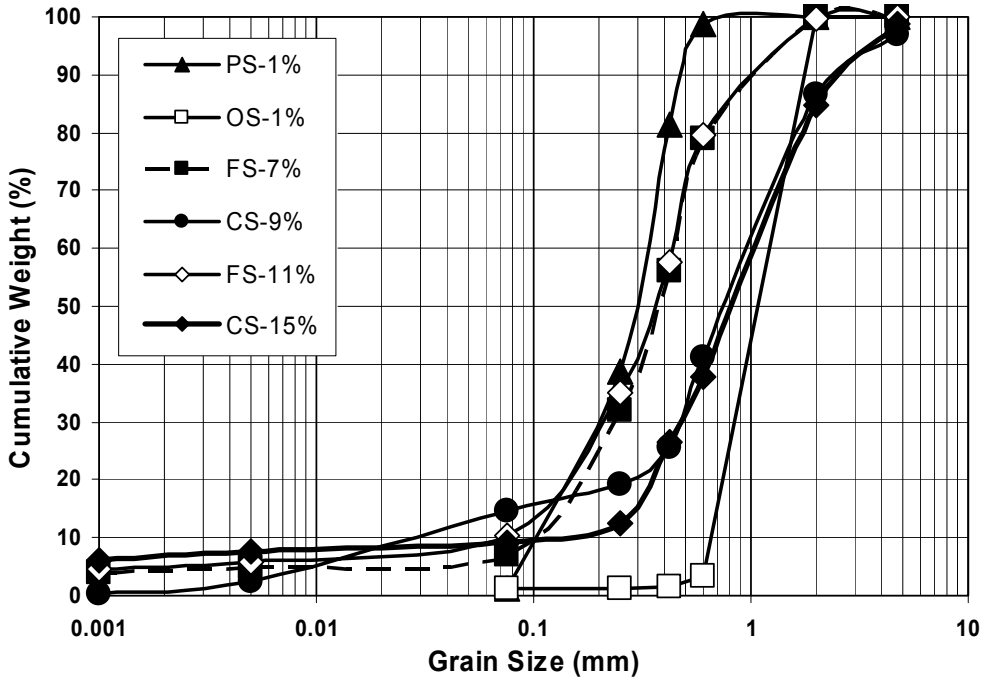

Figure 1.1 Grain size distribution of sediments used in permeameter studies.

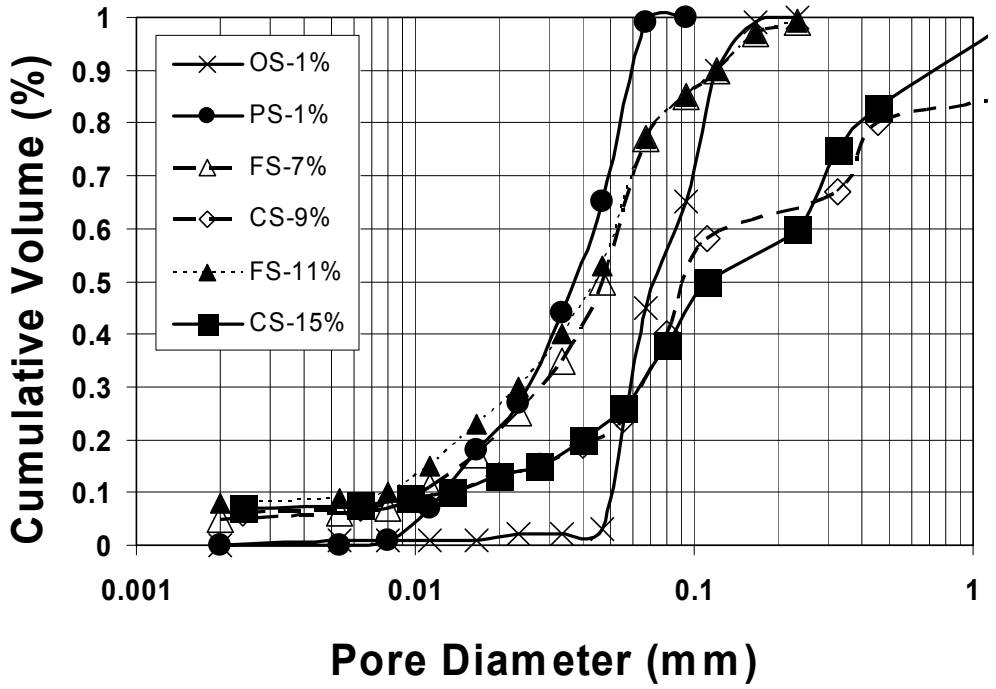

Figure 1.2 Cumulative pore diameter distribution of each sediment calculated using Barr (2001) procedure and grain size distribution from Fig 1.1.

The effect of oil injection on sediment permeability was measured in 11.4 cm dia. x 21.1 cm long columns (ASTM D2434 sand and gravel permeameter from ELE, Melbourne, Florida) with influent supplied by a peristaltic pump (Cole-Palmer Masterflex). Head loss was measured with wall mounted manometer tubes and the outflow recorded over time using a stopwatch. The columns were packed with dry sediment in 3 to 5 cm lifts. After each lift, the sediment was repeatedly compacted with a 5 cm rubber stopper mounted on a metal rod to achieve a density of approximately 1.8 g/cm^3. After packing, a vacuum was applied to the column and it was slowly flooded to minimize entrapped air. Deaired tap water was then pumped through the column until the permeability stabilized (0.5 to 2 hours depending on the sediment) and then the initial hydraulic conductivity (K_o) was measured at least twice over a 10-25 min period.

NAPL soybean oil injection was evaluated by pumping ~2.4 L of liquid soybean oil (~ 4 pore volumes) through each sediment followed by deaired tap water until the permeability stabilized (minimum of 20 pore volumes (PV)). All materials were tested in triplicate. Changes in head loss in the manometer tubes were monitored with time to evaluate the change in effective permeability of the sediment as oil was injected and then displaced with water. The final oil residual saturation was determined by volatile solids (VS) analysis of three ~2.5 cm dia. by 13 cm long sediment cores. Sediment moisture content was determined by weight loss after drying at 105 ºC for 24 hours (48 h for liquid samples). VS was determined by weight loss on ignition for 1 hour at 550 ºC.

Emulsion injection was evaluated following the same general procedures used for NAPL oil injection. A minimum of 3 pore volumes of emulsion were injected followed by deaired tap water until permeability stabilized (6 to 10 PV). At the end of each PV, an effluent sample was collected and the permeability was measured. The sediment moisture content and final oil retention were determined by VS analysis.

1.2.2. Emulsion Preparation

The food preparation industry has tremendous experience in producing stable oil-in-water emulsions with a uniformly small droplet size (Becher, 2001; Binks, 1998, Torrey, 1984). The key factors in generating the desired emulsion are: (1) the oil-water interfacial tension; and (2) the mixing energy. Small droplets can be generated using surfactants that result in a low interfacial tension (less than 1 dyne/cm). However, these emulsions may be unstable (Hofman and Stein, 1991) and the small droplets may coalesce forming larger droplets with time. The most stable emulsions are often produced at moderate interfacial tensions (5 – 10 dyne/cm) with very high mixing energy. Using this information, a series of studies were conducted to identify combinations of surfactants and mixers that generate stable oil-in-water emulsions with a small, uniform droplet size distribution. The droplet size distribution was measured visually with a Nikon™ microscope equipped with a Sensys™ calibrated camera and Metamorph™ software at a 400x magnification.

Several of food grade surfactants were first screened to identify those with desirable properties. Air-water and oil-water interfacial tension was measured with a surface tensiometer equipped with a platinum iridium ring (Fisher Scientific). Once several potential surfactants were identified, emulsification studies were conducted to evaluate the effect of mixing energy on the resulting oil droplet size distribution. Coarse emulsions were first prepared using a fixed ratio of oil to surfactant to water in a kitchen blender. These emulsions were then subjected to progressively higher levels of mixing energy.

Nine different food-grade emulsifiers were initially screened for their ability to generate stable soybean oil-in-water emulsions. A mixture of 160 ml tap water, 40 ml oil and 2, 4 or 6 g of each emulsifier were manually shaken for three minutes and then stored for 24 hours. The emulsifiers that were easiest to blend with water and yielded a stable emulsion

were considered the best. Based on this initial screening, lecithin with hydrophilic lipophilic balance (HLB) of 4 (Centrophase C from Central Soya), polysorbate 20, polysorbate 21, polysorbate 85 (from UNIQUEMA) and a surfactant mixture (38% polysorbate 80, 56% glycerol monooleate (GMO) and 6% water from Lambent Technologies) were selected for further evaluation. The soybean oil-water interfacial tension of 2% solutions of surfactant in water were as follows: 28 dyne/cm for no surfactant, 8 dyne/cm for polysorbate 20, 8.3 dyne/cm for polysorbate 21, 9.7 dyne/cm for polysorbate 85 and 11 dyne/cm for the polysorbate 80-GMO mixture. The interfacial tension of the lecithin could not be measured because the low HLB prevented it from dissolving in water.

Several tests were then conducted to evaluate the effect of different surfactants and mixers on the resulting droplet size distribution. The following mixing procedures were evaluated (table 1.2): (1) mixing at high speed in a standard kitchen blender (Westinghouse) for 5 minutes; (2) mixing for 5 minutes using a hand-held homogenizer at the highest setting (Ultra Turrax RKA T18, Fisher Scientific); (3) mixing for 5 minutes using a lab sonicator (Sonic Dismembrator Model 550, Fisher Scientific); (4) repeated passage through a Silverson high shear laboratory mixer (LART-W) with the EMSC-F mixing heads; (5) one pass through a commercial dairy homogenizer (Gaulins two stage 300 GCI) at 1000 psi; (6) mixing for 3 minutes at low speed in a 1 gallon Waring Commercial Blender; and (7) mixing for 5 minutes at high speed in the same blender. Photomicrographs of several of the emulsions are shown in Figure 1.3.

Table 1.3 Characteristics of droplet size distributions from different surfactant – mixer combinations. Statistics are for Log_{10} transformed distribution of the oil droplet diameter**.**

#	Surfactant	Mixer	Mixing time	Median (μm)	Mean (μm)	Standard Deviation (μm)	Skewness of Log Dia.
1	Centrophase C lecithin	Kitchen blender on high speed	5 min.	2.7	3.9	3.1	0.7
2	Centrophase C lecithin	Silverson high shear mixer	3 passes	2.4	3.0	2.2	1.2
3	Centrophase C lecithin	Silverson high shear mixer	10 passes	3.2	3.6	1.5	0.5
4	Polysorbate 85	Kitchen blender on high speed	5 min.	4.6	4.8	1.7	0.4
5	Polysorbate 85	Lab. homogenizer	5 min.	3.2	3.4	1.7	0.7
6	Polysorbate 85	Lab. sonicator	5 min.	1.4	1.5	1.6	0.6
7	Polysorbate 80-GMO	Waring blender on low speed	3 min.	7.4	7.2	1.6	-0.3
8	Polysorbate 80-GMO	Waring blender on high speed	5 min.	1.2	1.2	1.3	0.2
9	Polysorbate 80-GMO	Gaulins homogenizer	1 pass	0.7	0.7	1.3	-0.3

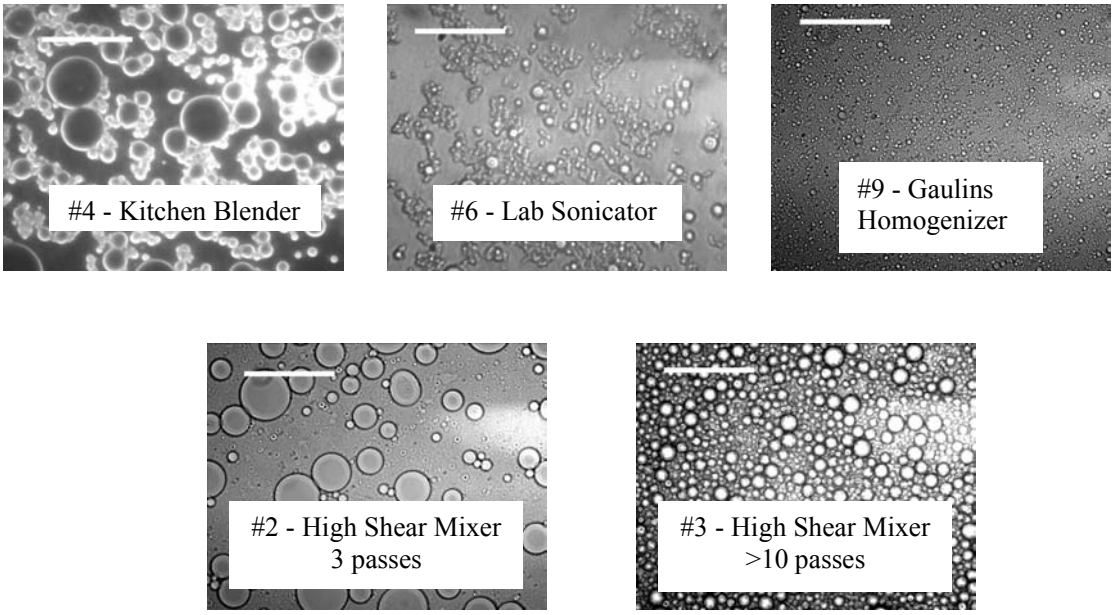

Figure 1.3 Emulsion droplets produced with different surfactants and mixing devices as described in Table 1.3. White scale bar is 25 μm.

Most of the oil droplet size distributions are strongly non-symmetric with many small droplets and a few large droplets. However the few large droplets contain a substantial portion of the total oil since the droplet volume is proportional to the diameter cubed. To provide a more useful presentation of these results, a statistical summary of the Log_{10} transformed droplet size distribution is presented in Table 1.3. The cumulative oil volume vs. droplet diameter for the different mixers is presented in Figure 1.4.

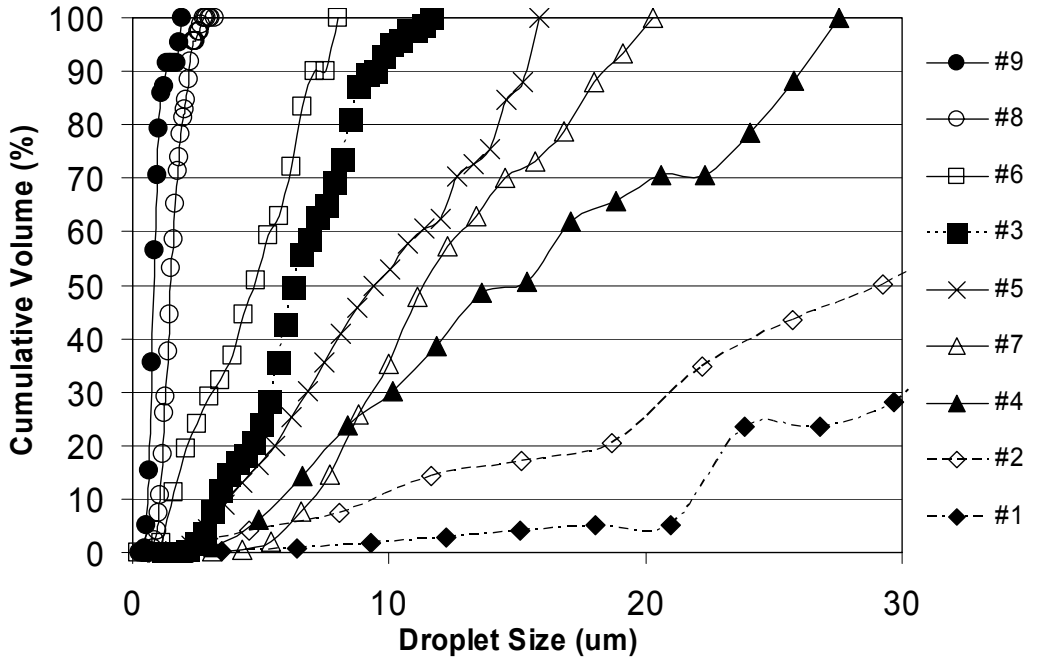

Figure 1.4 Cumulative droplet volume distributions for different emulsion preparation methods. Emulsion numbers and preparation methods are listed in Table 1.3.

The modified lecithin (Centrophase C) resulted in coarse emulsion with a large average droplet size and wide range of droplets. In contrast, both the polysorbate 85 and polysorbate 80 - GMO mixture generated droplet size distributions with smaller, more uniform droplets. A single pass through the Silverson mixer generated a very coarse emulsion that separated rapidly (data not shown). However, over 10 passes through the Silverson laboratory mixer (equivalent to > 4 passes through a full-size mixer) generated a good emulsion that was stable with small, uniform droplets. The Gaulins homogenizer and

the Waring commercial blender at high speed for 5 minutes provided the smallest, most uniform droplets. Emulsions prepared with polysorbate 80 - GMO and both the Silverson high shear mixer and dairy homogenizer were stable for at least one month when stored at 4 ^{o}C. Droplet size distributions from both mixers were measured immediately after preparation, after storage for one week and after storage for one month. For both mixers, there was no significant change in the droplet size distribution (data not shown).

The median droplet size of all emulsions generated in this study were significantly smaller than the median pore size of all the sediments suggesting that most droplets could be easily transported through the different sands. However some of the emulsions have a highly variable droplet size distribution with a few very large (> 50 μm) droplets. In these emulsions, much of the oil is present in largest droplets which could be rapidly removed by straining. Therefore for the remaining experiments we used emulsions prepared with the Lab Blender and the Gaulins Homogenizer with Polysorbate 80-GMO as the surfactant.

1.3. NAPL OIL INJECTION RESULTS

The laboratory column tests demonstrated that NAPL soybean oil can be distributed in sands with little or no clay. However, with the equipment available in our laboratory, it was not practical to inject soybean oil in sediments with any significant clay content. For the three sands tested, oil residual saturation after flushing with over 30 pore volumes (PV) of water varied from 22 to 54% (Table 1.2). Residual saturation was the lowest in the most uniform material (OS-1%) and was the highest in the more broadly graded CS-9%. This is consistent with the results of Chatzis and Morrow (1984) who observed that a broader grain size range results in a higher residual saturation. Even though two fluid were injected, permeability was measured initially with water only and at the end of the experiment when no more oil was coming out in the effluent. Therefore the reduction in permeability was

assessed by quantifying the change in hydraulic conductivity. For the three sands tested, the final permeability after over 20 PV of water displacement was just below half of the initial permeability, indicating that if the oil could be displaced to residual saturation, the permeability loss would not be excessive.

Table 1.2 Residual saturation and change in hydraulic conductivity following injection with NAPL soybean oil.[a]

Media	Oil Residual Saturation (% by volume of pore space)	Initial Hydraulic Conductivity (K_o) (cm/s)	Final Hydraulic Conductivity (K) (cm/s)	K/K_o
OS-1%	21.7 (3.7)	0.427 (0.035)	0.185 (0.057)	0.46(0.12)
PS-1%	36.5 (2.5)	0.027 (0.006)	0.011 (0.001)	0.46 (0.18)
CS-9%	54.2 (7.9)	0.051 (0.002)	0.026 (0.007)	0.45 (0.00)
CS-15%	31.0 (0.1)	0.019 (0.004)	0.008 (0.003)	0.39 (0.14)

[a] Residual saturation and permeability change are the average of triplicate column tests. Standard deviations are shown in parentheses.

A number of operational problems were identified during injection that would complicate application of NAPL oil injection in the field. At typical groundwater temperatures (10 to 20 ºC), soybean oil has a viscosity 60 to 70 times that of water which makes it very difficult to move NAPL oil any significant distance from the injection point. Figure 1.5 shows the hydraulic gradient (m of water head/m) required to pump 2 pore volumes of water, 3 PV of liquid soybean oil and then 7 PV of water through Ottawa sand (OS-1%) at a constant flow rate. There is an almost two order of magnitude increase in the hydraulic gradient during soybean oil injection if the same flow rate is maintained. Once the oil is displaced to residual saturation, hydraulic conductivity returns to roughly half of the pre-injection value. However, over 20 PV of water flushing is required to achieve this. In the field, extended flushing with water to reach residual saturation would not be practical. However, if the soybean oil is not displaced to residual saturation, it will float upward due to its lower density. Finally, the high residual saturation of soybean oil would require injection

of large volumes of oil. In summary, the high pressure buildup, large volume of oil required, and very large volume of flush water required are expected to significantly limit the used of NAPL oil injection for enhanced anaerobic bioremediation.

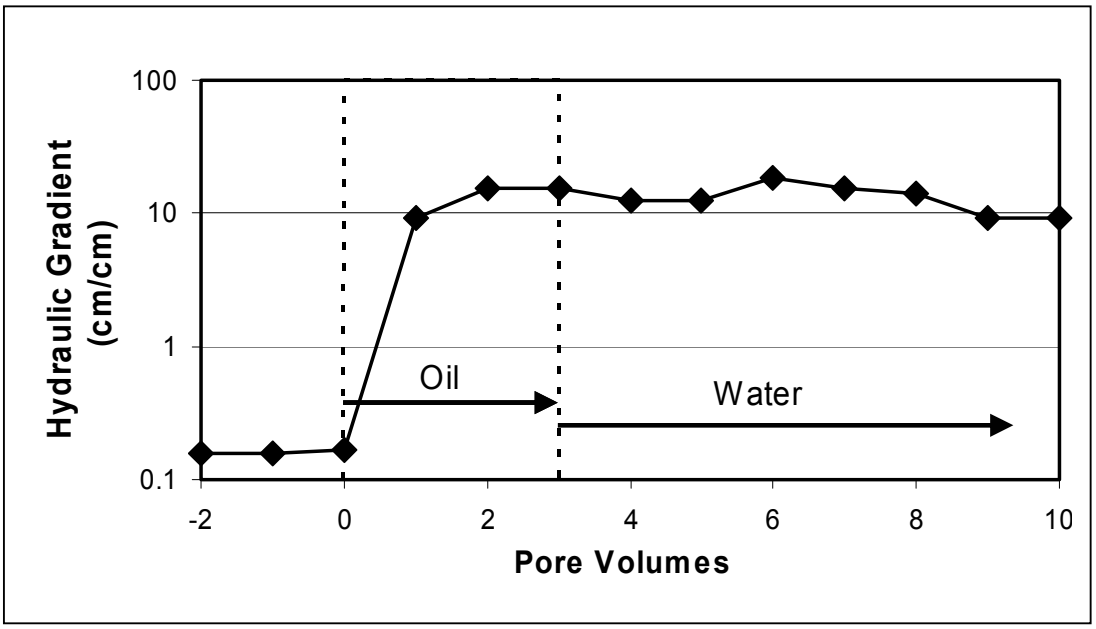

Figure 1.5 Variation in hydraulic gradient during injection of Ottawa Sand (OS-1%) with 3 pore volumes of NAPL soybean oil followed by plain water at constant flow rate**.**

The remainder of this work will focus on the development of methods for distributing soybean oil-in-water emulsions in representative aquifer materials. Injection of oil-in-water emulsions appears to provide a promising method for distributing soybean oil without many of the problems associated with NAPL oil injection.

1.4. EMULSION INJECTION RESULTS

The most commonly adopted model for emulsion transport in porous media was proposed by Soo and Radke (1984) to describe emulsion transport and associated clogging in petroleum reservoirs. These investigators conducted a series of experiments examining the

transport of emulsions with different droplet size distributions through fine Ottawa sand cores (intrinsic permeability = 1.5 μm^2 and 0.57 μm^2). The emulsions used by Soo and Radke were prepared with refined mineral oil (Chevron 410H) stabilized with sodium oleate and oleic acid, mixed with sodium hydroxide to minimize droplet sticking to the surface of sediment particles and also minimize droplet coalescence. Results of these experiments demonstrated that oil droplets smaller than the sediment pores could be transported significant distances through porous media with low interception by solid surfaces and low permeability loss to the porous media. However, injection of oil droplets larger than the sediment pores resulted in rapid droplet removal by straining with a large, permanent permeability loss.

Our objective was to develop a method for distributing oil-in-water emulsions significant distances away from the injection point with low to moderate permeability loss and moderate oil retention. Preliminary calculations indicate that depending on environmental conditions, a 3 m wide barrier with 0.5 to 2 % residual oil should contain enough organic substrate to support anaerobic biodegradation for 10 years or more. Excessive permeability loss could cause contaminated groundwater to flow around the emulsion impacted zone and not be treated. High oil retention could increase the amount of oil required above that necessary for treatment of the contaminants. However too low an oil retention could allow the oil droplets to migrate out of the target treatment zone requiring more frequent injection and possibly affecting down gradient receptors. The sediments examined in this study had median pore sizes (D_{50}) between 35 and 125 μm with some pores less than 10 μm (Figure 1.2). Adding kaolinite to the concrete sand and FS significantly reduced the estimated D_{50} of the pores indicating that sediments with higher clay contents will require emulsions with smaller droplet size distributions. In addition, the added kaolinite may increase interception since the small oil droplets may be more likely to stick to the charged clay surfaces. Based on the work of Soo and Radke (1986a; 1986b), we concluded

that an emulsion was needed with small (less than 10 μm), uniformly sized droplets. Ideally, the sediment-droplet collision efficiency should be low to moderate allowing the oil droplets to be transported some distance before they are immobilized on the sediment surfaces.

1.4.1. Emulsion Transport and Permeability Loss

Column experiments were conducted to evaluate emulsion transport and associated permeability loss in CS-9%, FS-7% and FS-11% with both coarse and fine emulsions. The cumulative oil volume vs. droplet diameter for the coarse and fine emulsions are shown in Figure 1.4 as emulsions #7 and #8. The variation in emulsion concentration in the column effluent and effective hydraulic conductivity of FS-7% treated with fine emulsion is shown in Figure 1.6. The emulsion concentration is presented as the measured volatile solids (VS) concentration of the column effluent divided by the VS of the injected emulsion (C/Co). Hydraulic conductivity is calculated as the observed hydraulic gradient divided by the flowrate per unit area. During injection, the emulsion rapidly breaks through in the column effluent with little evidence of retardation. Then during the post-injection water flush, the emulsion rapidly declines to background levels with little evidence of tailing or flushout of trapped emulsion. The effective hydraulic conductivity declines to ~ 66% of the preinjection value and then returns to background levels during the water flushing. Most of the observed reduction in hydraulic conductivity is due to the higher viscosity of the emulsion (1.44 centipoise) compared to water (0.95 centipoise) at the ambient temperature (23 ºC).

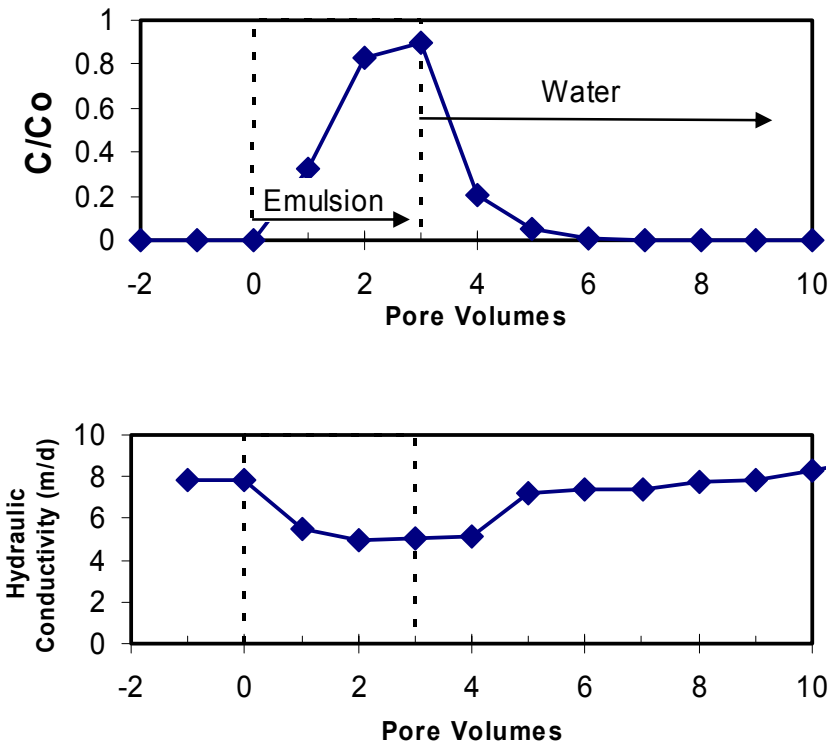

Figure 1.6 Variation in emulsion concentration (C/Co) in column effluent and effective hydraulic conductivity during injection of field sand (FS-7%) with 3 pore volumes of fine emulsion followed by plain water.

Figure 1.7 shows the effective hydraulic conductivity (K) when CS-9%, FS-7% and FS-11% are treated with coarse or fine emulsion. For each material, the initial hydraulic conductivity of the material can vary by 30% or more due to minor differences in packing of the columns. The effective hydraulic conductivity (K) of the CS-9% dropped by 40-44% during injection of the coarse emulsion and then rebounded during water flushing resulting in a final permeability loss of 12-19%. The small hydraulic conductivity reduction and low oil retention (Table 1.4) is due to the large ratio of pore size to droplet size.

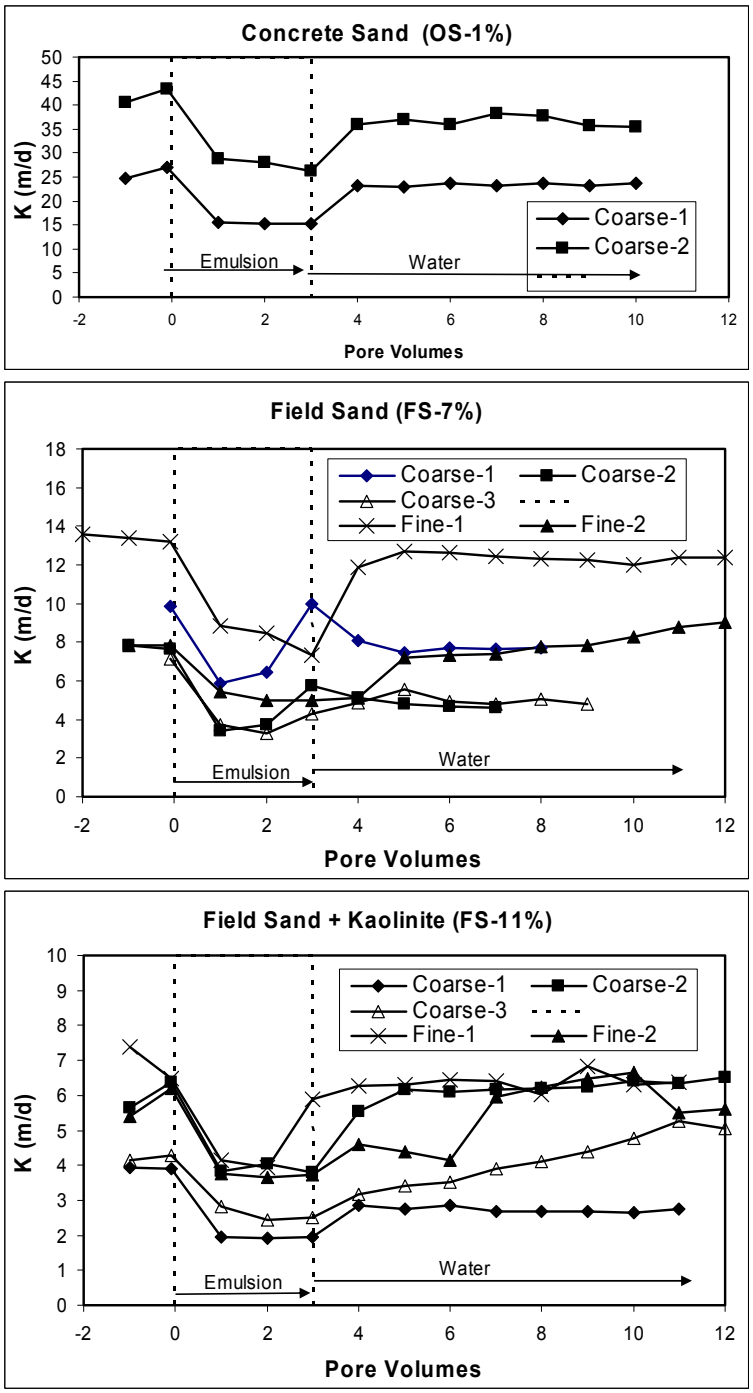

Figure 1.7 Variation in hydraulic conductivity (K) during injection of concrete sand, field sand, and field sand + kaolinite with three volumes of either coarse or fine emulsion followed by water flushing.

Table 1.4 Comparison of observed permeability loss and oil retention with best fit results for Soo and Radke model. Standard deviations of experimental results are shown in parentheses.

Material	CS-9%	FS-7%	FS-7%
Median Pore Diameter, Dp (μm)	90.7	45.0	45.0
Standard Deviation of Pore Diameter (μm)	13.7	5.4	5.4
Maximum Potential Surface Coverage, θ (dimensionless)	0.4	0.45	0.55
Emulsion Type	Coarse	Fine	Coarse
Median Droplet Diameter, Dd (μm)	7.39	1.17	7.39
Experimental k/k_o (dimensionless)	0.88 (0.02)	0.97(0.12)	0.69(0.08)
Simulated k/k_o (dimensionless)	0.87	0.95	0.67
Experimental Retention (%)	0.39 (0.99)	1.15(0.11)	1.79 (0.38)
Simulated Retention (%)	0.98	0.37	2.7

During injection of fine emulsion into the FS-7%, K declined by roughly 40% and then recovered to near preinjection values (93-115% of initial K). However when the coarse emulsion was injected into the FS-7%, there was a permanent permeability loss of 20 to 40%. The largest oil droplets in the coarse emulsion are ~20 μm in diameter which is significantly smaller than the median pore size of the FS-7%. The greater permeability loss with the coarse emulsion is presumably due to clogging of some of the smaller pores with the larger oil droplets.

Results from emulsion injection into the FS with kaolinite added (FS-11%) were more variable. Permeability declined during injection of the fine emulsion and then recovered to near the preinjection values following the same general pattern observed with the FS-7% and fine emulsion. However when the coarse emulsion was injected into the FS-11% columns,

there was a permanent permeability loss of 30% in one column, no permanent permeability loss in a second column, and a gradual increase in permeability in the third column to 120% of the preinjection value. The exact cause of these variable results in the FS-11% columns is not known but may be related to mobilization and rearrangement of the added kaolinite by the surfactants used to prepare the emulsions (Sabbodish, 2002).

1.4.2. Mathematical Model of Emulsion Transport and Oil Retention

Soo and Radke (1984; 1986a; 1986b) develop a model based on the deep bed filtration theory (Tien and Payatakes, 1979) to describe the transport and retention of emulsion droplets in porous media. Their model assumes that oil droplets may be captured by straining in pore constrictions smaller than the droplet diameter and by interception on pore walls due to various physical forces leading to a permanent loss in permeability and unrecoverable residual oil. Interception is most important when the oil drops are smaller than the pores of the media. Permeability reduction is described by the relationship

$$k/k_0 = 1 - \beta\sigma/\varepsilon_0$$

where β is the flow restriction parameter, σ is the oil retention and ε_0 is the initial porosity. Intrinsic permeability (k) is calculated as $k = K\eta/\rho g$ where K is the effective hydraulic conductivity, η is the viscosity of the injection fluid, ρ is the density of the injection fluid, and g is the gravitational acceleration constant. The model does not explicitly consider the various electrostatic forces that may influence droplet interception. However it does include a surface coverage parameter (θ) that varies between 0 – 1 and represents the fraction of pore wall surface that can be covered by the droplets. The model input parameters with the greatest impact on simulated permeability loss are the average pore size of the sediment, median pore diameter (Dp), median droplet diameter (Dd), the standard deviation of the pore

size distribution, and θ. There is no method for independently estimating θ, so this parameter was used as a fitting parameter to achieve the best fit between simulated and observed k/k_o. The model was coded in Visual Basic for application in a spreadsheet, then θ was varied manually to match the observed values. Model parameters are presented in Table 1.4.

Figure 1.8 shows the simulated and observed changes in intrinsic permeability during injection of the CS-11% and FS-7% with 3 PV of coarse or fine emulsion followed by 7 PV of plain water. All of the experimental curves show the same general trend with an initial drop in k/k_o during emulsion injection followed by no significant change in k/k_o during water flushing. There is no recovery in k/k_o during water flushing since plotting intrinsic permeability automatically accounts for differences in the viscosity and density of the water and emulsion. The Soo and Radke model reproduces the experimental reduction in k/k_o very well. This model was not nearly as accurate in simulating oil retention (Table 1.4). The match between simulated and observed oil retention could be improved by increasing θ. The required increases in θ are not physically realistic because they would result in excessively high simulated k losses. A major limitation of the Soo and Radke model is the assumption of a perfectly uniform droplet size distribution. However in practice, emulsions have a range of droplet sizes with most of the oil present in the larger droplets. For the coarse emulsion, over 85% of the total oil volume was present in oil droplets greater than the median droplet diameter (7.5 μm).

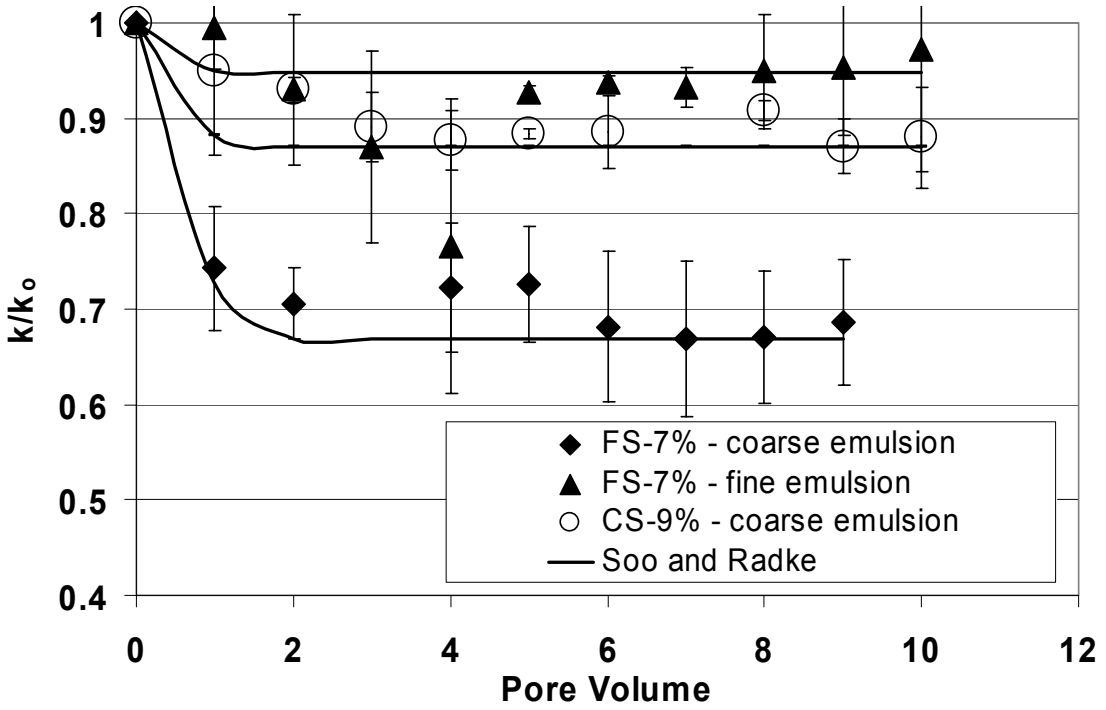

Figure 1.8 Comparison of Soo and Radke model with observed variation in relative permeability when CS-9% and FS-7% are flushed with 3 PV of coarse or fine emulsion followed by plain water. Error bars show the range of experimental measurements in triplicate columns.

1.4.3. Effect of Clay Content on Emulsion Residual Saturation and Permeability Loss

Figure 1.9 shows the variation in oil residual saturation (oil content after emulsion injection followed by over 8 PV of water flushing) with clay content and includes results using a variety of different emulsion preparation methods (lecithin and polysorbate - GMO with both coarse and fine emulsions). Oil retention increases with sediment clay content (r^2= 0.81, $p<0.0001$). This is not unexpected since when oil droplets are smaller than the sediment pores, straining losses are low and oil capture should be dominated by interception. The large surface area and negative charge associated with the clay particles may significantly enhance oil droplet interception.

Figure 1.10 shows the variation in k/k_o versus residual saturation after >8 PV of water flushing for several different emulsion preparation methods. The CS-9% treated with lecithin, CS-9% treated with polysorbate 80 - GMO and FS-7% treated with polysorbate 80 - GMO all appear to follow a relatively consistent trend where increasing oil residual saturation results in a greater permanent permeability loss. The FS-11% columns do not follow this general pattern, possibly due to mobilization of the added clay particles as discussed above.

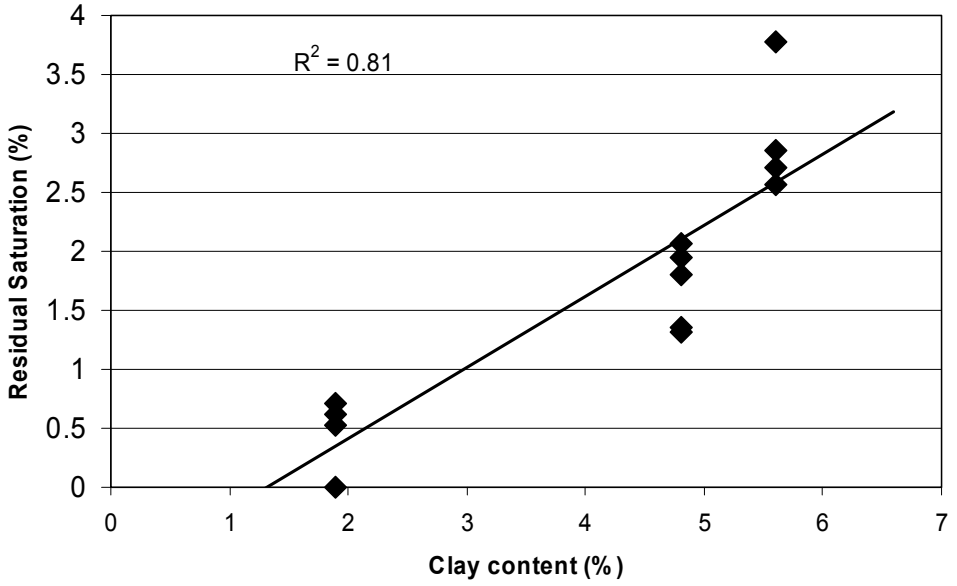

Figure 1.9 Variation in oil residual saturation with sediment clay content**.**

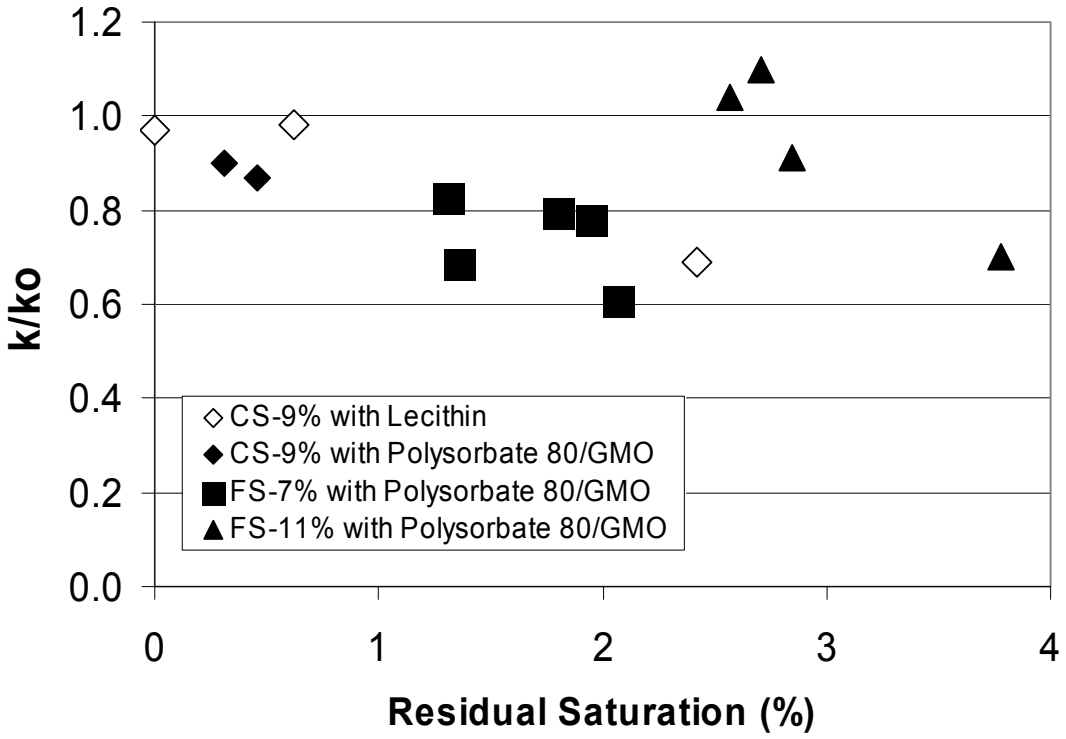

Figure 1.10 Variation in k/k_o with oil residual oil saturation for three different sediments.

1.4.4. Modeling Permeability Loss from Residual Oil

A number of different relationships have been proposed to describe the permeability loss resulting from entrapped particles (bacteria, clay and other colloids). One of the first relationships was proposed by Ives and Pienvichitr (1965) for describing permeability reduction due to biofilm growth. This relationship is:

$$k/k_o = (1-\alpha)^{3-P}$$

where α is the fraction of the total pore space occupied by entrapped particles (particle volume/pore volume) and P is a parameter to account for tortuous pores. Tien (1989) observed that the Pienvichitr relationship consistently under-predicted permeability loss and proposed the relationship

$$k/k_o=(1-\alpha)^3(1+\eta_o*\alpha/(1-\eta_o))^{-4/3}$$

where η_o is the initial porosity. Renshaw et al. (1997) introduced a different approach where retained particles are considered as an equivalent clay fraction and

$$k_{final}=k_o^{(1-vclay)}\ k_{clay}^{vclay}$$

where k_{clay} is the permeability of the retained clay and vclay is the volume fraction of clay.

Figure 1.11 shows a comparison of computed versus observed permeability loss in the FS-7% and CS-9% for both the Tien and Renshaw relationships. ν_{clay} was computed from the oil residual saturation and bulk density of the porous media and oil. Tien's model could not be successfully fit to the experimental results, significantly underestimating permeability loss for the full range of experimental results. The Renshaw model was adjusted to match the experimental data (RMSE=0.072) using k_{clay} as a fitting parameter since k_{clay} could not be independently estimated. The best fit for the Renshaw model was obtained with a k_{clay} value of 5.64×10^{-27} cm^2 (5.64×10^{-16} Darcys) implying that the trapped oil droplets are essentially impermeable to water.

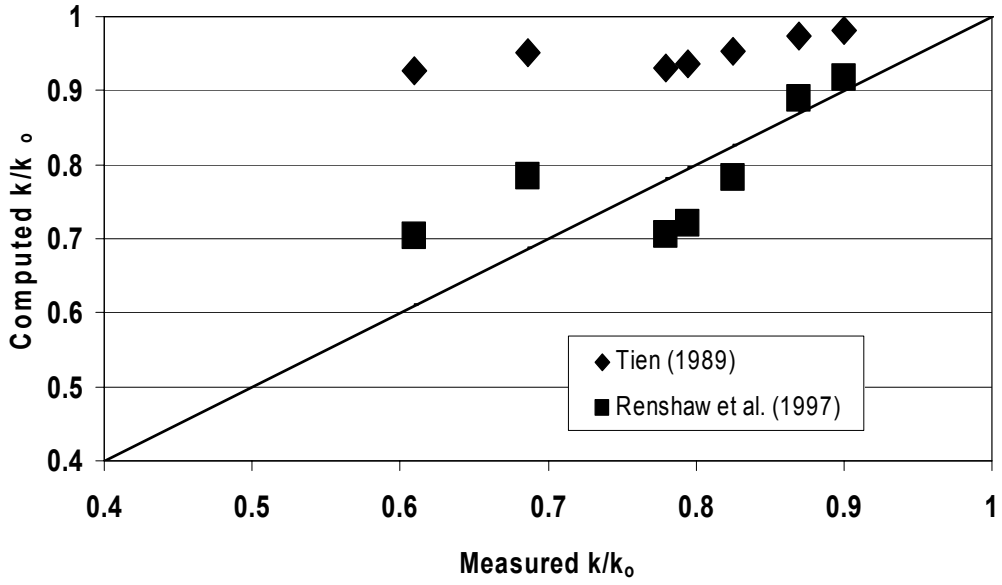

Figure 1.11 Comparison of measured and computed values of k/k_o for Tien (1989) and Renshaw et al. (1997) models.

1.5. DISCUSSION AND CONCLUSIONS

Our experimental results demonstrate that NAPL soybean oil can be distributed short distances in sands without excessive permeability loss if the oil can be displaced to residual saturation. However in the field, oil displacement to residual saturation may be very difficult because of the high viscosity of the soybean oil and the large volumes of injection water required. If the oil is not displaced to residual saturation, permeability losses will be significantly higher and there is potential for upward migration of the oil due to buoyancy effects.

Injection of soybean oil as an oil-in-water emulsion appears to offer many advantages over injection as a NAPL. Soybean oil-in-water emulsions can be prepared using only food-grade, Generally Recognized As Safe (GRAS) materials to aid in gaining regulatory approval. Using appropriate combinations of surfactants and high-energy mixers, emulsions

with very small droplets can be prepared. These droplets will easily pass through the pores of most sandy sediments. For the fine emulsions used in this study, the primary mechanism of oil retention is believed to be interception, where oil droplets collide with pore surfaces and stick. Retention of these emulsions is very low in pure sand and increases linearly with clay content. Emulsion injection into aquifer material does result in some permeability loss. However for sands with low to moderate clay content, the permeability loss is modest (0 to 40% loss) and is proportional to the oil residual saturation.

The low permeability loss observed in our work differs from results by Jain and Demond (2002) who observed large permeability losses when columns packed with pure silica sand were flushed with emulsions prepared with tetrachloroethene (PCE) and two different nonionic surfactants (Witconol 2722 – a polyoxyethylene(20) sorbitan monooleate, and Witconol SN 120 – an ethoxylated dodecyl alcohol). The difference in results observed by Jain and Demond and our own results is likely due to the surface characteristics of the emulsions and sediments. In the work by Jain and Demond, the zeta potential of the silica sand was -25 mV and the zeta potentials of the two emulsions were 0.3-0.5 mV and 1.2-1.3 mV. The small absolute value of the emulsion zeta potential reduces inter-particle repulsion, causing the emulsion droplets to stick to each other when they collide. Overtime, large masses of flocculated droplets can form which then clog the sediment pores. Retention of these masses of droplets is further encouraged by the difference in charge between the emulsion and silica sand surface.

Table 1.5 Zeta potential of different emulsions and sediments. Standard deviation of triplicate measurements shown in parentheses**.**

Material	Zeta Potential
Soybean oil emulsion prepared with polysorbate 80 and GMO	-17.6 (1.3)
Soybean oil emulsion prepared with polysorbate 80	-12.3 (0.1)
Soybean oil emulsion prepared with GMO	-25.2 (0.9)
CS-9%	5.5 (0.6)
FS-7%	-22.2 (2.5)
Kaolinite	-24.4 (1.1)

Conditions in our studies were very different from those of Jain and Demond. Table 1.5 shows the zeta potential for soybean oil emulsions prepared with polysorbate 80 - GMO and sediments used in our work. Zeta potential was measured with a Pen Kem model 501 Lazer Zee Meter after diluting in tap water (the eluent in our work). Similar results were observed when measurements were conducted using deionized water for dilution (data not shown). The polysorbate 80 - GMO surfactant mixture generated an emulsion with a strongly negative zeta potential (-17.6 mV) which results in strong droplet-droplet repulsion and minimizes flocculation of the oil droplets. The FS-7% and kaolinite also had a strongly negative zeta potential which reduces the potential for droplets to stick to the sediment surfaces. In contrast, the CS-9% had a positive zeta potential. The difference in zeta potential between the CS-9% and the emulsion may explain why there was some significant retention of oil, even though the clay content of the CS-9% was very low.

Results of our work indicate that appropriately prepared emulsions can be distributed in representative aquifer material without excessive loss of aquifer permeability, and suggests that edible oil emulsions can potentially be used to form biologically active permeable reactive barriers. However additional work is needed to evaluate the effect of biological growth and/or gas production on changes in permeability of the barrier zone and downgradient aquifer.

1.6. REFFERENCES

Arya, L.M., Leij, F.J., Shouse, P.J. and Van Genuchten, M.Th., 1999. Relationship between the hydraulic conductivity function and the particle-size distribution. Soil Sci. Soc. Am. J., 63, 1063-1070.

Barr, D.W., 2001. Coefficient of permeability determined by measurable parameters. Ground Water, 39, 356-361.

Becher P. (2001). Emulsions: Theory and practice. 3rd edition. Oxford Univ. Press New York. 513p

Binks B. P. (1998). Emulsion – Recent advances in understanding. Modern aspects of emulsion science. Royal Society of Chemistry. Cambridge, UK. 430p

Borden, R.C., Coulibaly, K.M., Long, C.M., and, Harvin A.S., 2001. Development of permeable reactive barriers (PRBs) using edible oils, Annual Report to the Strategic Environmental Research and Development Program.

Boulicault, K.J., Hinchee, R.E., Wiedemeier, T.H., Hoxworth, S.W., Swingle, T.P., Carver, E., Haas, P.E., 2000. Vegoil: A Novel Approach for Stimulating Reductive Dechlorination. In: Wickramanayake, G.B., Gavaskar, A.R., Alleman, B.C., Magar, V.S. (Eds) Bioremediation and Phytoremediation of Chlorinated and Recalcitrant Compounds, Battelle Press. pp. 1-7.

Chatzis, I., Morrow N.R., 1984. Correlation of capillary number relationships for sandstones. Society Petro. Engr. J. 24, 555-562.

De Bruin, W.P., Kotterman, M.J.J., Posthumus, M.A., Schraa, G. and Zehnder, A.J.B., 1992. Complete biological reductive transformation of tetrachloroethene to ethane. Appl. Environ. Microbiol. 58, 1996-2000.

Dybas, M.J., Tatara, G.M., Witt, M.E. and Criddle, C.S., 1997. Slow-release substrates for transformation of carbon tetrachloride by Pseudomonas strain KC. In Situ and On Site Bioremediation, Vol. 3, Columbus, Battelle Press, p. 59.

Ellis, D.E., Lutz, E.J., Odom, J.M., Buchanan, R.J., Bartlett, C.L., Lee, M.D., Harkness, M.R., Deweerd, K.A., 2000. Bioaugmentation for accelerated in situ anaerobic bioremediation. Env. Sci. Tech. 34, 2254-2260.

Freedman, D.L., Gossett J.M., 1989. Biological reductive dechlorination of tetrachloroethylene and trichloroethylene to ethylene under methanogenic conditions. Appl. Environ. Microbiol. 55, 2144-2151.

Hunter, W.J., 2001. Use of vegetable oil in a pilot-scale denitrifying barrier. J. Cont. Hydro. 53, 119-131.

Hunter, W. J., 2002. Bioremediation of chlorate or perchlorate contaminated water using permeable barriers containing vegetable oil. Current Microbiol., 45, 287-292.

Ives, K.J. and Pienvichitr V., 1965. Kinetics of filtration of dilute suspensions. Chemical Engr. Sci. 20, 965-973.

Jain, V. and Demond, A. H., 2002. Conductivity reduction due to emulsification during surfactant enhanced-aquifer remediation. 1. Emulsion transport. Environ. Sci. Technol. 36, 5426 -5433.

Koenigsberg, S.S., Farone, W.A. and Sandefur, C.A., 2000. Time-release electron donor technology for accelerated biological reductive dechlorination. In: Wickramanayake, G.B., Gavaskar, A.R., Alleman, B.C., Magar, V.S. (Eds) Bioremediation and Phytoremediation of Chlorinated and Recalcitrant Compounds, Battelle Press. pp. 39-46.

Lee, D.M., Lieberman T.M., Borden R.C., Beckwith W., Crotwell T. and Haas P.E., 2001. Effective distribution of edible oils – results from five field applications. – In: Wickramanayake, G.B., Gavaskar, A.R., Alleman, B.C., Magar, V.S. (Eds.), Proc. In Situ and On-Site Bioremediation: The Sixth Internal. Sym., San Diego, CA, Battelle Press, Columbus, OH.

Lee, M.D., Odom J.M., Buchanan R.J., 1998. New perspectives on microbial dehalogenation of chlorinated solvents: Insights from the field. Ann. Rev. Microbiol. 52, 423-452.

Major, D.W., McMaster, M.L., Cox, E.E., Edwards, E.A., Dworatzek, S.M., Hendrickson, E.R., Starr, M.G., Payne, J.A., Buonamici, L.W., 2002. Field demonstration of successful bioaugmentation to achieve dechlorination of tetrachloroethene to ethene. Environ. Sci. Technol. 36, 5106-5116.

Martin, J.P., Sorenson, K.S., Peterson, L.N., 2001. Favoring efficient in situ dechlorination through amendment injection strategy. In: G. B. Wickramanayake, G.B., Gavaskar, A.R., Alleman, B.C., Magar, V.S. (Eds.): Proc. In Situ and On-Site Bioremediation: The Sixth Internal. Sym., San Diego, CA, pp. 265-272.

Renshaw C.E., Zynda G.D. and Fountain J.C., 1997. Permeability reductions induced by sorption of surfactant. Water Resour. Res. 33, 371-378.

Sabbodish, M. S. Jr, 2002. A Physicochemical Investigation of the Soil Clogging Phenomena During Surfactant Enhanced Remediation. Doctoral Dissertation, Dept. Civil Engr., North Carolina State Univ.

Sewell, G.W., Gibson S.A. and Russell, H. H., 1990. Anaerobic in-situ treatment of chlorinated ethenes. Proc., 1990 Water Pollution Control Federation Annual Conference: In-situ Bioremediation of Groundwater and Contaminated Soil, 68–79.

Sewell, G. W. and Gibson, S. A., 1991. Stimulation of the reductive dechlorination of tetrachloroethene in anaerobic aquifer microcosms by the addition of toluene. Environ. Sci. Technol. 25, 982-984.

Soo H. and Radke C. J., 1984. The flow mechanism of dilute stable emulsions in porous media. Ind. Eng. Chem. Fundam. 23, 342-347.

Soo, H. and Radke C.J., 1986a. A filtration model for the flow of dilute stable emulsions in porous media – I. Parameter evaluation and estimation. Chemical Engr. Sci. 41, 273-281 1986.

Soo, H. and Radke C.J., 1986b. A filtration model for the flow of dilute stable emulsions in porous media – I. Theory. Chemical Engr. Sci. 41, 263-272.

Tien, C., 1989. Granular filtration of aerosols and hydrosols. Butterworth, Boston, 1989.

Tien, C., and Payatakes, A.C., 1979. Advances in deep bed filtration. A.I.Ch.E.J. 25, 737-7359.

Torrey S. (1984). Emulsions and emulsifier applications: recent developments. Noyes Data Corp., 319 p

Wu, M., 1999. A pilot study using HRC^{TM} to enhance bioremediation of CAHs. Engineered approaches for In Situ Bioremediation of Chlorinated Solvent Contamination, Battelle Press, Columbus, Ohio, pp 177-180.

Zenker, M.J., Borden, R.C., Barlaz, M.A., Lieberman, M.T. and Lee M. D., 2000. Insoluble substrates for reductive dehalogenation in permeable reactive barriers. In: Wickramanayake, G.B., Gavaskar, A.R., Alleman, B.C., Magar, V.S. (Eds) Bioremediation and Phytoremediation of Chlorinated and Recalcitrant Compounds, Battelle Press. pp. 47-53.

CHAPTER 2: Emulsion transport modeling

ABSTRACT

The main purpose of this work was to develop a model that could describe and predict the movement of soybean oil emulsion in the subsurface. This model would be used to design field implementation of PRBs using emulsified soybean oil. The transport and retention of a soybean oil-in-water emulsion was evaluated in long (80 cm long, 1 inch diameter) and short (20 mL sediment) laboratory columns packed with a medium to fine clayey sand amended with varying amounts of kaolinite. Emulsion was injected in one end followed by deaired water and effluent collected at the other end. At the end of the experiment the long column was cut in 8 pieces of 10 cm each and their oil content assessed thus providing oil spatial distribution. A standard colloidal transport model that includes a Langmuirian blocking function was used to model the columns. The long column experiments demonstrated that appropriately prepared soybean oil-in-water emulsions can be distributed in clayey sand at least 80 cm away from the injection point. The empty bed collision efficiency (α') and the maximum retention capacity (Smax) are the parameters governing emulsion transport. Kaolinite addition to the clayey sand resulted in an increase in the maximum oil retention. Model parameters determined in replicate columns and at varying velocities were reasonably reproducible. Kaolinite addition to the clayey sand resulted in an increase in the maximum oil retention. However, the empty bed collision efficiencies in columns packed with clayey sand amended with kaolinite were lower than in columns packed with clayey sand only suggesting that kaolinite is a less efficient collector of oil droplets than natural clayey sand. The empty bed collision efficiency (α') in the short columns closely matched parameter estimates from the long columns. The maximum oil retention in the short columns was significantly lower than for the long columns.

2.1. INTRODUCTION

In-situ anaerobic bioremediation processes are being implemented for treatment of a wide variety of groundwater contaminants including chlorinated solvents, nitrate, perchlorate and acid mine drainage (Morse et al., 1998; Hunter, 2001, 2002; ARCADIS, 2002; ITRC, 2002). In all of these processes, one or more biodegradable organic substrates are distributed throughout the treatment zone to provide a carbon source for cell growth and an electron donor for energy generation.

Recently, there has been considerable interest in using soybean oil as a substrate for in-situ bioremediation because of its' low cost, food-grade status, and longevity in the subsurface. However several studies (Zenker et al., 2000; Lee et al., 2001) suggest that injection of soybean oil into the subsurface as a separate non-aqueous phase liquid (NAPL) may be difficult because of the very limited spread of the oil and large amount of chase water required to displace the oil to residual saturation.

To overcome these problems, Coulibaly and Borden (2003) developed a process for distribution of soybean oil (and other materials) as an oil-in-water emulsion. The emulsion was prepared to: (1) be stable for extended time periods (e.g. non-coalescing); (2) have small, uniform droplets to allow transport in most aquifers; and (3) have a negative surface charge to reduce droplet capture by the solid surfaces. The emulsion would be distributed throughout the proposed treatment zone by injecting a dilute emulsion followed by one or more pore volumes (PV) of water to distribute and immobilize the oil droplets. Laboratory permeameter studies demonstrated that these emulsions can be effectively distributed in sands and clayey sands with only modest reductions in aquifer permeability (0 to 40% reduction in K). Oil retention and associated reductions in permeability increased with sediment clay content and with the ratio of droplet size to pore size.

In the work presented here, we demonstrate an approach for simulating the transport of these emulsions in representative aquifer materials using a standard advection-dispersion transport model. Emulsion retention by the aquifer material is represented by a colloidal filtration model with a Langmuirian blocking function. Once validated, this approach could be used to evaluate different alternatives for distribution of emulsified oil in contaminated aquifers.

2.2. EMULSION AND COLLOID TRANSPORT

Soo and Radke (1984, 1986a, 1986b) studied emulsion transport, deposition and associated permeability loss in porous media. All experimental work was conducted using emulsions that were prepared to minimize droplet coalescence and sticking to particle surfaces. Experimental results demonstrated that oil droplets smaller than the sediment pores could be transported significant distances through porous media with low interception by solid surfaces and low permeability loss. However, injection of oil droplets larger than the sediment pores resulted in rapid droplet removal by straining with a large, permanent permeability loss. This suggests that when oil droplets are smaller than the sediment pores, they can be transported without significant permeability loss and droplet transport and retention may be described by colloidal transport theory (Westall and Gschwend, 1993).

Colloid transport and deposition in porous media has been an area of intense research due the important implications for facilitated transport of contaminants sorbed on colloids, dispersal of bacteria for in-situ bioremediation, and transport of groundwater pathogens. The emulsions developed by Coulibaly and Borden (2003) have characteristics similar to many bacteria including the oil droplet size (~ 1 μm) and surface charge characteristics (zeta potential ~ - 18 mV). As a consequence, much of what has been learned about bacterial transport in the subsurface maybe useful for describing transport of colloidal size oil droplets.

Two general approaches have been employed to describe bacterial transport in the subsurface. In the first approach, transport of bacteria (and other colloids) is simulated using a rate limited sorption approach (Lindqvist et al., 1994; Bengtsson and Lindqvist 1995; Bolster et al., 1998; Kretzschmar and Sticher 1998; Bengtsson and Ekere, 2001) where the rate of mass transfer between the aqueous and solid phase is proportional to the concentration gradient between the two phases.

In the second approach, bacterial transport and retention is simulated using deep-bed filtration theory where particle capture by the sediment surfaces is a function of: (1) the rate that particles approach a single collector or sand grain; (2) the single collector efficiency (η) which is the fraction of particles approaching a collector that actually strike the collector; and (3) the sticking efficiency (α) which is the fraction of particles colliding with the collector that are actually retained (Westall and Gschwend, 1993; Ryan and Elimelech 1996; Logan 1999). The rate that particles approach a collector is determined based on a simple mass-balance approach (Ryan and Elimelech, 1996; Chen et al., 2001). The single collector efficiency is most commonly determined using the Rajagopalan and Tien equation (1976) which includes terms for diffusion (η_D), interception (η_I) and gravitational settling (η_S). α is an empirical term that reflects a variety of particle – collector interactions that affect adhesion including pH, ion strength, colloid and sand grain surface coatings, and prior coverage of the collector surface by previously trapped particles (Rijnaarts et al.,1996a, Bolster et al., 2001).

In this work, we evaluate the use of a deep-bed filtration approach for simulating emulsion transport in 2.9 cm diameter by 80-cm long columns packed with medium to fine sand amended with varying amounts of kaolinite. Independent estimates of emulsion retention parameters were obtained using the short column protocol presented by Jewett et al. (1995, 1999).

2.2.1 Deep-Bed Filtration Model of Emulsion Transport

The transport and retention of oil-in-water emulsions may be simulated using the standard advection-dispersion equations with terms representing colloid capture by the sand grain surfaces and droplet release back to the mobile phase where (Bolster et al., 1998; Camesano et al., 1999).

$$\frac{\partial C_m}{\partial t} = \frac{\partial}{\partial x}\left(D \frac{\partial C_m}{\partial x} \right) - \frac{\partial}{\partial x_i}\left(v C_m \right) - K_a v\, C_m + \frac{\rho}{\varepsilon_0} R \qquad (1)$$

and

$$\frac{\partial C_{im}}{\partial t} = K_a v \frac{\varepsilon_0}{\rho} C_m - R \qquad (2)$$

where

C_m = mobile phase concentration (ML^{-3})

C_{im} = immobile phase concentration ($M\ M^{-1}$)

t = time (T)

x = distance (L)

D = dispersion coefficient (L^2T^{-1})

v = pore water velocity (LT^{-1})

K_a = filter coefficient attachment rate (L^{-1})

ρ = bulk density (ML^{-3})

ε_0 = porosity (dimensionless)

R = immobile phase release rate (T^{-1})

For an empty bed, the filter coefficient, K_a, can be calculated as

$$K_a = \frac{3}{2}\left(\frac{1-\varepsilon_0}{d_c}\right)\alpha\eta \qquad (3)$$

α = collision efficiency (dimensionless)

η = single collector efficiency (dimensionless)

d_c = equivalent collector diameter (L)

However a variety of studies have shown that sticking efficiency declines as the collector surfaces become covered with retained colloids. Rijnaarts et al. (1996b) proposed that the decline in sticking efficiency with prior coverage of the collector surfaces could be represented using a Langmuirian blocking function of the form $\alpha = \alpha'(\theta_{max} - \theta)/\theta_{max}$ where α' is the empty bed sticking efficiency, θ is the area of collector surface occupied by particles and θ_{max} is the maximum area available for particle capture. Under controlled laboratory conditions, θ_{max} can be calculated based on dimensions of the colloidal particles and sand grains. However in natural aquifers with a wide range of grain sizes and surface characteristics, accurate estimation of θ_{max} may be difficult and it may be more useful to represent surface blockage by the relationship $\alpha = \alpha'(C_{im}^{max} - C_{im})/C_{im}^{max}$ where C_{im}^{max} is an empirical measure of the maximum mass of particles captured per mass sediment. Substituting this relationship for α in equation 3 we obtain:

$$K_a = \frac{3}{2}\left(\frac{1-\varepsilon_0}{d_c}\right)\alpha'\left(\frac{C_{im}^{max} - C_{im}}{C_{im}^{max}}\right)\eta \qquad (4)$$

At present, the mechanisms controlling release of attached colloids is poorly understood. Most previous investigators have assumed colloid release to be neglible (i.e. R = 0). However in the experimental work described below, we observed a low but steady

release of volatile solids (VS) from columns treated with emulsified oils. To simulate this release, we propose use of the function

$$R = K_d \left(\frac{S}{C_m + S} \right) C_{im} \tag{5}$$

K_d = immobile phase release coefficient (T^{-1})

S = mobile phase concentration which reduces release rate by half (ML^{-3})

At high mobile phase concentrations (i.e. $C_m >> S$) and/or low immobile phase concentrations, the release rate goes to zero. However, when the mobile phase concentration is low, this function will result in a slow steady release of VS similar to what would be observed during the dissolution of a trapped residual oil phase.

2.3. MATERIALS AND METHODS

All experiments were conducted with a medium to fine sand amended with 0%, ~2.5% or ~5% kaolinite (Thiele Kaolin Company, Sandersville, Georgia). The original material termed Field Sand (FS-7%) was obtained from a local supplier (Caudle Sand and Rock, Raleigh, NC) and used in Chapter 1. Characteristics of each material are summarized in Table 2.1. The -_% designation is used to indicate the weight fraction finer that 75 μm (silt + clay fraction). Kaolinite addition had little effect on the median grain diameter (D_{50}) but increased the coefficient of uniformity (D_{60}/D_{10}) by an order of magnitude.

Table 2.1 Characteristics of sediments used in column experiments.

Material	D_{50} (mm)	D_{10} (mm)	D_{60} / D_{10}	% Finer than 75 μm (#200 sieve)
Field Sand (FS-7%)	0.38	0.1	4.5	6.9
Field Sand + 2.5% kaolinite (FS-9%)	0.36	0.074	6.0	9.2
Field Sand + 5% kaolinite (FS-12%)	0.37	0.0067	67.0	11.5

Coulibaly and Borden (2003) demonstrated that oil-in-water emulsions with small, uniform droplets can be prepared using soybean oil and food grade surfactants. The emulsions used in this work were prepared by blending 33% by volume soybean oil, 62% water and 5% premixed surfactant (38% polysorbate 80, 56% glycerol monooleate (GMO) from Lambent Technologies and 6% water) in a Waring Commercial blender at high speed for 5 minutes. The droplet size distribution was measured visually with a Nikon™ microscope equipped with a Sensys™ calibrated camera and Metamorph™ software at a 400x magnification and is shown in Figure 2.1. The zeta potential of the oil droplets, sand, and kaolinite were -17.6, -22.2 and -24.4 mV indicating unfavorable conditions for droplets to stick to collectors (Chapter 1).

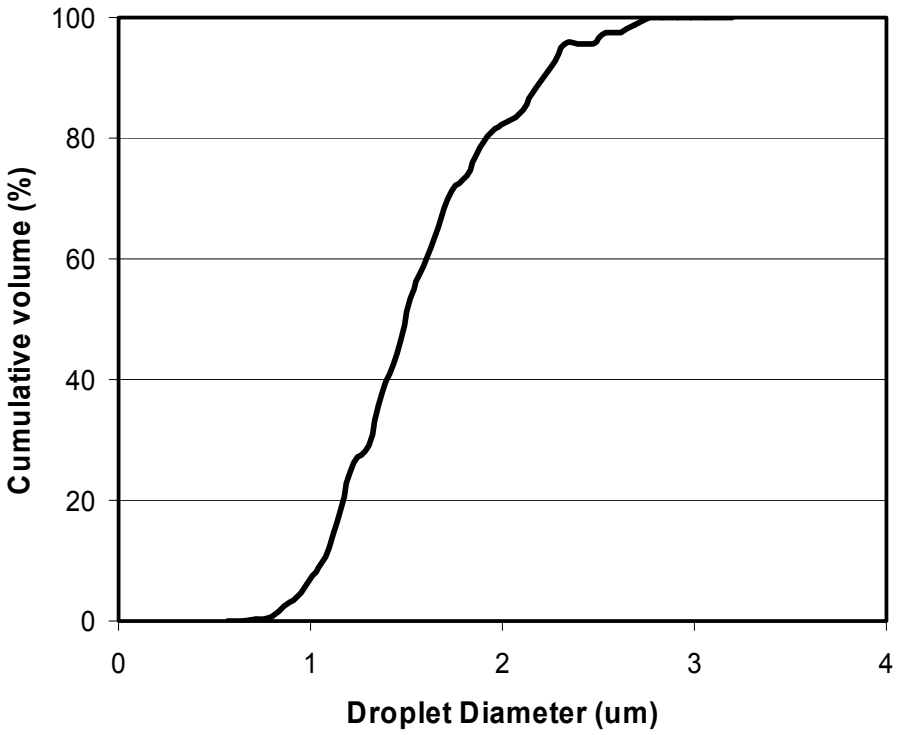

Figure 2.1 Oil droplet size distribution in emulsion prepared with polysorbate 80/GMO in laboratory mixer on high speed for 5 minutes.

2.3.1 Colloid Transport Parameter Determination

In this work, the empty bed sticking efficiency (α') was independently determined for each sediment using the short column protocol (SCP) developed by Jewett et al. (1995, 1999). Emulsion concentrations were varied from 0.4% to 33% oil by volume to evaluate the effect of oil loading on sticking efficiency. Sixty mL plastic syringes with a glass fiber filter were packed with 20 mL of sediment and then saturated with deaired water. Oil droplet capture by the sediment was determined by vacuum pumping 10 mL of emulsion (approximately 1.5 pore volumes) followed by 50 ml of water at 5 mL/min. Preliminary studies demonstrated that emulsion concentrations typically declined to less than 1% of the injection concentration after flushing 50 mL of water through the sediment. Oil

concentrations in the sediment and column effluent were determined by volatile solids analysis (VS). Moisture content was determined by weight loss after drying at 105 ºC for 24 hours for solid samples and 48 h or more for liquid samples). The VS was determined by weight loss on ignition for 1 hour at 550 ºC. Blank samples of field sand were analyzed to account for background VS.

Collision efficiency (α) for each experiment was calculated by the relationship (Gross et al., 1995):

$$\alpha = -\frac{2}{3}\frac{d_c}{(1-\varepsilon_0)\eta L} Ln(\frac{M}{M_0}) \qquad (6)$$

Where M and M_0 are the mass of VS recovered in the column effluent and mass injected, and L is the column length. In this work, we assume the equivalent collector diameter (d_c) is equal to the sediment D_{10} based on the work of Huber (2000) and Martin et al. (1996) who showed that D_{10} provided the most representative estimates of collector diameter in well graded sediments. Martin et al. (1996) reported that using D_{50} or arithmetic averages lead to an underestimation of η resulting in α higher than 1. The single collector efficiency (η) was computed using the Rajagopalan and Tien (1976) relationship:

$$\eta = A_s N_{Lo}^{1/8} N_R^{15/8} + 0.00338 A_s N_G^{6/5} N_R^{-2/5} + 4 A_s^{1/3} N_{Pe}^{-2/3} \qquad [7]$$

Where:

$$A_s = \frac{2(1-\gamma^5)}{2-3\gamma+3\gamma^5-2\gamma^6}$$

$$N_{Lo} = \frac{4H}{9\pi\mu d_p^2 v}$$

$$N_R = \frac{d_p}{d_c}$$

$$N_G = \frac{g(\rho_p - \rho)d_p^2}{18\mu v}$$

$$N_{Pe} = \frac{3\pi\mu v d_c d_p}{kT}$$

and

$$\gamma = (1-\theta)^{1/3}$$

d_p and ρ_p are the equivalent diameter and density of the bacteria (here of the droplets), d_c the collector diameter (grain diameter), v the approach velocity (pore velocity), μ and ρ the viscosity and density of the fluid, T the temperature, H the Hamaker constant, g the gravitational constant and k the Boltzmann constant. Values for the most important parameters used in the computation of μ are: equivalent droplet diameter of 1.25 μm, droplet density of 0.95 g/cm^3, water viscosity of 9.37 x 10^{-4} N/sm^{-2}, water density of 1 g/cm^3, and temperature of 23°C .

2.3.2 Long column procedure (LCP)

Emulsion transport and retention was examined in 80 cm long by 2.9 cm (~1 inch) polyvinyl chloride (PVC) columns. The columns were dry packed with sediment while constantly tapping to induce settlement. Deaired water was then pumped upward through the columns at ~ 2.5 mL/min for 2 hours to saturate the columns. The emulsion injection test consisted of pumping 25 mL of 11% oil by volume emulsion (~0.05 PV of pure oil) followed by 1000 mL (~5 PV) of deaired water. The effluent was collected every 30 ml and analyzed for oil content by VS. After completion of the experiment, the column was frozen, cut into 8

sections of 10 cm each, with each section analyzed for oil content by VS analysis. Prior to emulsion injection, a non-reactive tracer test was conducted by pumping 25 mL of 175 mg/l NaBr solution through each column at a flow rate of ~2.5 mL/min followed by 1000 mL of deaired water. Effluent samples were analyzed for Br by ion chromatography.

2.4. PARAMETERS ESTIMATION USING SHORT COLUMN PROTOCOL

Figure 2.2 shows the variation in collision efficiency (α) for field sand (FS-7%), field sand amended with 2.5% kaolinite (FS-9%) and field sand amended with 5% kaolinite (FS-12%) as a function of oil concentration in the injected emulsion. These collision efficiencies were calculated assuming the equivalent collector diameter (d_c) is equal to D_{10} of the sediment. At low emulsion concentrations, α in FS-7% is relatively constant at 0.07-0.08. However, at higher emulsion concentrations, α declines to less than 0.01. This variation in α with loading is consistent with prior work by Johnson and Elimelech (1995) and others who have shown that particle deposition may increase or decrease as collector surfaces become covered with retained colloids. Deposition rate can increase as the collectors become covered with retained colloids (ripening) if conditions are favorable for colloid-colloid sticking. However, if conditions are not favorable for colloid-colloid sticking, collision efficiency will decline with increasing loading as favorable sites are filled leaving fewer sites available for colloid attachment (blocking).

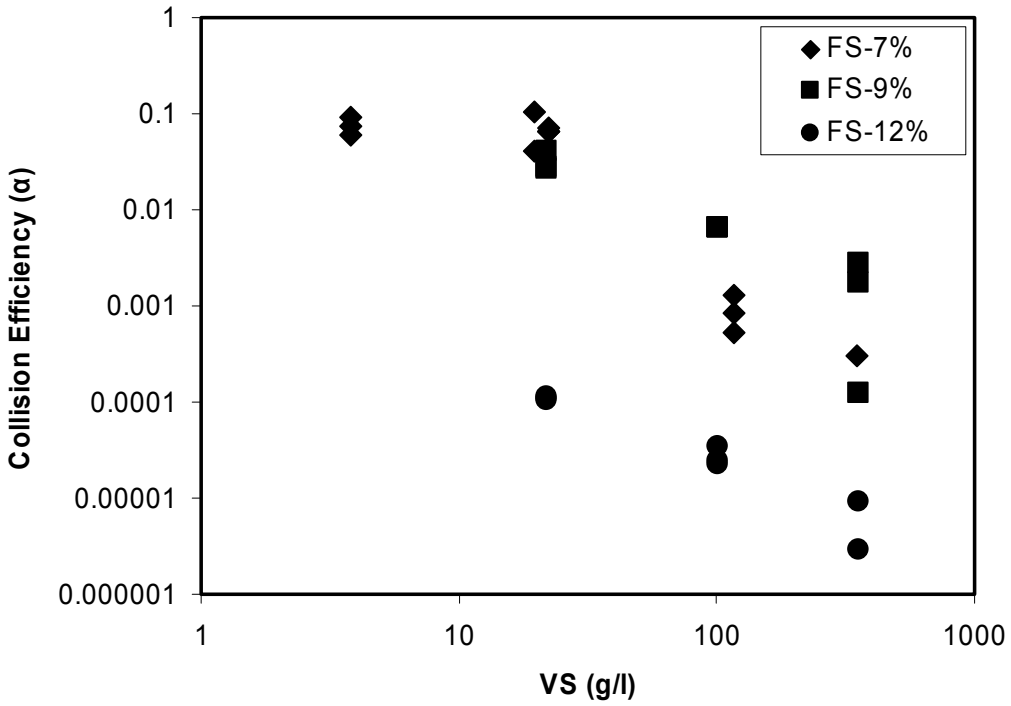

Figure 2.2 Collision efficiency versus volatile solids (VS) concentration in sands with varying silt+clay contents.

The overall oil retention in small columns packed with FS-9% and FS-12% was higher than with only FS-7% (data not shown). However the calculated collision efficiencies for FS-9% was a factor of 2 lower than for FS-7%, and were a factor ~300 lower for FS-12% because of the smaller value of d_c used in the calculations. If d_c is assumed to be equal to sediment D_{50}, the calculated collision efficiencies for the FS-9% and FS-12% would be 1.5 and 1.6 times the FS-7% collision efficiency.

The collision efficiencies for FS-7%, FS-9% and FS-12% all decreased with increasing oil concentration. In FS-7% at oil concentrations of 117 and 349 g/L, α was significantly lower than at 3.8 g/L (P=0.08). However there was no significant difference in the average α obtained in FS-7% with the three lowest concentrations (3.8, 19.7 and 22.1 g/L). The apparent decrease in collision efficiency with increasing emulsion concentration can be simulated using the Langmuirian blocking function shown in Equation 4. Using this

approach, the average empty bed collision efficiency (α') for FS-7%, FS-9%, and FS-12% were estimated using all α measurements for emulsion concentrations less than 22 g oil/L and are summarized in Table 2.2. With increasing clay content, the amount of oil retained increased. However α', decreased from 0.072 for FS-7% to 0.032 for FS-9% and 0.00011 for FS-12% due to the lower collector diameter used to calculate the single collector efficiency. This indicates that kaolinite addition does enhance oil droplet capture. However kaolinite appears to be a less efficient collector for oil droplets than the natural clayey sand.

Table 2.2 Colloid transport parameters estimated from SCP and long columns.

		SCP Parameters	Long Columns Parameters		
		α'	α'	K_d (min^{-1})	C_{im}^{max} (mg/g)
FS-7%	Fast	Ave. = 0.072 n = 8 range = 0.065	Ave. = 0.055 n=3 Range=0.052	Ave= 0.00057 n=3 range=0.0014	Ave. = 5.4 n=4 range=4.7
	Slow		0.036 n=1	0.00020 n=1	
FS-9% clay		Ave. = 0.032 n=3 range=0.015	0.030 n=1	0.0020 n=1	6.1 n=1
FS-12% clay		11×10^{-5} n=3 range=1.3×10^{-5}	7.7×10^{-5} N=1	0.0040 n=1	9.5 n=1

2.5. EMULSION TRANSPORT IN LONG COLUMNS

Experimental conditions and mass balance results for each of the long column experiments are summarized in Table 2.3. The FS-7%-#1, #2 and #3 were conducted at the same injection flowrate (2.25 to 2.38 mL/min). However minor differences in the sediment bulk density resulted in some variability in the solute transport velocity. The FS-7%-slow was conducted with a lower injection rate (0.5 mL/min) to evaluate the effect of transport velocity on oil retention. FS-9% and FS-12% examined the effect of increasing clay content on oil

retention. Overall mass balances for most experiments were close to 100% with the exception of FS-7%-#3 where only 65% of the injected mass was recovered in the column effluent and the sediment at the end of the experiment.

Experimental results for the three replicate FS-7% injection experiments are shown in Figure 2.3. In all three experiments, peak effluent emulsion concentrations were observed at approximately one pore volume indicating no significant enhancement or retardation of the oil droplets (Figure 2.3a). The maximum emulsion concentrations in the effluent of the three fast columns were 2.55, 0.66 and 0.7 g/L or 0.6 to 2.4% of the injection concentration. By contrast, the maximum non-reactive tracer concentrations were 13 to 27 % of the injection concentration (data not shown). Oil released in the column effluent varied from 4 to 12 % of the injected mass.

Table 2.3 Mass balance results for long columns**.**

Material	Bulk Density (g/cm^3)	Velocity (m/d)	Mass balance (%)	Experimental oil released (%)
FS-7%-#1	1.82	15.5	93	12.1
FS-7%-#2	1.44	11.1	105	6.5
FS-7%-#3	1.52	12.1	65	4.35
FS-7%-slow	1.66	2.9	87	1.23
FS-9%	1.73	18.4	120	0.51
FS-12%	1.74	18.6	126	0.008

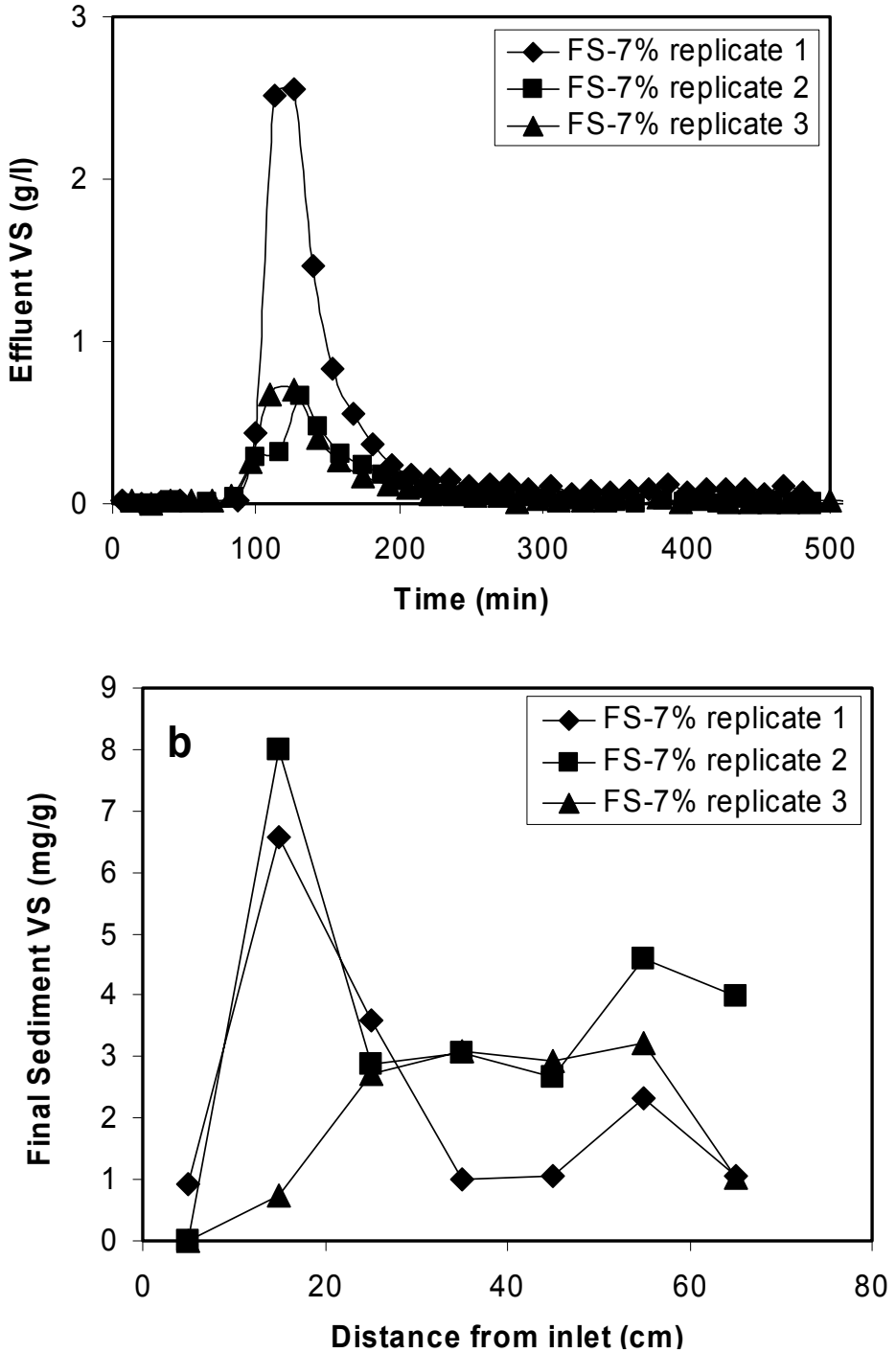

Figure 2.3 Experimental results from three replicate injection experiments with FS-7%: (a) variation in volatile solids (VS) concentrations in the column effluent; and (b) spatial variation in sediment oil concentration at the end of the experiment. Sediment values are the average concentration for a 10 cm increment corrected for the background VS.

There was also considerable variability in the final oil distribution in the sediment between the three replicate FS-7% columns (Figure 2.3b). In FS-7%-#1 and FS-7%-#2, the final oil concentrations were very low in the first sediment sample, reached their highest value in the 10-20 cm sample, and then declined. Final oil concentrations were also low in the first sediment sample in FS-7%-#3. However the oil concentration in the 10-20 cm sediment sample in FS-7%-#3 was much lower than in the first two columns and there was no clearly defined peak in final oil distribution.

In the emulsion injection tests conducted at lower velocity (FS-7%-slow) and with added kaolinite (FS-9% and FS-12%), oil retention was significantly higher. However appreciable amounts of oil were released from all columns with the exception of FS-9% and FS-12%. The higher oil retention in the FS-7%-slow test is consistent with prior work by Elimelech and Omelia (1990) and Camesano and Logan (1998) who demonstrated that colloid retention is a non-equilibrium process with lower transport velocities leading to increased contact time and greater colloid retention. The transport velocities employed in this work are higher than typically observed under ambient groundwater flow conditions but are comparable to velocities commonly encountered near emulsion injection wells. The trend of increasing oil retention with increasing clay content is consistent with prior results in chapter1.

These experimental results show that appreciable amounts of emulsified oils can be transported at least 80 cm from the injection point and will result in a reasonably uniform oil distribution in the experimental columns. However there was significant variability in experimental results between replicate columns. The greater amount of oil released from FS-7%-#1 could be due to the slightly higher transport velocity in this column. The cause of the observed variability in retained oil distribution is unknown, but may be related to minor variations in packing between columns.

2.6. MATHEMATICAL MODEL OF EMULSION TRANSPORT

2.6.1 Model development and implementation

Emulsion transport was simulated using MODFLOW (MacDonald and Harbaugh, 1988) and RT3D (Clement, 1997) as implemented in GMS 3.1 (Brigham Young University, 1999). Colloid transport is not currently implemented in RT3D, so a user defined module was developed to simulate colloid transport using equations 2, 3, and 4. RT3D uses the operator splitting method to separate the advection part of equation 1 from the reaction part. In the user defined module implemented as part of this work, the change in mobile emulsion concentration (C_m) and immobile emulsion concentration (C_{im}) due to oil droplet retention by the solid phase were represented by equations 7 and 8 coded in the RT3D user-defined module. This module is then compiled as a dynamic link library (dll) that is called by RT3D at runtime.

$$\frac{\partial C_m}{\partial t} = -K_a v \left(\frac{C_{im}^{\max} - C_{im}}{C_{im}^{\max}} \right) C_m + \frac{\rho}{\varepsilon_0} K_d \left(\frac{S}{C_m + S} \right) C_{im} \tag{7}$$

and

$$\frac{\partial C_{im}}{\partial t} = K_a v \frac{\varepsilon_0}{\rho} \left(\frac{C_{im}^{\max} - C_{im}}{C_{im}^{\max}} \right) C_m - K_d \left(\frac{S}{C_m + S} \right) C_{im} \tag{8}$$

where:

$$K_a = \frac{3}{2} \left(\frac{1 - \varepsilon_0}{d_c} \right) v \alpha' \left(\frac{C_{im}^{\max} - C_{im}}{C_{im}^{\max}} \right) \eta \tag{9}$$

The long columns (80 cm) used in the emulsion transport experiments were represented by a one-dimensional grid of 160 cells that were 0.5 cm long by 2.5 cm wide by

2.5 cm high. The column inlet was simulated as an injection well and the outlet was simulated as a drain. Dispersivity was estimated by fitting the RT3D non-reactive tracer module to match bromide tracer results (Appendix A2). Porosity was estimated from the measured bulk density and specific gravity of the sediment. The maximum oil retention capacity ($C_{im}^{\max}$) was assumed equal to the maximum observed oil concentration in the sediment. The immobile phase release coefficient (K_d) was adjusted to match the quasi-steady state concentrations observed in the column effluent after the peak of emulsion breakthrough curve (BTC) had passed. When the BTC was well defined, the best fit value of the empty bed collision efficiency (α') was found by comparing simulated and observed BTCs. However when less than 2% of injected emulsion was discharged in column effluent, α' was adjusted to match the observed oil distribution in the sediment. The best fit value of each parameter was found by the bisection method using the root mean square error as the primary objective function.

2.6.2 Simulation results

The colloid transport parameters, α', K_d, and $C_{im}^{\max}$, estimated from the SCP and long columns are summarized in Table 2.2. In Figure 2.4 observed BTC and the final oil distribution in each field sand column are compared with model simulation results generated using two different approaches. In the 'best fit' simulations, the model parameters were adjusted (alpha and K_d) to match observed results. In the 'K_d=0' simulations, the release rate was assumed to be negligible and K_d was set equal 0. Arithmetic mean of the parameter values from the best fit runs were used for each run.

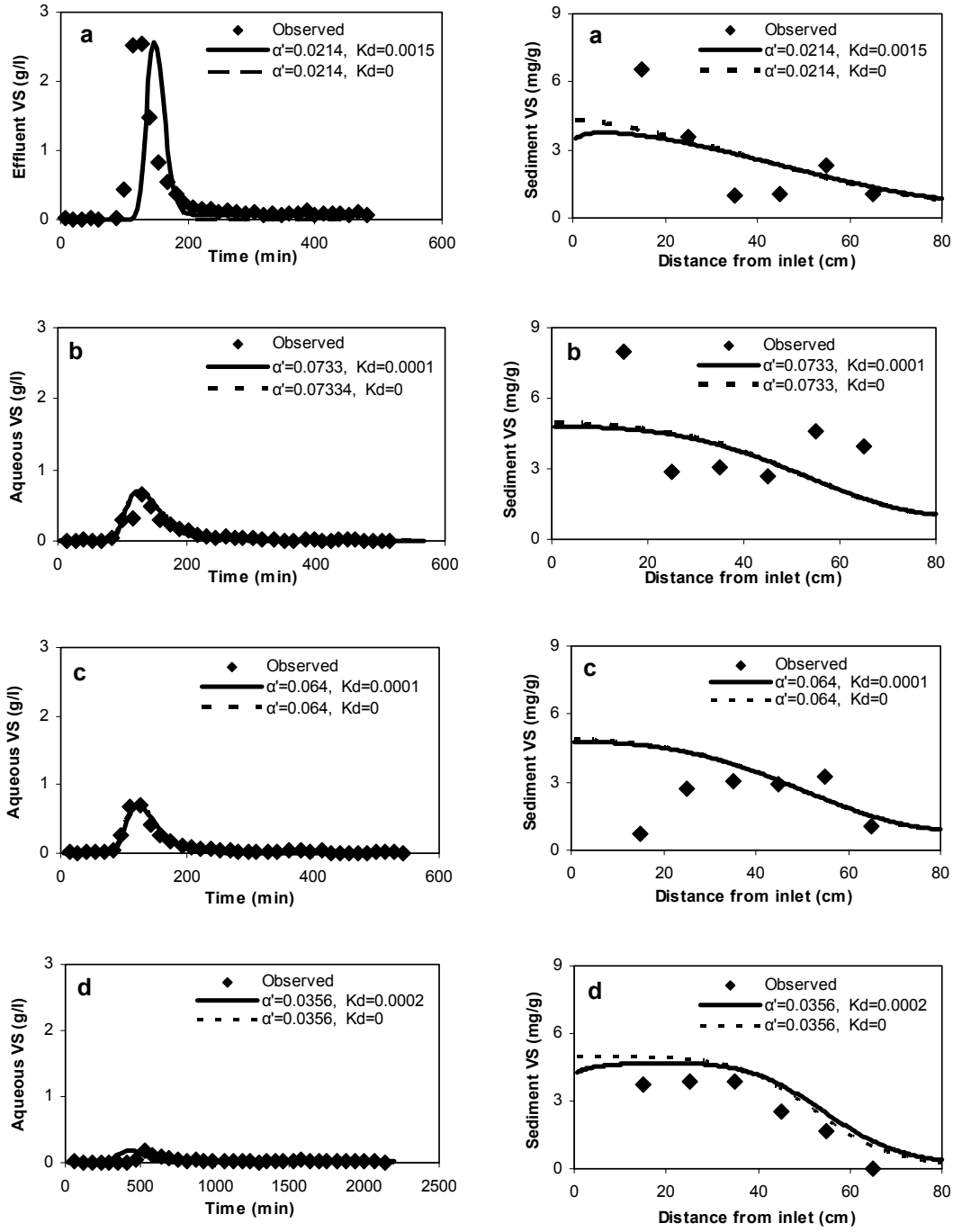

Figure 2.4 Comparison of simulated and observed volatile solids (VS) concentrations in column effluent (left) and final sediment (right) in field sand columns: (a) FS-7%-#1; (b) FS-7%-#2; (c) FS-7%-#3; and (d) FS-7%-slow.

Using the best fit parameter values, the model provides a very good fit between simulated and observed BTC for each of the FS-7% experiments. There was significant variability in the measured oil distribution in the columns at the end of the experiment so it was not possible to precisely match the oil distribution in any specific columns. However the best fit calibrated model appears to accurately simulate the general trend in the final oil distribution, with higher retention close to the inlet and gradually decreasing concentrations towards the outlet. Values of α' between the SCP and the long columns match for the FS-7% (fast and slow) and FS-9%. While significant variations in α' were observed, this variability is not unreasonable given that 1 or 2 orders of magnitude in α' have been reported in replicate experiments (Jewett et al., 1995). $C_{im}^{\max}$ could not be estimated from the SCP results because of the high velocity and short duration of these experiments.

Figure 2.5 shows a comparison of simulated and observed BTC and final oil distributions for the FS-9% and FS-12% columns. In the FS-9% column, the experimental results indicate that more oil is captured near the column inlet with lower concentrations further away. FS-12% shows a shift of the retention front, with peak concentrations approximately 40 cm from the injection point, resulting in a higher estimated release rate. In these experiments, over 99% of the oil was retained in the column.

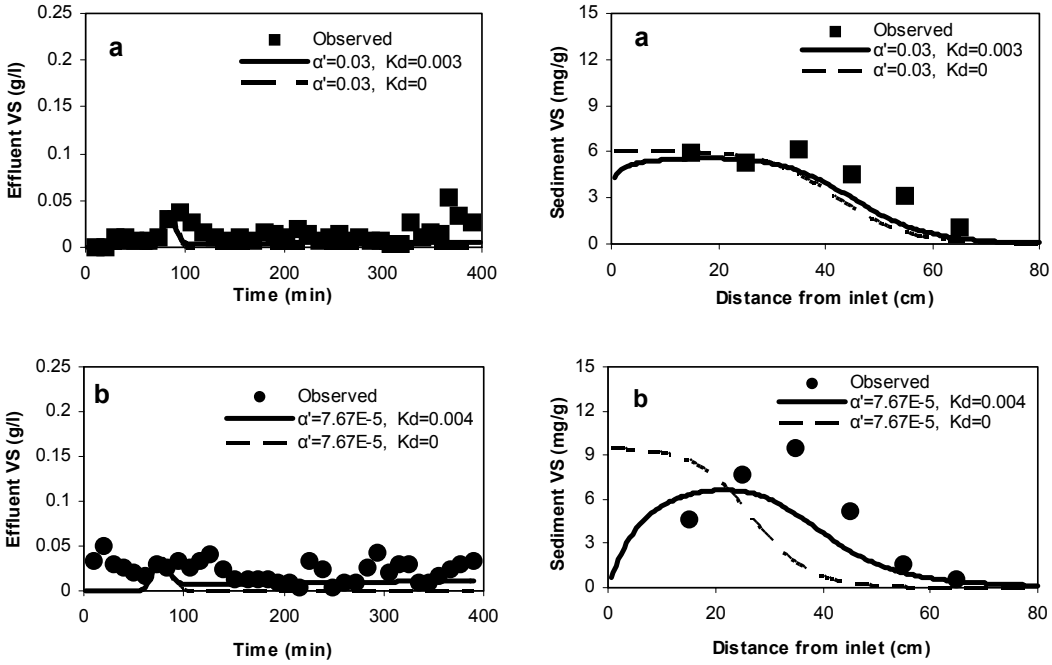

Figure 2.5 Comparison of simulated and observed volatile solids (VS) concentrations in column effluent (left) and final sediment (right) in columns packed with field sand amended with varying amounts of kaolinite: (a) FS-9%; and (b) FS-12%.

Table 2.4 Oil released as a percent of injected mass - comparison of experimental and model simulation results.

Material	Experimental Results (%)	Simulation Results (%)	
		Best fit parameters	With Kd=0
FS-7%-#1	12.1	8.97	7.45
FS-7%-#2	6.5	4.40	4.12
FS-7%-#3	4.35	4.02	3.78
FS-slow	1.23	1.21	0.75
FS-9%	0.51	0.22	0.06
FS-12%	0.008	0.38	0.08

Overall mass balance results for each of the simulations are compared with experimental results in Table 2.4. Between 88% and 99.9% of the injected oil was retained by the columns with the highest percent retained in FS-7% at a low flow rate and for the FS-9% and FS-12% columns. The mathematical model was able to reproduce this general trend very well both using Kd as a fitting parameter and when setting Kd equal to zero. In general,

Kd had very little impact on the observed oil distribution or the mass balance results. The only exception to this general trend was for the FS-12% column. For this one experiment, a relatively high release rate (Kd = 0.004 min^{-1}) resulted in the best fit between simulated and observed residual oil distribution as determined by the root mean squared error. With this high release rate, the model predicts that oil is flushed from the upstream end of the column. However, no experimental data is available in this portion of the column to confirm or refute this prediction. Given the high variability observed between the three replicate FS-7% columns, the prediction of oil being flushed from the upstream portion of the column should be treated with caution. Also, the higher clay content in the FS-12% required higher injection pressures to maintain flow which could have resulted in some flow bypassing.

While setting K_d equal to zero has little effect on the amount of oil retained in the column, setting K_d equal to zero does have a significant impact on the simulated VS concentrations in the column effluent once the main emulsion pulse has been flushed through the column. Figure 2.6 shows a comparison of observed and simulated effluent concentrations for the FS-7%-2 experiment where VS concentrations are plotted on a Log scale. The model accurately simulates the initial breakthrough and peak concentrations of VS using K_d= 0.0001 min^{-1} and K_d = 0. However when K_d = 0, the model significantly under estimates the VS concentrations in the column effluent after the emulsion peak has passed. Similar results were obtained in all other column experiments.

2.7. CONCLUSIONS

1. Oil-in-water emulsions prepared with small, uniformly sized droplets and a negative surface charge can be distributed in sands with varying clay content at least 80 cm away from injection point.

2. A mathematical model based on deep bed filtration theory and colloid transport can be used to simulate emulsion transport and retention in laboratory columns. The model provides a good description of effluent breakthrough curves and the final oil distribution in laboratory columns packed with field sand containing 7%, 9% and 12% silt and clay size material. Model parameters measured in replicate columns and at varying velocities were reasonably reproducible.

3. Kaolinite addition to field sand resulted in an increase in the maximum oil retention. However, the empty bed collision efficiencies in columns packed with field sand amended with kaolinite were lower than in columns packed with field sand only suggesting that the added kaolinite is a less efficient collector of oil droplets than the natural clayey sand.

4. Laboratory columns treated with emulsified oil, release a low, reasonably constant concentration of volatile solids that could be used to support anaerobic bioremediation processes. A mathematical function has been proposed that reasonably matches the observed effluent concentrations in the limited studies conducted to date. However, more work is needed to determine if this function can be used to reliably simulate VS release from entrapped oil under a range of experimental conditions. Until this work is completed, it may be more prudent to model emulsion transport and retention assuming zero oil release.

5. Additional work is needed to determine if the model parameters determined in laboratory columns can be used to predict emulsion transport and retention in larger scale systems.

2.8 REFERENCES

ARCADIS Geraghty & Miller, Inc. (ARCADIS). 2002. Final: Technical Protocol for Using Soluble Carbohydrates to enhance reductive Dechlorination of Chlorinated Aliphatic Hydrocarbons. Prepared for the Air Force Center for Environmental Excellence, San Antonio, Texas and the Environmental Security Technology Certification Program, Arlington, Virginia. December 19, 2002.

Bengtsson, G. and Ekere, L. 2001. Predicting sorption of groundwater bacteria from size distribution, surface area, and magnetic susceptibility of soil particles Water. Resources. Res., 37, pp 1795-1812.

Bengtsson, G and Lindqvist, R. 1991. Dispersal dynamics of groundwater bacteria. Microbial Ecology, 21, pp 49-72.

Bengtsson, G., Lindqvist, R. 1995. Transport of soil bacteria controlled by density dependent sorption kinetics, Water Resources Research, 31, 1247-1256.

Bengtsson, G, Lindqvist, R. 1995. Transport of soil bacteria controlled by density dependent sorption kinetics, Water Resources Research, 31, 1247-1256.

Bolster, C. H., Hornberger, G. M. and Mill A. L. 1998. A method for calculating deposition coefficients using the fraction of bacteria recovered from laboratory columns. Environ. Sci. Technol., 32, pp 1329-1332

Bolster, C. H., Mills A.L., Hornberger, G. M., Herman, J.S. 2001. Effect of surface coatings, grain size, and ionic strength on the maximum attainable coverage of bacteria on sand surfaces. J. Contaminant Hydrology, 50, pp 287-305.

Borden, R.C., Coulibaly, K.M., Long, C.M., and, Harvin, A.S. 2001. Development of permeable reactive barriers (PRBs) using edible oils. Annual Report to the Strategic Environmental Research and Development Program.

Brigham young University, Environmental Modeling Laboratory. 1999. The Department of Defense Groundwater Modeling System, GMS v3.1

Camesano, T.A. and Logan, B.E. 1998. Influence of Fluid velocity and Cell Concentration on the Transport of Motile and Non-motile Bacteria in Porous Media. Environmental Science & Technology. 32:1699-1708

Camesano T. A., K.M. Unice and B.E. Logan, 1999, Blocking and ripening of colloids in porous media and their implications for bacterial transport. Colloids Surf.

Chen, J. Y., Ko, C. H., Bhattacharjee, S. and Elimelech, M. 2001. Role of spatial distribution of porous medium surface charge heterogeneity in colloid transport. Colloids and surfaces A: Physicochemical and Engineering Aspects, 191, pp 3-15.

Clement, T. P. 1997. RT3D – A modular computer code for simulating reactive multi-species transport in 3-Dimensional groundwater aquifers. Battelle Pacific Northwest National Laboratory Research Report, draft version, PNNL-SA-28967.

Coulibaly, K. M., Borden, R. C. 2003. Distribution of edible oil emulsions and permeability loss in sandy sediments, In Situ and On-Situ Bioremediation: The Seventh Internat. Sym., Orlando, FL (accepted for publication).

Elimelech, M. and O'Melia, C.R. 1990. Kinetics of Deposition of Colloidal Particles in Porous Media. Environ. Sci. Technol. 24:1528-1536

Gross, M. J., Albinger, O., Jewett, D. G., Logan, B. E., Bales, R. C., and Arnold, R. G. 1995. Measurement of bacterial collision efficiencies in porous media. Wat. Res., 29, pp1151-1158.

Harvey, R. W., Kinner, N. E., Bunn, A., MacDonald, D. and Metge, D. 1995. Transport of groundwater protozoa and protozoan sized microspheres in sandy aquifer sediments. Appl. Env. Microbiol.. 61, pp 209-217.

Hunter, W. J., 2002. Bioremediation of chlorate or perchlorate contaminated water using permeable barriers containing vegetable oil. Current Microbiol., 45, pp 287-292.

Hunter, W.J., 2001. Use of vegetable oil in a pilot-scale denitrifying barrier. J. Cont. Hydro., 53, pp 119-131.

Huber, N., Baumann, T. and Niessner, R. 2000. Assessment of colloid filtration in natural porous media by filtration theory. Environ. Sci. Technol., 34, pp 3774-3779

Interstate Technology and Regulatory Council (ITRC) In Situ Bioremediation Team. 2002. Technical/Regulatory Guidelines: A systematic approach to in situ bioremediation in groundwater including decision trees on in situ bioremediation for nitrates, carbon tetrachloride, and perchlorate.

Jewett, D. G., Hilbert, T. A., Logan, B. E., Arnold, R. G., and Bales, R. C. 1995. Bacterial transport in laboratory columns and filters: influence of ionic strength and pH on collision efficiency. Wat. Res., 29, pp 1673-1680.

Jewett, D. G., Logan, B. E., Arnold, R. G., and Bales, R. C. 1999. Transport of *Pseudomonas fluorescens* strain P17 through quartz sand columns as a function of water content. Journal of Contaminant hydrology, 36, pp 73-89.

Johnson, P. R. and Elimelech, M. 1995. Dynamics of colloid deposition in porous media: blocking based on random sequential adsorption. Langmuir, 11, pp 801-812.

Kretzschmar, R., Sticher, H., 1998. Colloid transport in natural porous media: Influence of surface chemistry and flow velocity. Phys. Chem. Earth, 23, pp 133-139.

Lindqvist, R., Cho, J. S. and Enfield, C. G. 1994. A kinetic model for cell density dependent bacterial transport in porous media. Wat. Res., 30 pp 3291-3299

Lee, D. M., T. M. Lieberman, R. C. Borden, W. Beckwith, T. Crotwell and P. E. Haas, 2001. "Effective distribution of edible oils – results from five field applications." In G. B. Wickramanayake, A. R. Gavaskar, B. C. Alleman and V. S. Magar (Eds.), *Proc. In Situ and On-Site Bioremediation: The Sixth Internal. Sym.*, San Diego, CA.

Logan, B.E., 1999. *Environmental Transport Processes*, John Wiley & Sons, New York, 654 pg.

Martin, J. M., Logan, B. E., Johnson, W. P., Jewett, D. G. and Arnold, R. G. 1996 Scaling bacterial filtration rates in different sized porous media. J. Env. Eng., pp 407-415

McDonald, J. M. and Harbaugh, A. W., 1988. A modular three-dimensional finite-difference groundwater flow model. Techniques of water resources investigations of the U.S. Geological Survey Book 6, 586.

Morse, J.J., Alleman, B.C., Gossett, J.M., Zinder, S.H., Fennell, D.E., Sewell, G.W., and Vogel, C.M. 1998. Draft technical protocol: A treatability test for evaluating the potential `applicability of the reductive anaerobic biological in situ treatment technology (RABITT) to remediate chloroethenes. ESTCP, February 23, 1998.

Rajagopalan, R. and Tien, C. 1976 Trajectory analysis of deep-bed filtration with the sphere-in-cell porous media model. A.I.C.H.E.J. 28, pp 871-872.

Ren, J., Packman, A I. and Welty, C. 2001. Analysis of an observed relationship between colloid collision efficiency and mean collector grain size. Colloids and surfaces A: Physicochemical and engineering aspects, 191, pp 133-144.

Rijnaarts, H. H. M, Norde, W, Bouwer, E. J., Lyklema, J., Zehnder, A.J.B. 1996a. Bacterial deposition in porous media related to the clean bed collision efficiency and to substratum blocking by attached cells. Environ. Sci. Tech., 30, 2869-2876.

Rijnaarts, H. H. M., Norde, W., Bouwer, E.J., Lyklema J. and Zehnder, A.J.B. 1996b. Bacterial deposition in porous media: Effects of cell-coating, substratum hydrophobicity, and electrolyte concentration. Environ. Sci. Tech., 30, pp 2877-2883.

Ryan, J. N. and Elimelech, M. 1996. Colloid mobilization and transport in groundwater. Colloids and Surfaces: A-Physicochemical and Engineering Aspects. pp 1-56

Soo, H. and Radke, C.J. 1984. The flow mechanism of dilute stable emulsions in porous media. Ind. Eng. Chem. Fundam. 23, 342-347.

Soo, H. and Radke C.J., 1986a. A filtration model for the flow of dilute stable emulsions in porous media – I. Parameter evaluation and estimation. Chemical Engr. Sci. 41, 273-281 1986.

Soo, H. and Radke C.J. 1986b. A filtration model for the flow of dilute stable emulsions in porous media – I. Theory. Chemical Engr. Sci. 41, 263-272.

Westall, J. C. and Gschwend, P. M. 1993. Mobilizing and depositing colloids. Manipulation of groundwater colloids for Environmental Restoration. Lewis Publishers. Ann Harbor.

Zenker, M. J., Borden, R. C., Barlaz, M. A., Lieberman, M. T. And Lee, M. D. 2000. Insoluble Substrate for reductive Dehalogenation in Permeable Reactive Barriers. Bioremediation and phytoremediation of Chlorinated and recalcitrant Compounds. 2nd International Conference on Remediation of Chlorinated and Recalcitrant Compounds. Monterey, California. May 22-25, 2000

CHAPTER 3: Transport of Emulsified Edible Oil in a 3-Dimensional Sandbox: Experimental and Modeling Results

ABSTRACT

Injection of edible oils into the subsurface can provide an effective, low-cost alternative for stimulating anaerobic bioremediation processes. However concerns have been raised about the effects of oil buoyancy and variations in aquifer permeability on the final distribution of oil in the subsurface. 3-D sandbox experiments (1.2 m x 0.98 m x 0.98 m) were conducted to study the distribution of edible oil emulsions. In the first homogeneous experiment, the sandbox was packed with fine clayey sand (D_{50} = 0.38 mm, 6.9 % passing #200 sieve). In the second heterogeneous experiment, the sandbox was packed in three layers with the fine clayey sand amended with varying amounts of kaolinite (2.5%, 0%, and 5%). A continuously screened injection well was located in one corner of the sandbox. No flow boundaries were located on the two sides directly adjoining the well and constant head boundaries were located on the two sides opposite from the well to simulate ¼ of the flow-field surrounding an injection well. A fine emulsion was first injected through the well followed by chase water to distribute the emulsion throughout the sandbox. This approach was very effective in distributing emulsified oil throughout the sandbox and resulted in a reasonably uniform volatile solids distribution in the top, middle and bottom layers, measured 5 and 7 weeks after the completion of emulsion injection.

A standard colloidal transport model that includes a Langmuirian blocking function was used to simulate emulsion transport and retention in the 3-D sandbox. All model parameters were measured independently. Simulations results were in close agreement with observed values for both the homogeneous and heterogeneous injection tests demonstrating that this approach can be used to describe the transport and distribution of emulsified oil under representative aquifer conditions.

3.1. INTRODUCTION

A variety of anaerobic bioremediation processes are being developed for the in-situ treatment of groundwater contaminants including chlorinated solvents, perchlorate (ClO_3^-), chromate (CrO_4^{-2}), nitrate (NO_3^-) and acid mine drainage (Morse et al., 1998; Hunter, 2001; Hunter, 2002; ARCADIS, 2002; ITRC, 2002). Essentially all of these processes require that the contaminant be brought in contact with a biodegradable organic substrate (Nyer, 1985; Thomas et al., 1989). This substrate serves as a carbon source for cell growth and as an electron donor for energy generation.

The most common approach for stimulating in-situ anaerobic biodegradation is to flush a dissolved substrate through the contaminated zone using a series of injection and production wells. This approach has been very effective at some sites (Ellis et al., 2000; Martin et al., 2001; Major et al., 2002). However continuously feeding a soluble, easily biodegradable substrate can be expensive. There is a significant initial capital cost associated with installation of the required tanks, pumps, mixers, injection and pumping wells, and related process controls. In addition, operation and maintenance (O&M) costs can be high because of problems with injection well clogging and the labor for monitoring and process control. An alternative approach employed at some sites has been to distribute a 'slow-release' organic substrate to support anaerobic biodegradation of the target contaminants. A variety of slow-release substrates have been proposed including chitin (Harkness, 2003; Martin et al., 2002), Hydrogen Release Compound (Koenigsberg, 2000; Wu, 1999), and emulsified edible oils (Zenker et al., 2000; Lee et al., 2001; Wiedemeier et al., 2001).

We are working to develop an effective, low cost process for stimulating in-situ anaerobic bioremediation processes using food-grade edible oils. In this process, an oil-in-water emulsion is prepared using edible oil, food-grade surfactants and an appropriate high-shear mixer. This emulsion is then injected into the sediment followed by chase water to

distribute and immobilize the oil. The immobilized oil then serves as a slow-release carbon source to support anaerobic biodegradation of the problem contaminants. Capital costs for stimulating anaerobic bioremediation processes using emulsified oils are expected to be much lower than competing technologies since most of the injection equipment can be reused at multiple sites. Long-term operation and maintenance costs should also be lower since much less frequent substrate addition would be required (Harkness, 2000).

Coulibaly and Borden (2003) have presented laboratory results showing that emulsions prepared using food-grade soybean oil can be effectively distributed in sands and clayey sands with only modest reductions in aquifer permeability (0 to 40% reduction in K). The key to effective oil transport appears to be in preparing an emulsion with small, uniformly sized oil droplets. When the oil droplets are smaller than the pore diameters, the droplets can be transported significant distances through porous media (Soo and Radke, 1986). Oil retention and associated reductions in permeability increases with sediment clay content and with the ratio of droplet size to pore size (Chapter 1). Emulsion droplet transport in sandy sediments can be described using a colloids transport model based on deep bed filtration (chapter 2).

While the available laboratory and field data indicate that emulsions can be effectively distributed in typical aquifer materials, some questions still remain.

- Edible oils are less dense than water so there is potential for buoyancy effects that could result in poor oil distribution in deeper portions of the aquifer where contaminant concentrations may be high.
- In-situ treatments are often complicated to implement because difficulties associated with distributing treatment agents throughout heterogeneous aquifers.

In this work, radial flow injection experiments were conducted in a 3-dimensional (3-D) laboratory sandbox to study the oil injection process and validate an emulsion transport

model under representative conditions. Emulsion injection tests were conducted for two aquifer conditions: (1) homogenous sand; and (2) a moderate permeability sand layer between two lower permeability clayey sand layers. These experimental results were then used to validate the numerical model implemented as a user defined-module in RT3D (Clement, 1997) for simulating emulsion transport where emulsion movement in the subsurface is described by a colloids transport model based on deep bed filtration (Chapter 2).

3.2. MATERIALS AND METHODS

The experimental setup was designed to simulate one quarter of the flow-field adjoining an emulsion injection point. A plan view of the sandbox and injection well is shown in Figure 3.1. The inside dimensions of the sandbox were 0.98 m wide x 0.98 m deep x 1.2 m high. A double layer of geonet drainage material and single layer of non-woven geotexile fabric are installed along the back and right boundaries. These drainage layers are connected by several different ports to a single reservoir that maintained the back and right sides as constant head boundaries. A 2.5 cm diameter x 100 cm long slotted well screen (#20 slot) was located in the front left corner of the sandbox and connected to a constant head reservoir. With the front and left sides of the tank acting as no-flow boundaries, this setup reasonably represented one quarter of the flow field surrounding an injection point. The 1.0 m injection radius in the laboratory experiment is at a scale comparable to field conditions.

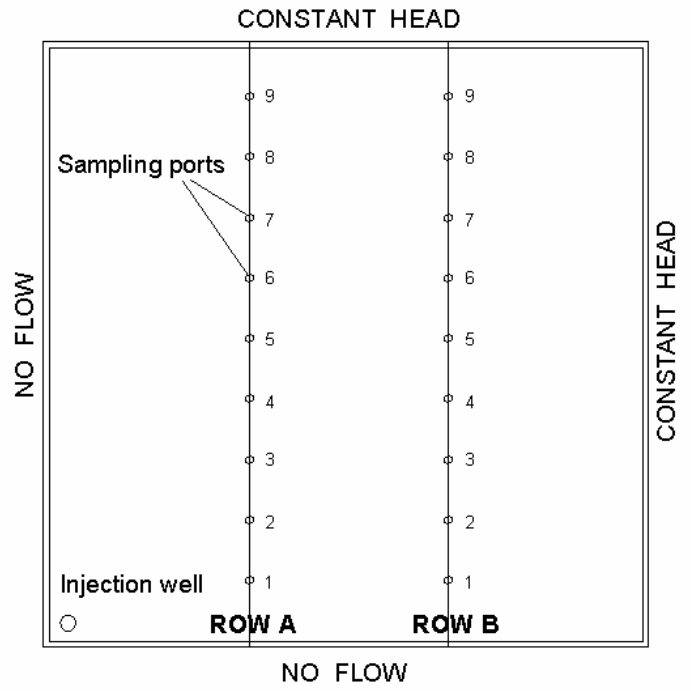

Figure 3.1 Schematic Plan view of the 3-D sandbox showing the sample/manometer tube locations**.**

The concentrated oil-in-water emulsions used in these experiments were prepared by blending 33% soybean oil with 5% premixed surfactant (38% polysorbate 80, 56% glycerol monooleate and 6% water) and 62 % tap water. The emulsion used in the first homogeneous test was prepared in a standard high-speed lab blender (Waring Commercial Blender) while the emulsion used in the second heterogeneous test was prepared in a high pressure dairy homogenizer (Gaulins two stage 300 GCI at 1000 psi). The concentrated emulsions described above were diluted 3:1 with water prior to injection resulting in the following composition for the injection solution 87.3 % tap water, 11 % soybean oil, and 1.7 % premixed surfactant. The droplet size distribution for each emulsion was measured visually with a Nikon™ microscope equipped with a Sensys™ calibrated camera and Metamorph™ software at a 400x magnification. In the homogeneous test, the median droplet diameter was 1.2 μm while the median diameter in the heterogeneous tests was 0.7 μm. The cumulative oil

volume versus droplet diameter for the emulsions used in the homogeneous and heterogeneous injection tests are presented in Figure 3.2.

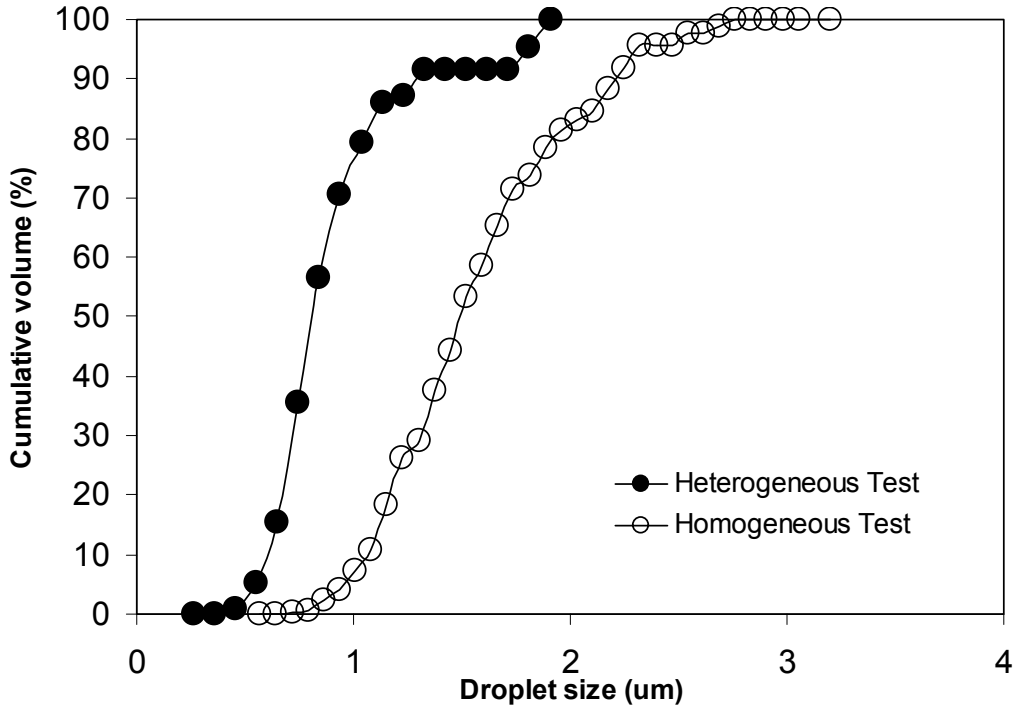

Figure 3.2 Cumulative droplet volume distributions for homogeneous and heterogeneous injection tests**.**

Liquid samples were collected throughout both tests to monitor emulsion breakthrough with time. Soil cores were collected 5 weeks after completion of the homogeneous and 7 weeks after completion of heterogeneous test to measure the final oil distribution. Liquid and sediment samples were analyzed for volatile solids (VS) by weight loss on ignition for 1 hour at 550 ºC.

3.2.1. Homogeneous Injection Test

For the homogeneous test, a 5 cm thick bentonite layer was placed in the bottom of the tank followed by 110 cm of field sand (fine clayey sand, D_{50} = 0.38 mm, D_{10} = 0.09 mm, D_{60}/D_{40} = 3.9, 6.9 % passing #200 sieve, termed FS-7%). A second 10 cm thick bentonite

layer was placed above the sand to form a confining layer allowing emulsion injection under a slight pressure (~ 18 cm of water). During sand placement, 10 – 20 cm of water was maintained above the sand surface. Approximately 10 L of sand was placed at a time followed by gentle mixing of the sand surface and compaction to remove entrapped air. On a macroscopic scale, this resulted in reasonably uniform packing with little entrapped air. However visual inspection of the sand through the clear acrylic plastic showed some small-scale segregation of sediments where some thin layers appeared to have more clay than others. Two rows (shown as A and B on Figure 3.1) of 2 mm ID stainless steel tubes with nylon screens were installed at 25 cm, 50 cm, and 75 cm from the top of the sand layer for sample collection and to measure changing water levels via a manometer board. Additional details on the tank construction and sampling tube locations are presented in Appendix A3. Based on the weight of added sand, the final porosity (n) and bulk density (ρ_B) were 0.36 and 1.77 g/cm^3, respectively. Hydrodynamic parameters were estimated using results from a non-reactive tracer test where 60 L (~0.2 PV) of a 200 mg/L NaBr solution was injected followed by 450 L (~1.5 PV) of tap water over a 5 day period. During the emulsion test, 30 L (~ 0.1 PV) of oil-in-water emulsion were injected followed by 450 L of tap water (~1.5 PV) to distribute and immobilize the oil.

2.2. Heterogeneous Injection Test

In the heterogeneous test, a 5 cm bentonite layer was installed on the bottom of the tank, followed by 23 cm of field sand amended with ~5% kaolinite (n = 0.26, ρ_B = 1.96 g/cm^3 termed FS-12%), 48 cm of field sand (n = 0.22, ρ_B = 2.07 g/cm^3, termed FS-7%), 29 cm of field sand amended with ~2.5% kaolinite (n = 0.30, ρ_B = 1.84 g/cm^3, termed FS-9%) and 20 cm of bentonite to form a confining layer. The field sand – kaolinite mixtures were prepared by blending known weights of field sand and kaolinite (Standard Industrial Mineral Inc.

Bishop, CA) in concrete mixer for ~ 15 minutes per batch. The stainless steel sampling tubes were screened at 20 cm, 50 cm, and 90 cm from the top of the sand box layer. Additional details on the tank construction and sampling tube locations are presented in Appendix A3. In the heterogeneous test, the non-reactive tracer was injected as part of the emulsion. Prior to injection, tap water was flushed through the tank for 2 weeks to establish steady-state conditions. The emulsion injection test consisted of injecting 120 L (~0.5 PV) of emulsion amended with 1000 mg/l NaCl followed by 1000 L (~5.0 PV) of tap water.

3.3. EMULSION INJECTION TEST RESULTS

3.3. 1. Homogeneous Injection Test

Prior to the start of emulsion injection, a non-reactive tracer test was run and the spatial variation of head with distance was determined to collect data required for calibration of a groundwater flow and solute transport model (described in Section 4). During emulsion injection, the flowrate dropped to 0.06 m^3 /d from a pre-injection value of 0.13 m^3 /d (std. dev. = 0.01). Shortly after the start of the post-emulsion water flush, the flowrate recovered to 0.10 m^3 /d and then remained relatively constant for the remainder of the test (ave. flow = 0.11 m^3 /d, std. dev. = 0.01). Water levels in the injection well and constant head boundaries were held constant throughout the test, so the decline in flowrate during emulsion injection indicates a temporary reduction in the effective hydraulic conductivity. Most of this reduction appears to be due to the somewhat higher viscosity (μ = 1.44 centipoises) and lower density (ρ = 0.99 g/cm^3) of the emulsion compared to that of water (μ = 0.95 centipoises, ρ = 1 g/cm^3). The recovery in injection flowrate during the post-emulsion water flush indicates that there was no significant, long-term permeability loss associated with the emulsion injection. These results are consistent with prior work by Coulibaly and Borden (2003) who showed that flushing 3 pore volumes (PV) of a similar emulsion (median droplet

diameter = 1.2 μm) followed by 7 PV of water through FS-7% resulted in only 3% reduction in hydraulic conductivity.

Figure 3.3 shows the variation in emulsion concentration versus time in monitoring points close to the injection well (Figure 3.3a) and away from the injection well (Figure 3.3b). The maximum concentrations observed in the closest monitoring points were 110%, 37% and 90% of the injection concentration indicating essentially complete emulsion breakthrough at up to 44 cm from the injection well. In the more distant sampling points, emulsion breakthrough was more limited and occurred later in the test as the chase water distributed emulsion throughout the sandbox. In sampling points over 70 cm from the injection well, emulsion concentrations never exceeded 0.5% of the injected concentration. This is in contrast to the non-reactive tracer test results which showed 50% to 100% breakthrough at the same locations and indicates that most of the emulsion was captured by the soil matrix.

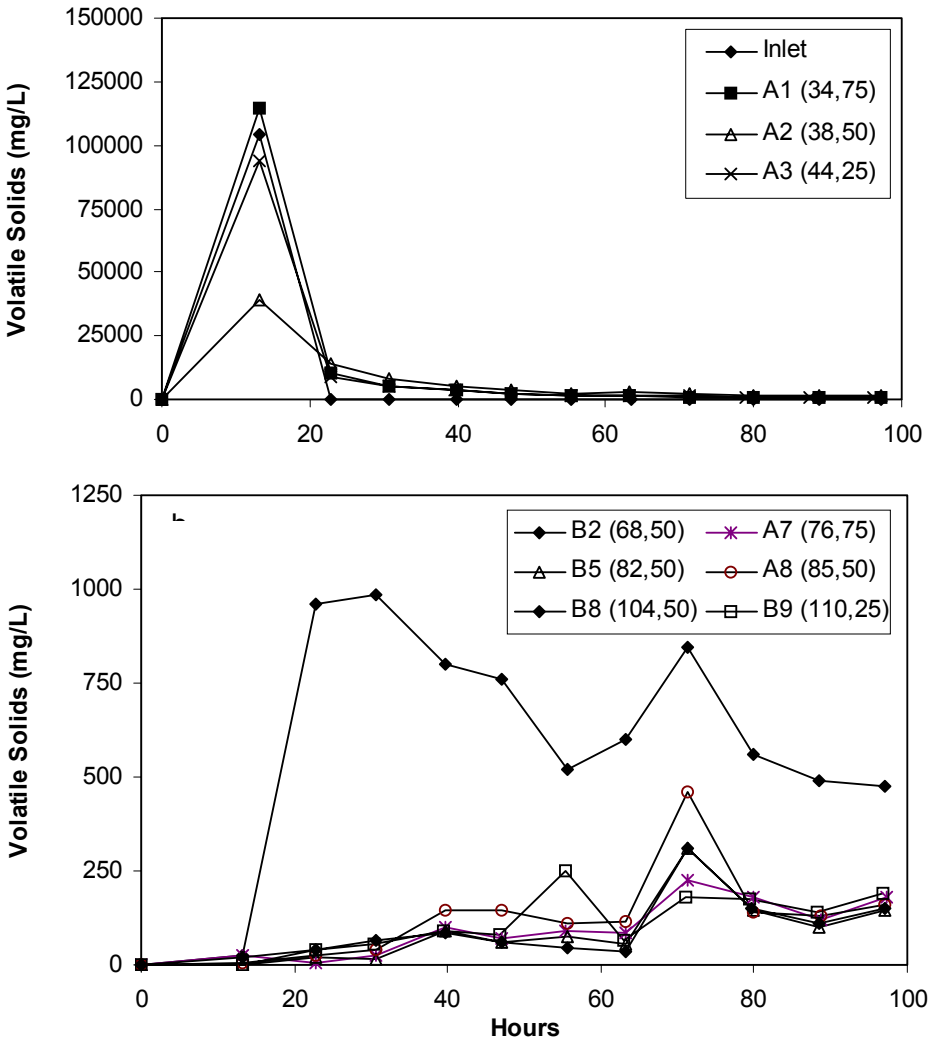

Figure 3.3 Volatile solids concentration versus time in the injection feed and monitoring points. Values in parentheses indicate radial distance from the injection well (cm) and depth from the top of sand (cm).

Five weeks after the end of the emulsion injection test, sediment cores were collected from 9 locations to determine the spatial distribution of residual emulsion in the sediment. During this post-injection period, there was no flow through the tank to evaluate the potential for oil droplets to float upward due to buoyancy effects. Figure 3.4 shows the sediment volatile solids (VS) concentration (mg/g) after correcting for the sediment VS prior to injection (5.39 mg/g). The VS results show that emulsion was effectively distributed

throughout the tank. However there was a statistically significant trend in VS concentration with radial distance at each depth with slightly higher concentrations in samples collected closer to the injection well. There was no significant difference in sediment VS concentrations between the three sampling zones indicating that buoyancy effects were not significant.

Approximately 67.5% (95% confidence limits = ± 24 %) of the added emulsion was retained by the sediment based on the average VS in the sandbox (mean = 1.85 mg/g, std. dev. = 1.66, n = 27) and the amount of sediment in the sandbox. Sampling from one of several discharge ports on the constant head boundaries indicated that 2.5% of the emulsion was released in the sandbox effluent with up to 30% of the emulsion unaccounted. However visual observations indicated considerable variability in emulsion concentration between the different constant head discharge ports, suggesting that more emulsion may have been released in the sandbox discharge than the sampling results indicate.

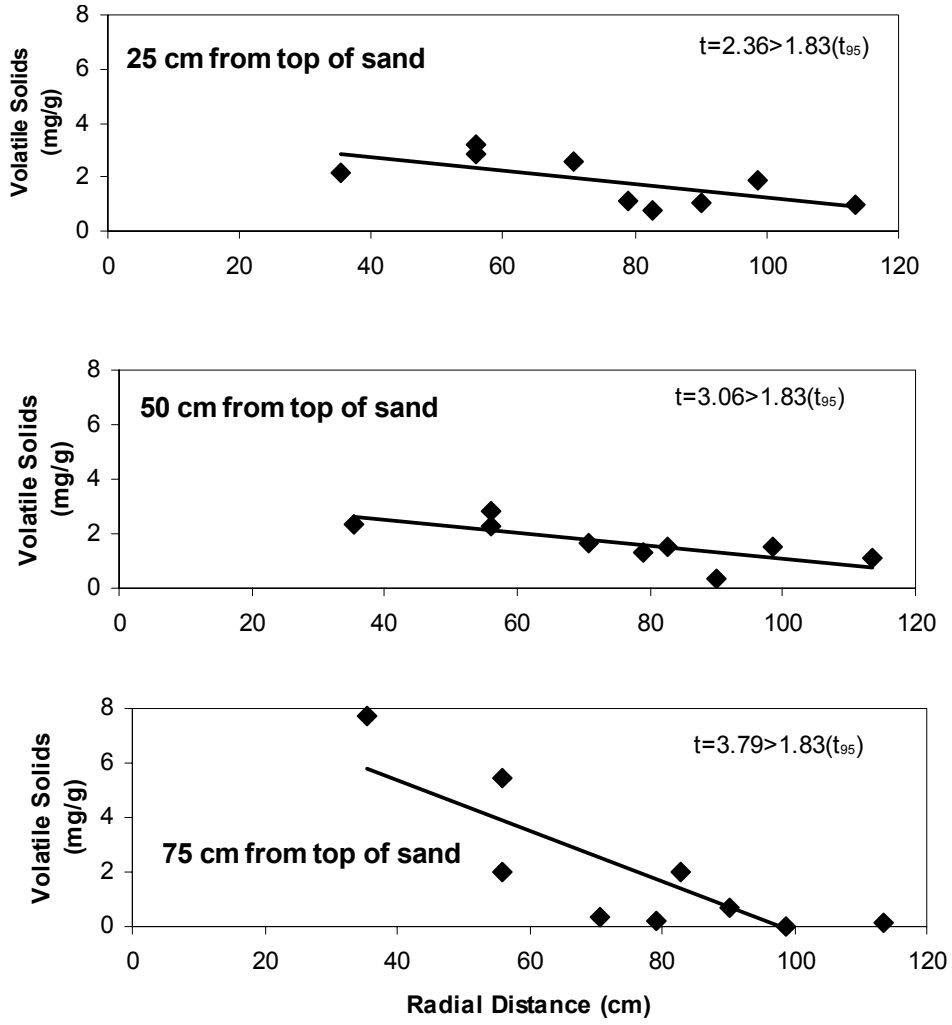

Figure 3.4 Volatile solids concentration in sediment samples collected 5 weeks after the end of homogeneous injection test. T is the t-value and t_{95} the critical t-value at 95% confidence limit

3.3.2. Heterogeneous Injection Test

Prior to the start of emulsion injection, tap water was run through the tank at a flowrate of 0.6 m^3/d for 2 weeks to establish steady-state conditions. The spatial variation of head with distance was determined for groundwater model calibration (described Appendix A3). The emulsion injection test consisted of injecting 120 L (~0.5 PV) of emulsion amended with 1000 mg/l NaCl followed by 1000 L (~5.0 PV) of tap water.

During the emulsion injection portion of the test (0 to 10 hr), the flowrate dropped from a pre-injection value of 0.6 m^3/d (std. dev. = 0.03) to 0.2 – 0.4 m^3/d (Figure 3.5A). When the injection solution was switched back to tap water at 10 hr, the injection flowrate recovered to near pre-injection values and then declined toward the end of the test. Towards the end of the heterogeneous test, we also observed an increase in head in monitoring points directly adjoining the constant head boundaries suggesting that the non-woven fabric forming the constant head boundary was being gradually clogged with fine sediment. We hypothesize that this clogging was due to mobilization of the added kaolinite by the surfactants used to form the emulsion. In prior studies, Sabbodish (2002) reported clay mobilization due to surfactant injection. The variation in transmissivity with time was evaluated by fitting injection flowrate and hydraulic head results from six different monitoring points to the steady-state Theim equation (Figure 3.5B). These results show an apparent reduction in hydraulic conductivity immediately after emulsion injection and then an immediate recovery to pre-injection values. Towards the end of the heterogeneous test, there appears to be a slight increase in transmissivity (T), possibly due to mobilization of some fraction of the kaolinite. However the slight increase in T was not significant at the 95% confidence level.

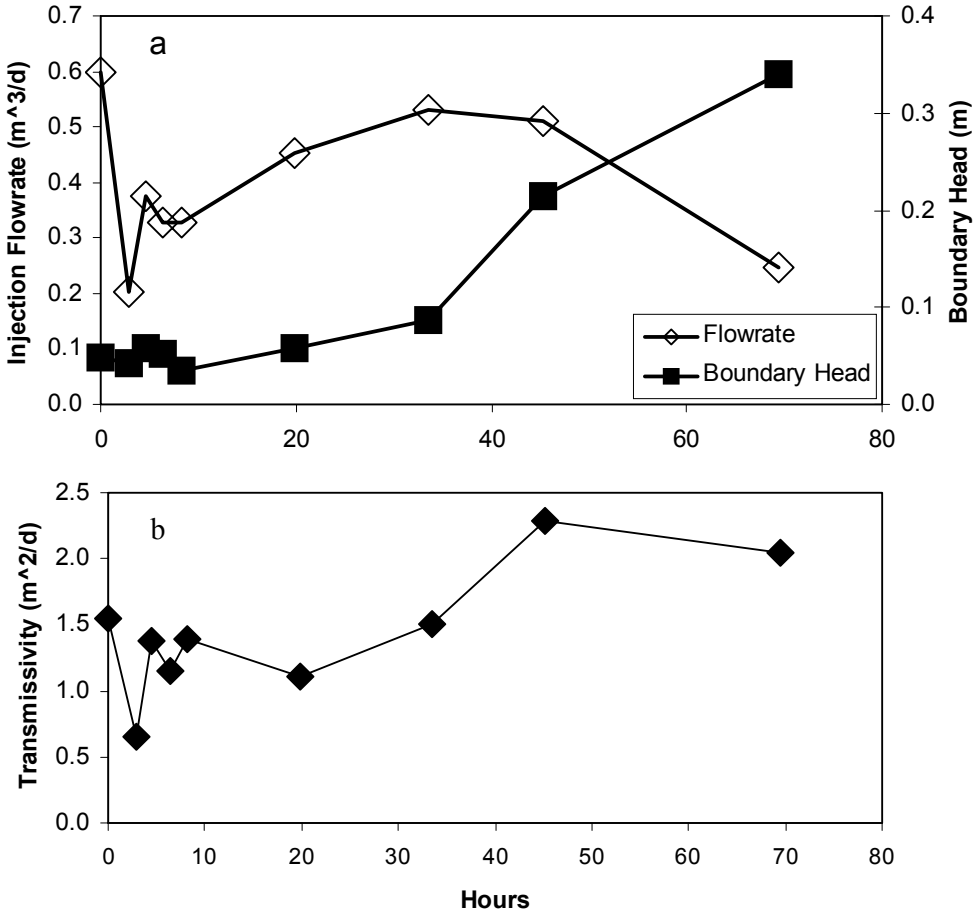

Figure 3.5 Variation in injection flowrate and head in monitoring point closest to constant head boundary during heterogeneous test (a). Variation in transmissivity with time (b) determined by fitting water levels in different monitoring points to steady-state Theim equation.

During the heterogeneous test, the emulsion contained a non-reactive tracer (1000 mg/L NaCl) for comparison with the emulsion breakthrough results. Figure 3.6 shows the breakthrough in relative concentrations of volatile solids and conductivity in sampling ports in the top, middle and bottom layers of the sandbox at different radial distances. Relative concentrations were calculated as the concentration measured at the sampling point (C) divided by concentration in the initial emulsion/tracer solution (Co). Electrical Conductivity was used as a surrogate measure of NaCl. In all the sampling points, the peak emulsion concentration was observed at the same time or slightly before the peak tracer concentration.

Early colloid breakthrough has been observed in a number of previous studies (Enfield et al., 1989; Higgo et al., 1993; Grindrod et al., 1993; 1996, Kretzschmar et al., 1995, 1998) and has generally been attributed to colloid exclusion from the smaller soil pores.

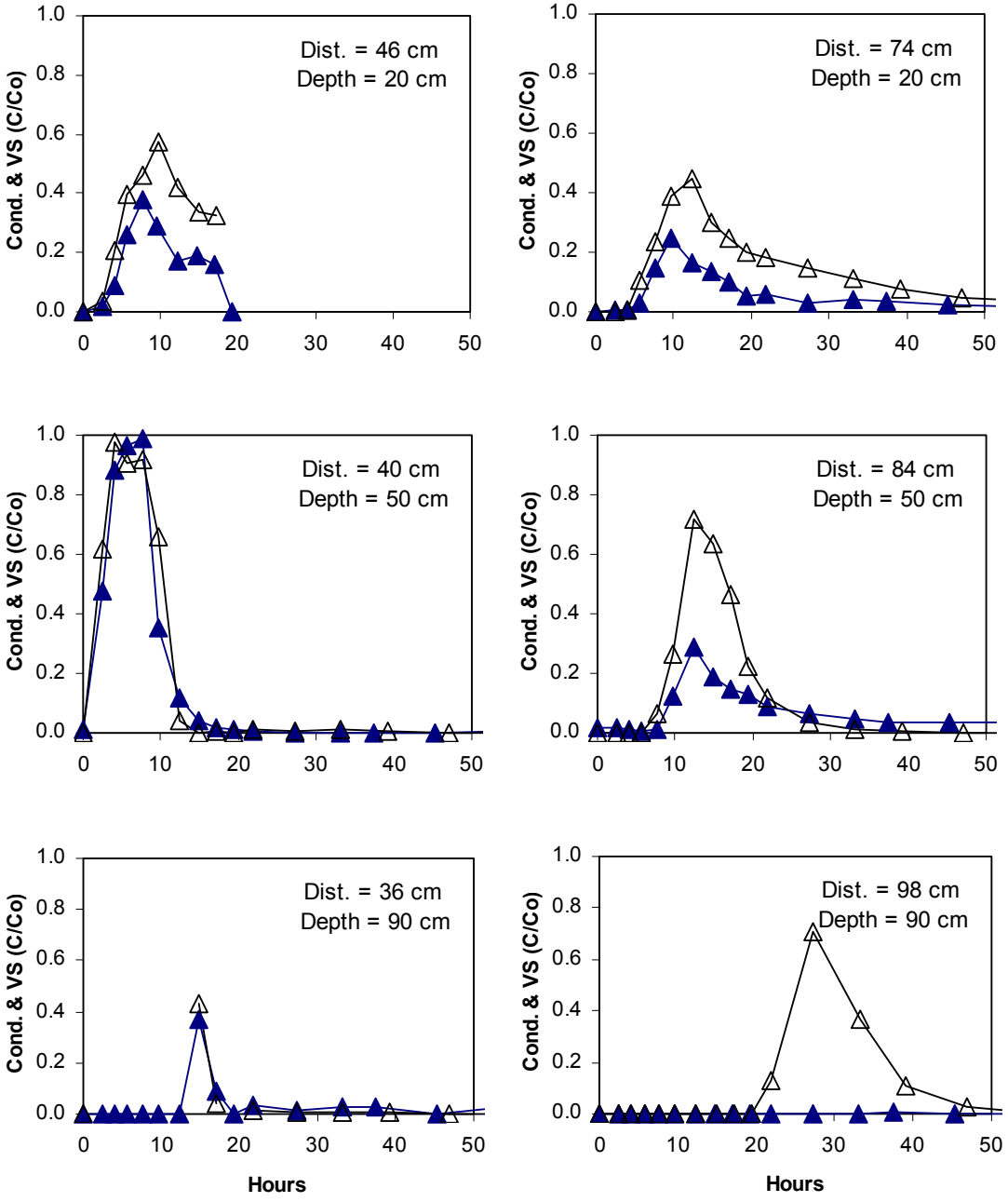

Figure 3.6 Variation in relative conductivity (Cond., open triangles) or volatile solids (VS, filled triangles) with time in selected sampling ports during heterogeneous injection test. Concentrations are plotted as measured concentration (C) divided by emulsion concentration (Co).

Figures 3.7a, 3.7b and 3.7c show the emulsion breakthrough with time in the upper (FS-9%), middle (FS-7%) and lower (FS-12%) layers. In the FS-7% layer, the maximum emulsion concentration in sampling points closest to the injection wells were close to 100% of the injection concentration, similar to results obtained during the homogeneous test. However in the heterogeneous test, high emulsion concentrations were observed farther out in the FS-7% layer, possibly due to the greater amount of emulsion injected (0.5 PV of emulsion) and higher amount of water flushed (1000 L vs 450 L in homogeneous sand box).

In the FS-9% and FS-12% layers, emulsion quickly reached the wells closest to the injection well but maximum concentrations were lower than in the FS-7% layer and concentrations declined much more rapidly with distance from the injection point. This may be due to the higher capacity of the field sand amended with kaolinite to retain emulsion (Coulibaly and Borden, 2003).

Figures 3.8a, 3.8b and 3.8c shows the VS concentration of sediment samples collected at 20 cm (FS-9%), 50 cm (FS-7%) and 90 cm (FS-12%) from the top of the sandbox, 7 weeks after the completion of the emulsion injection. As in the homogeneous experiment, there was no flow through the box for this period to evaluate the effects of oil buoyancy. VS associated with the emulsion was determined by subtracting the background VS of the sediment (FS-7% = 3.83 mg/g, Std. dev. = 2.33; FS-9% = 1.59 mg/g, Std. dev. = 1.71; FS-12% = 2.07 mg/g, Std. dev. = 1.70). The sediment coring results show that emulsion was very effectively distributed throughout the FS-7% layer with no significant trend in VS concentration with distance. However, in the FS-12% layer, VS concentrations were highest close to the injection well with lower concentrations farther out. The more limited emulsion distribution in this layer is presumably due to the lower hydraulic conductivity of this layer. Results from the FS-9% layer were intermediate between two other layers. The VS concentrations appear

to be somewhat higher near the injection well; however this trend was not significant at the 95% confidence level. As in the homogeneous test, there was no significant difference in VS in the bottom, middle and top layers indicating buoyancy effect on the final emulsion distribution.

In the heterogeneous test, a total of 13.2 kg of VS were injected as emulsion or 11.87 mg/g of sediment. Seven weeks after the end of the injection, the average VS of the sediment was 3.97 mg/g (95% confidence limits = ± 0.94 mg/g) or 59.5% of the amount injected. In addition, 32.8% of the injected emulsion was observed in the sandbox effluent leaving 7.7% unaccounted. The close mass balance obtained in the heterogeneous test is likely due to switching the sampling point to the constant head reservoir which included the discharge from all outflow ports. The greater amount of emulsion discharged from the sandbox in the heterogeneous test is presumably due to the much larger amount of emulsion injected and greater amount of water flushing.

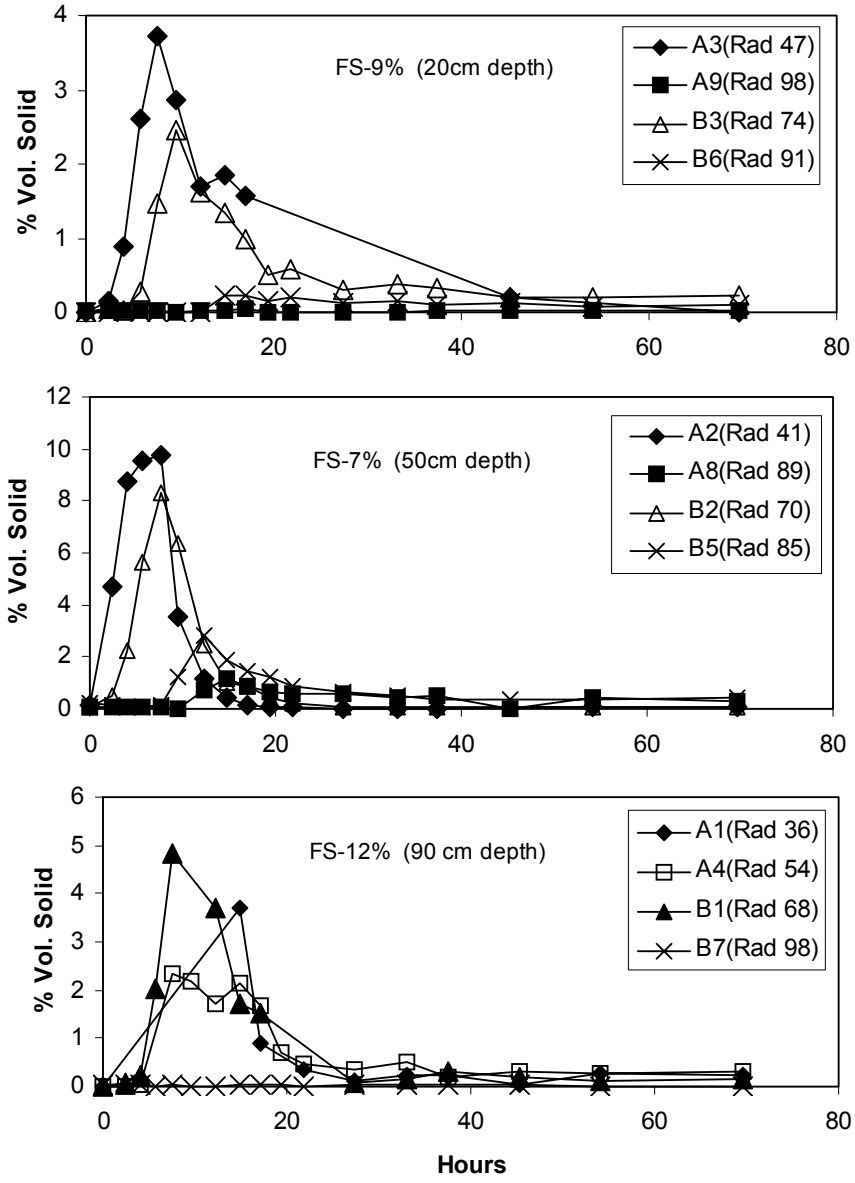

Figure 3.7 Volatile solids variation in liquid phase with time in the monitoring points during the heterogeneous test. Values in parentheses indicate radial distance from the injection well (cm).

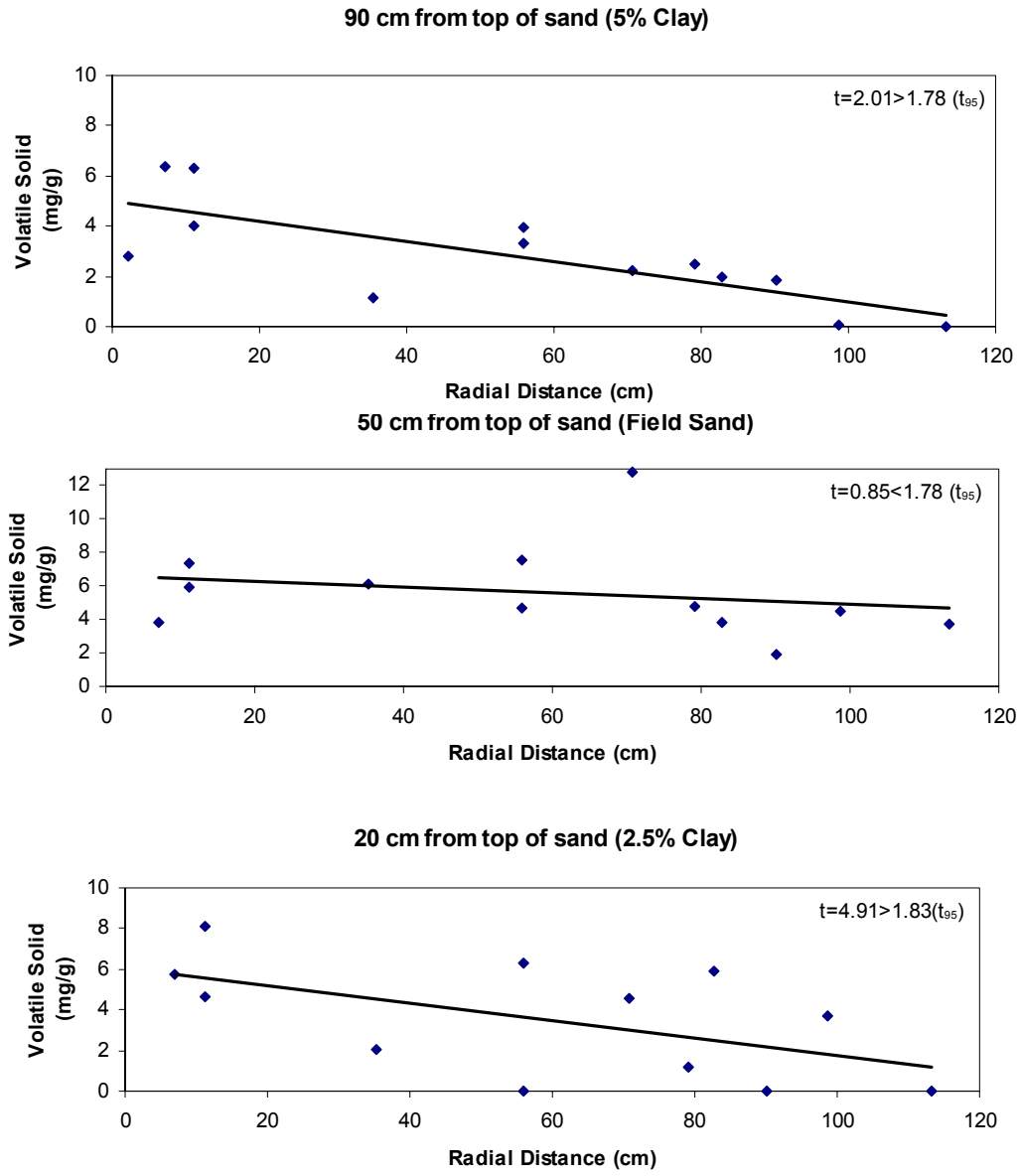

Figure 3.8 Volatile solids concentration in sediment samples collected 7 weeks after the end of heterogeneous test.

3.4. MATHEMATICAL MODELING OF EMULSION TRANSPORT AND IMMOBILIZATION

The transport and retention of oil-in-water emulsions may be simulated using the standard advection-dispersion approach with terms representing colloid capture by the sand grain surfaces and droplet release back to the mobile phase (Bolster et al, 1998; Camesano et al, 1999). In chapter 1 we have shown that emulsion transport and retention can be simulated using

$$\frac{\partial C_m}{\partial t} = \frac{\partial}{\partial x_i}\left(D_{ij} \frac{\partial C_m}{\partial x_j} \right) - \frac{\partial}{\partial x_i}\left(v_i C_m\right) - K_a v_i C_m + \frac{\varepsilon_o}{\rho} R \tag{1}$$

$$\frac{\partial C_{im}}{\partial t} = K_a v \frac{\varepsilon_o}{\rho} C_m - R \tag{2}$$

where

C_m mobile phase concentration (ML^{-3})

C_{im} immobile phase concentration ($M\ M^{-1}$)

K_a = filter coefficient attachment rate (L^{-1})

ρ = bulk density (ML^{-3})

ε_o = porosity (dimensionless)

R = immobile phase release rate (T^{-1})

The filter coefficient, K_a, can be calculated as

$$K_a = \frac{3}{2}\left(\frac{1-\varepsilon_o}{d_c}\right)\alpha'\left(\frac{C_{im}^{\max} - C_{im}}{C_{im}^{\max}}\right)\eta \qquad (3)$$

α' = empty bed collision efficiency (dimensionless)

η = single collector efficiency (dimensionless)

d_c = equivalent collector diameter (L)

$C_{im}^{\max}$ = maximum oil retention by sediment (MM^{-1})

The immobile phase release rate, R, represents the release of organic carbon to the aqueous phase which supports anaerobic bioremediation processes. However when the primary objective is to describe the initial transport and retention of the emulsion (Chapter 2) we have showed that droplet release can be neglected. This approach has been adopted in this work and R is assumed equal to zero.

The sandbox was represented in plan view by a 20 x 20 grid where each cell was 5 cm x 5 cm. In the homogeneous experiments, the sandbox was simulated as a single vertical layer. In the heterogeneous experiments, the sandbox was represented by three separate layers. No flow and constant head boundary conditions were implemented where appropriate. Porosity was calculated from the sediment specific gravity and the dry weight of sediment added to each layer. For both the homogeneous and heterogeneous tests, the total transmissivity of sandbox was obtained by fitting water level monitoring results to the steady-state Thiem equation. For the heterogeneous test, the transmissivity of each layer was estimated based on the layer thickness and hydraulic conductivity measurements in standard laboratory permeameters (ASTM d 2434). Dispersivity was estimated by fitting MT3D (Zheng, 1990) to match results from non-reactive tracer tests (calibration results not shown).

Emulsion transport and retention in the 3-D homogeneous and heterogeneous sandbox experiments was simulated using two different sets of values for α'. Emulsion transport in

each sand box was first predicted using of α' previously measured in chapter 2 in 2.9 cm diameter by 80 cm long laboratory columns packed with FS-7%, FS-9% and FS-12%. The model was then calibrated to match the observed sediment volatile solids (VS) concentrations by adjusting α'. The best fit value of α' was found using the bisection method with the root mean square error (RMSE) as the primary objective function. The match between simulated and observed aqueous concentrations (C_m) was not used as a calibration criterion. For both simulations, the values of C_{im}^{max} measured by Coulibaly et al. (submitted) were used without calibration. Best fit and independently measured values of α' are shown in Table 3.1. All other parameter values are presented in Table 3.2.

Table 3.1 Comparison of best fit and independently measured values of the empty bed collision efficiency (α').

Parameters	Material	Best Fit	Coulibaly et al. (submitted)
Homogeneous Test	FS-7%	0.03	0.048
Heterogeneous Test	FS-9%	0.00065	0.03
	FS-7%	0.015	0.048
	FS-12%	4.5×10^{-6}	76.7×10^{-6}

Table 3.2 Physical and chemical parameters for homogeneous and heterogeneous injection tests.

	Homogeneous test	**Heterogeneous test**
Hydraulic Conductivity, K (m/d)	1.47	Layer 1 = 4.27
		Layer 2 = 7.0
		Layer 3 = 2.43
Porosity	0.27	Layer 1 = 0.30
		Layer 2 = 0.22
		Layer 3 = 0.26
Dispersivity (m)	0.08	0.08
Pumping rate before emulsion injection (m^3/d)	0.13	0.598
Bulk Density (kg/m^3)	1,700	Layer 1 = 1,840
		Layer 2 = 2,070
		Layer 3 = 1,960
Max. Oil Retention C_{im}^{max} (g/kg)	5.4	Layer 1 = 6.1
		Layer 2 = 5.4
		Layer 3 = 9.5
Emulsion Injection Concentration (g/L)	104	99

The variation in simulated and observed sediment VS concentrations versus radial distance is presented in Figure 3.9 for the homogeneous injection test. Reducing α' from the independently measured value of 0.048 to the best fit value of 0.03 reduced the computed RMSE from 1.86 to 1.43. However, given the variations observed in the sediment volatile solids (VS), it is difficult to say whether this improvement in the RMSE is really significant.

Figure 3.10 shows the effluent concentrations at different radial distances from the injection well during the homogeneous test. The predicted and best fit model simulations closely match observed values near the injection point. Farther away from the injection point, the independently measured α' (predicted simulation) appears to provide a slightly better fit to the aqueous concentrations than the α' obtaining by fitting to the sediment VS measurements. However the difference between these two simulations is really very small;

for both simulations, aqueous VS concentrations decline to less than 4% of the injection concentration within 70 cm of the injection point.

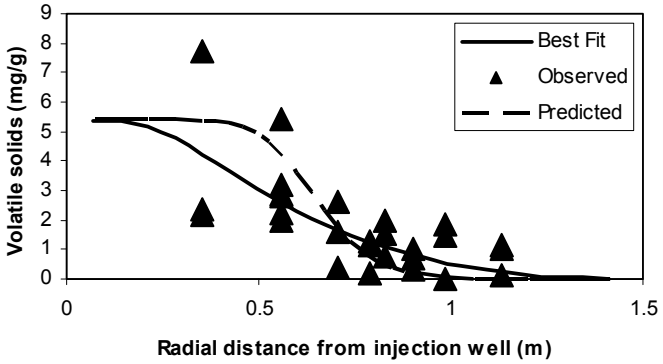

Figure 3.9 Variation in simulated (solid and dash line) and observed sediment volatile solids concentration versus radial distance from the injection well for the homogeneous injection experiment. Observed concentrations are corrected for background VS.

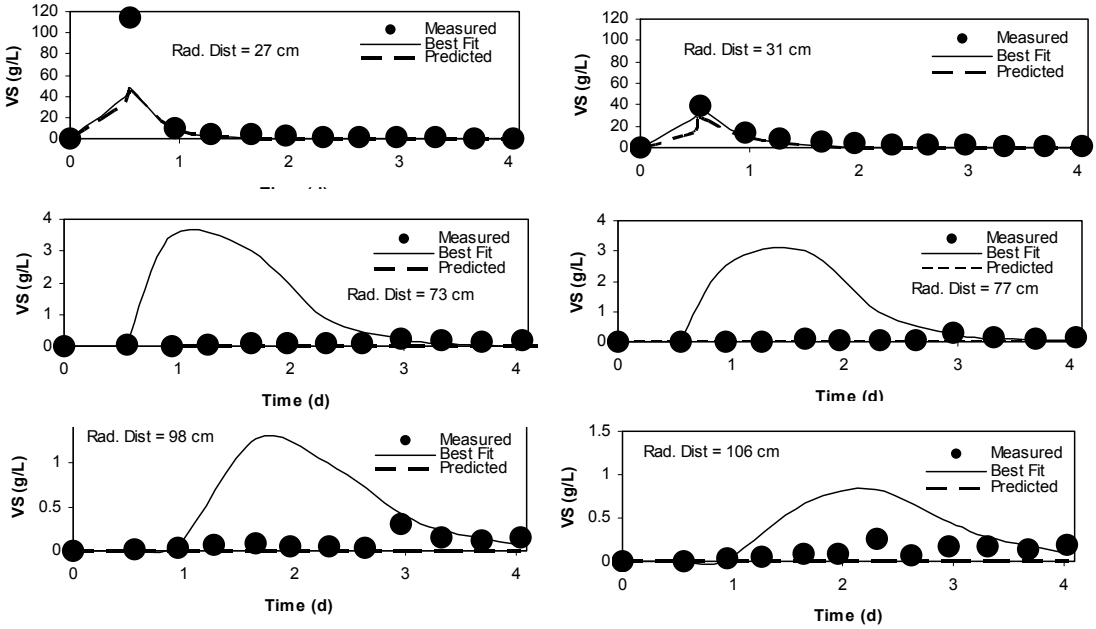

Figure 3.10 Simulated and observed emulsion breakthrough curves at different radial distances from injection well in the homogeneous sand box**.**

Predicted and best fit simulations of the sediment VS concentrations at the end of the heterogeneous test are compared in Figure 3.11. Again, reducing α' from the independently measured values to the best fit values results in some reduction in the sediment RMSE. However, it is not clear whether this reduction in the RMSE is really significant. Observed VS concentrations in the aqueous phase are compared to predicted and best fit model simulations in Figure 3.12. Throughout the middle FS-7% layer, both the predicted and best fit simulations closely match the observed aqueous concentrations. In the upper FS-9% layer, both simulations closely match observed concentrations close to the injection point. However farther away from the injection point, the independently measured α' appears to provide a slightly better fit to the aqueous data than the α' fit to the sediment VS measurements. In the lower FS-12% layer, the predicted and best fit simulations appear to match the aqueous measurements equally well.

Overall, the emulsion transport model provided a good prediction of the aqueous VS concentration versus time in multiple monitoring points and the final VS distribution in the sediment using independently measured parameter values. The only location where the model prediction is somewhat less than desired is for the FS+12% layer in the heterogeneous test. In this layer, the model predicts somewhat higher sediment VS concentrations than observed. The difference between simulated and observed VS concentrations could be due to higher uncertainties in the parameter estimates for this layer. In the prior work by Coulibaly et al. (submitted), the higher clay content in FS-12% required higher injection pressures which could have resulted in some flow bypassing.

Generally, the best fit values of α' were similar, but lower than the independently measured values previously reported in chapter 2 for these same materials. The differences between them could be due to differences in experimental conditions between the two

studies. However it appears more likely that the apparent difference between the best fit and independent estimates of α' is due to the uncertainty in model parameters generated from small experimental data sets. The α' value reported in chapter 2. for FS-7% is an average of four column experiments where observed values of α' varied from 0.02 to 0.07 indicating significant variability among replicate columns. These variations are not unreasonable given that prior investigators (Jewett et al., 1995) have reported 1 or 2 orders of magnitude variation in α' in replicate experiments. The α' values reported in chapter 2 for the FS-9% and FS-12% were each generated from a single column experiment. Given the variability observed for FS-7%, the parameter estimates for FS-9% and FS-12% could be an order of magnitude higher or lower than single observed value. It is also not clear that the 'best fit' parameter values provide a significantly improved match for the 3-D sandbox experiment compared to the independent parameter estimates. As discussed above, the independent estimates of α' frequently resulted in a better match with the aqueous emulsion measurements than the α' values obtained by fitting the model to the sediment VS.

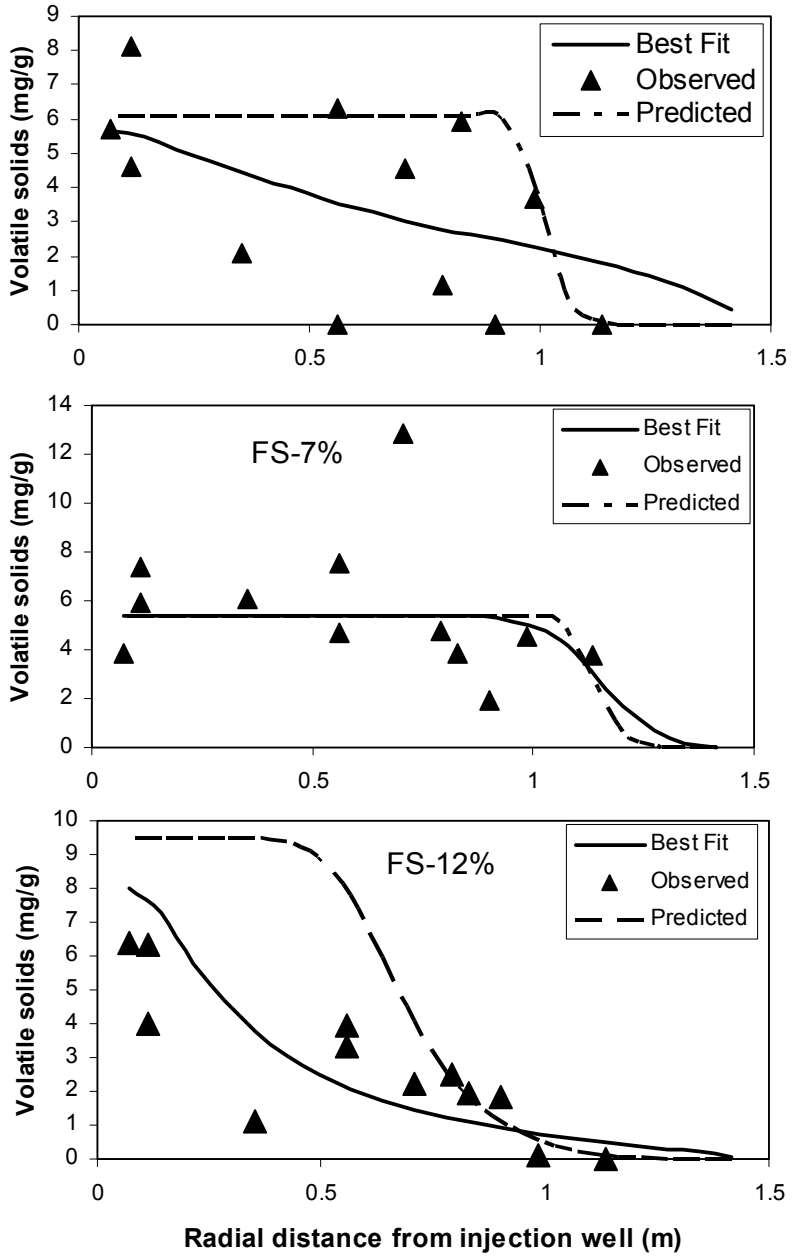

Figure 3.11 Variation in predicted and best fit model simulations and observed sediment volatile solids concentration versus radial distance from the injection well for the heterogeneous injection experiment. Observed concentrations are corrected for background VS.

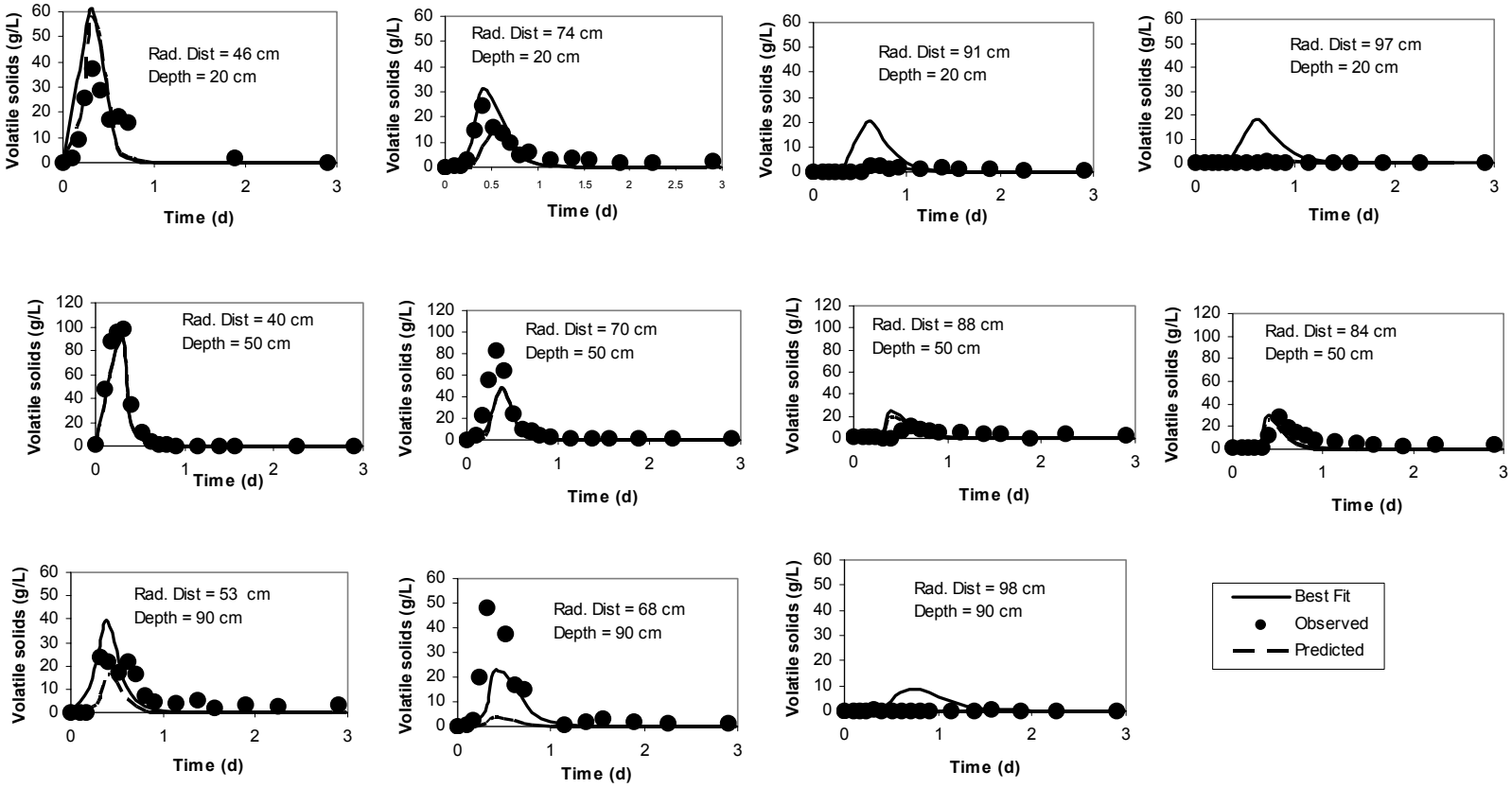

Figure 3.12 Variation in predicted (dashed line) and best fit (solid line) model simulations and observed (filled circles) aqueous volatile solids concentration versus time at different radial distance from the injection well for the heterogeneous injection experiment.

3.5. SUMMARY AND CONCLUSIONS

Emulsified edible oils can provide a low-cost, slow-release source of biodegradable organic carbon to support anaerobic bioremediation processes. However to be effective in the field, we must be able to effectively distribute the oil out away from the injection points without excessive permeability loss. Large-scale 3-D sandbox experiments were conducted for both homogeneous and heterogeneous conditions to evaluate the transport and distribution of emulsified edible oils under controlled laboratory conditions. Results from this work showed that injection of a fine oil-in-water emulsion (~ 0.1 PV for homogeneous, ~ 0.5 PV for heterogeneous) followed by chase water (~ 1.5 PV for homogeneous, ~ 5.5 PV for heterogeneous) resulted in excellent oil distribution throughout fine clayey sand with no significant reduction in hydraulic conductivity and no upward movement of the oil due to buoyancy effects. Data from both of these tests were used in the validation of a 3-D numerical model of emulsion transport. This model was calibrated using parameter values independently measured in a series of 1-D column experiments (chapter 2). Model predictions for both the homogeneous and heterogeneous injection tests were in close agreement with observed values. These results indicate that the transport and distribution of emulsified oil can be simulated using a colloidal transport model which incorporates a Langmuirian blocking function to simulate the effects of sediment surface saturation with attached emulsion droplets. This model was implemented as a user-defined function in RT3D.

Acknowledgements

The research presented in this chapter was conducted cooperatively with Yong Jung. Mr. Jung was primarily responsible for the planning and implementation of the 3-D sandbox experiments with support provided by Kapo Coulibaly. Mr. Coulibaly was primarily responsible for the model development and application with support provided by Mr. Jung.

3.6 REFERENCES

ARCADIS Geraghty & Miller, Inc. (ARCADIS)., 2002. Final: Technical protocol for using soluble carbohydrates to enhance reductive dechlorination of chlorinated aliphatic hydrocarbons. Prepared for the Air Force Center for Environmental Excellence, San Antonio, Texas and the Environmental Security Technology Certification Program, Arlington, Virginia. December 19, 2002.

ASTM (American Society for Testing and Materials)., 2000. Designation: D 2434-68, Standard test method for permeability of granular soils (constant head), West Conshohocken, PA.

Bolster, C. H., Hornberger, G. M. and Mill A. L. 1998. A method for calculating deposition coefficients using the fraction of bacteria recovered from laboratory columns. Environ. Sci. Technol., 32.

Borden, R. C., Coulibaly, K. M., Long, C. M., Harvin A. S., 2001. Development of permeable reactive barriers (PRBs) using edible oils, Annual Report to the Strategic Environmental Research and Development Program.

Brigham Young University, Environmental Modeling Laboratory, 1999. The Department of Defence Groundwater Modeling System, GMS v3.1.

Camesano T. A., K.M. Unice and B.E. Logan, 1999, Blocking and ripening of colloids in porous media and their implications for bacterial transport. Colloids Surf.

Clement, T. P., 1997. RT3D – A modular computer code for simulating reactive multi-species transport in 3-Dimensional groundwater aquifers. Battelle Pacific Northwest National Laboratory Research Report, draft version, PNNL-SA-28967.

Coulibaly, K. M., Long, C. M., Lindow, N. L., Borden, R. C., 2003. Transport of edible oil emulsions in aquifer sands: experimental and simulation results, submitted for review.

Ellis, D.E., Lutz, E.J., Odom, J.M., Buchanan, R.J., Bartlett, C.L., Lee, M.D., Harkness, M.R., Deweerd, K.A., 2000. Bioaugmentation for accelerated in situ anaerobic bioremediation. Env. Sci. Tech. 34, 2254-2260.

Enfield, C. G., Bengtsson, G., Lindqvist, R., 1989. Influence of macromolecules on chemical transport, Environ. Sci. Technol. 23, 1278-1286.

Grindrod, P., 1993. The impact of colloids on the migration and dispersal of radionuclides within fractured rock. In: Chemistry and migration of actinides and fission products. Journal of Contam. Hydrol. 13, 167-182.

Grindrod, P., Edwards, M. S., Higgo, J. J. W., Williams, G. M., 1996. Analysis of colloid and tracer breakthrough curves. Journal of Contam. Hydrol. 21, 243-253.

Harkness, M. R., 2000. Economic considerations in enhanced anaerobic biodegradation: Bioremediation and phytoremediation of chlorinated and recalcitrant compounds. 2nd Internat. Conf. Remediation of Chlorinated and Recalcitrant Compounds. Monterey, California, May 22-25, 2000.

Harkness, M. R., R. Farnum, B. Weesner, D. Foti, W. Wilke, D. Smith, 2003. The case for chitin, In Situ and On-Situ Bioremediation: The Seventh Internat. Sym., Orlando, FL (accepted for publication).

Higgo, J. J. W., Williams, G. M., Harrison, I., Warwick, P., Gardiner, M. P., Longworth, G. 1993. Colloid transport in a glacial sand aquifer. Laboratory and field studies. Colloids and Surfaces A. 73, 179-200.

Hunter, W. J., 2001. Use of vegetable oil in a pilot-scale denitrifying barrier. J. Cont. Hydro. 53, 119-131.

Hunter, W. J., 2002. Bioremediation of chlorate or perchlorate contaminated water using permeable barriers containing vegetable oil. Current Microbiol., 45, 287-292.

Interstate Technology and Regulatory Council (ITRC) In Situ Bioremediation Team. 2002. Technical/Regulatory Guidelines: A systematic approach to in situ bioremediation in groundwater including decision trees on in situ bioremediation for nitrates, carbon tetrachloride, and perchlorate. August.

Jewett, D. G., Hilbert, T. A., Logan, B. E., Arnold, R. G., and Bales, R. C. 1995. Bacterial transport in laboratory columns and filters: influence of ionic strength and pH on collision efficiency. Wat. Res., 29, pp 1673-1680.

Koenigsberg, S. S., 2000. Accelerated bioremediation of chlorinated compounds in groundwater. Selected Battelle Couference Papers. 1999-2000. Regenesis Bioremediation Products, San Clemente, CA.

Konikow, L. F., August, L. L., Voss, C. I., 2001. Effect of clay dispersion on aquifer storage and recovery in costal aquifers. Transport in porous media 43, 45-64.

Kretzschmar, R., Robarge, W. P., Amoozegar, A., 1995. Influence of natural organic matter on colloid transport through saprolite. Water Resources Research 31 (3), 435-445.

Kretzschmar R., Sticher, H., 1998. Colloid transport in natural porous media: Influence of surface chemistry and flow velocity. Phys. Chem. Earth.23 (2), 133-139.

Lee, D.M., Lieberman T.M., Borden R.C., Beckwith W., Crotwell T. and Haas P.E., 2001. Effective distribution of edible oils – results from five field applications. – In: Wickramanayake, G.B., Gavaskar, A.R., Alleman, B.C., Magar, V.S. (Eds.), Proc. In Situ and On-Site Bioremediation: The Sixth Internal. Sym., San Diego, CA, Battelle Press, Columbus, OH.

Major, D.W., McMaster, M.L., Cox, E.E., Edwards, E.A., Dworatzek, S.M., Hendrickson, E.R., Starr, M.G., Payne, J.A., Buonamici, L.W., 2002. Field demonstration of successful bioaugmentation to achieve dechlorination of tetrachloroethene to ethene. Environ. Sci. Technol. 36, 5106-5116.

Martin, J.P., Sorenson, K.S., Peterson, L.N., 2001. Favoring efficient in situ dechlorination through amendment injection strategy. In: G. B. Wickramanayake,

G.B., Gavaskar, A.R., Alleman, B.C., Magar, V.S. (Eds.): Proc. In Situ and On-Site Bioremediation: The Sixth Internal. Sym., San Diego, CA, pp. 265-272.

Martin, J. P., Sorenson, Jr. K. S., Peterson, L. N., Brennan, R. A., Werth, C. J., Sanford, R. A., Bures, G. H., Taylor, C. J., 2002. Enhanced CAH dechlorination in a low permeability variably-saturated medium, In: A.R. Gavaskar and A.S.C. Chen (Eds.), Remediation of Chlorinated and Recalcitrant Compounds, Battelle Press.

McAuliffe, C. D., 1973. Oil-in-water emulsions and their flow properties in porous media. Journal of Petroleum Technology, 727-733.

McDonald, J. M., Harbaugh, A. W., 1988. A modular three-dimensional finite-difference groundwater flow model, Techniques of water resources investigations of the U.S. Geological Survey Book 6, 586.

Morse, J. J., Alleman, B. C., Gossett, J. M., Zinder, S. H., Fennell, D. E., Sewell, G. W., Vogel, C. M. 1998. Draft technical protocol: A treatability test for evaluating the potential applicability of the reductive anaerobic biological in situ treatment technology (RABITT) to remediate chloroethenes. ESTCP, February 23, 1998.

Nyer, E. K., 1985. Groundwater treatment technology. Van Nostrand Reinhold, New York,

Ryan, J. N., Gschwend, P. M., 1994. Effect of solution chemistry on clay colloid release from an iron oxide-coated aquifer sand. Environ. Sci. Technol. 28, 1717-1726.

Sabbodish, M.S. Jr, 2002. A Physicochemical Investigation of the Soil Clogging Phenomena During Surfactant Enhanced Remediation. Doctoral Dissertation, Dept. Civil Engr., North Carolina State Univ.

Soo H., Radke, C. J., 1986. A filtration model for the flow of dilute stable emulsions in porous media – I. Theory. Chemical Engr. Sci. 41, 263-272.

Thomas, J. M., Ward, C. H., 1989. In situ biorestoration of organic contaminants in the subsurface. Environ. Sci. Tech., 23 (7), 760-766

Wiedemeier, T. H., Henry, B. M., Haas, P. E., 2001. Technical protocol for enhanced reductive dechlorination via vegetable oil injection. Proceedings of the Sixth In Situ and On-Site Bioremediation Symposium. Battelle Press, Columbus, OH.

Wu, M., 1999. A pilot study using HRC^{TM} to enhance bioremediation of CAHs. Engineered approaches for In Situ Bioremediation of Chlorinated Solvent Contamination, Battelle Press, Columbus, Ohio, pp 177-180.

Zenker, M.J., Borden, R.C., Barlaz, M.A., Lieberman, M.T., Lee M. D., 2000. Insoluble substrates for reductive dehalogenation in permeable reactive barriers. In: Wickramanayake, G.B., Gavaskar, A.R., Alleman, B.C., Magar, V.S. (Eds) Bioremediation and Phytoremediation of Chlorinated and Recalcitrant Compounds, Battelle Press. pp. 47-53.

Zheng, C. 1990. MT3D - A modular three-dimensional transport model for simulation of advection, dispersion and chemical reactions of contaminants in groundwater system prepared for the U.S. Environmental Protection Agency.

APPENDICES

Appendix A1 – Sand gravel permeameter experiment

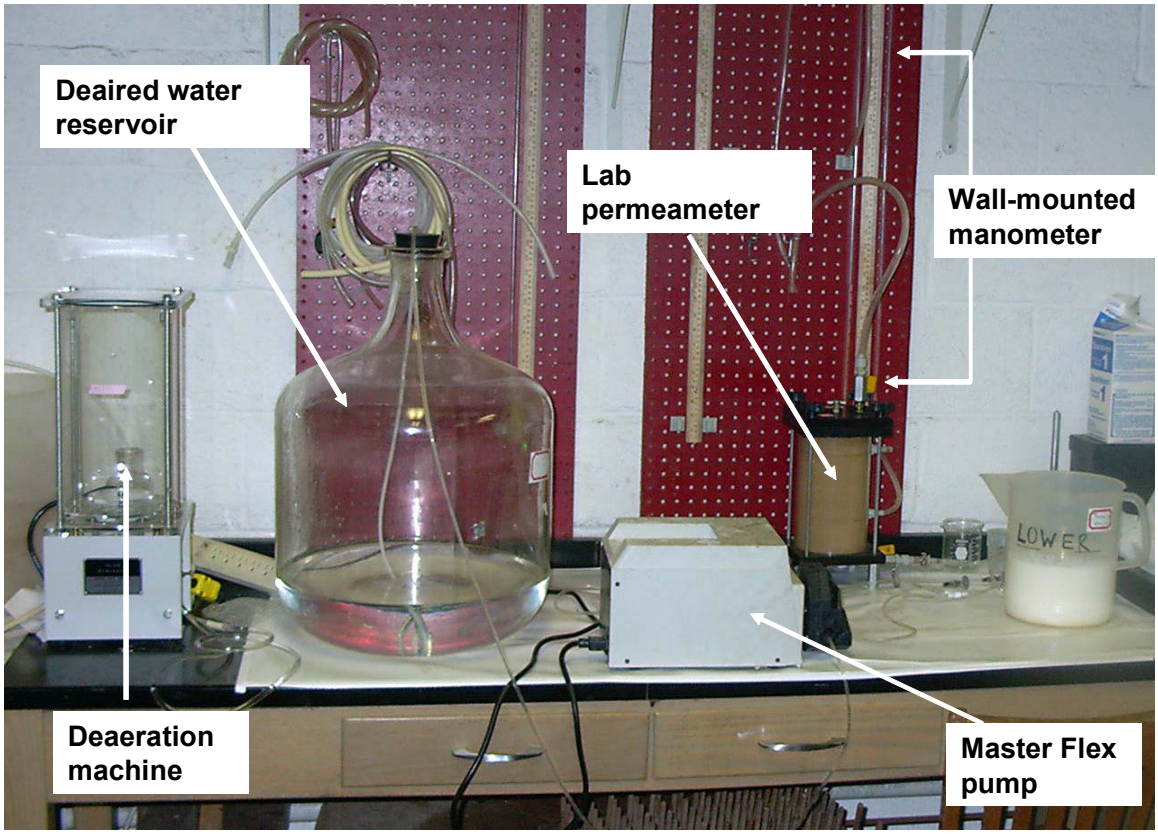

Figure A1.1: Sand gravel permeameter setup

Appendix A2 – Long columns experiment

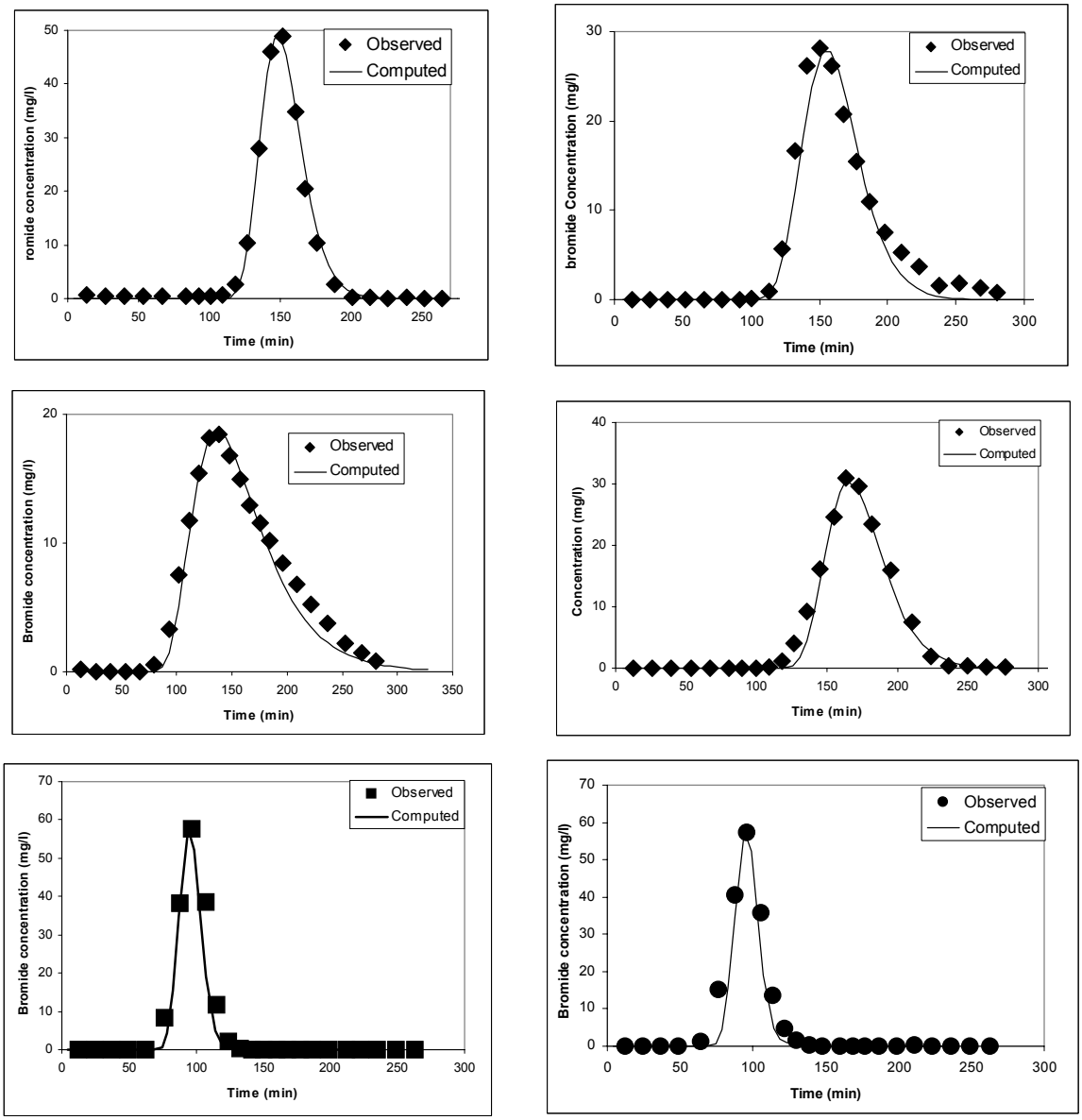

Figure A.2.1 : Long column tracer test results: FS-7% #1, FS-7% #2, FS-7% #3, FS-7% slow, FS-9% and FS-12%.

Table A.2.1: Long columns sediment VS concentrations.

(a)

Oil injected (g)	Concentration injected (g/L)	Oil relased (g)
0.195	19.52	0.1063
0.195	19.52	0.1543
0.222	22.15	0.1468
0.222	22.15	0.1519
0.222	22.15	0.1525
0.038	3.78	0.027
0.038	3.78	0.0247
0.038	3.78	0.0224
3.494	349.41	3.424
1.173	117.28	1.1322
1.173	117.28	1.0766
1.173	117.28	1.1081

(b)

Oil injected (g)	Concentration injected (g/L)	Oil relased (g)
0.218	21.78	0.0943
0.218	21.78	0.1245
0.218	21.78	0.1279
1.015	101.54	0.8891
1.015	101.54	0.8924
1.015	101.54	0.8924
3.534	353.40	3.3400
3.534	353.40	3.5250
3.534	353.40	3.4143

(c)

Oil injected (g)	Concentration injected (g/L)	Oil relased (g)
0.218	21.78	0.093
0.218	21.78	0.1022
0.218	21.78	0.0992
1.015	101.54	0.862
1.015	101.54	0.7906
1.015	101.54	0.8457
3.534	353.40	3.3061
3.534	353.40	3.4602

Table A.2.2: Long column effluent VS concentrations data (FS-7% fast 1, 2, 3)

Time	Concentration(mg/L)	Time	Concentration(mg/L)	Time	Concentration(mg/L)
7	16.67	14	0.00	14	15.99
20	3.33	27	0.00	27	3.29
33	10.00	40	16.91	40	19.37
47	20.00	53	-10.16	55	17.76
60	-10.00	67	6.45	70	23.34
73	-23.33	85	38.64	83	52.45
87	23.33	99	291.04	96	255.32
100	433.33	116	315.72	110	676.85
113	2513.33	130	661.62	126	698.41
127	2550.00	144	476.34	143	405.19
140	1470.00	158	306.11	157	268.41
154	830.00	175	234.01	174	165.68
167	550.00	188	173.58	192	114.36
181	363.33	202	140.68	206	95.59
195	236.67	217	90.42	222	64.21
208	180.00	231	57.44	239	61.84
222	146.67	244	48.70	253	50.13
235	150.00	261	53.66	269	47.42
249	106.67	274	43.51	282	13.56
263	123.33	287	43.82	296	26.89
276	116.67	303	33.48	311	24.67
290	86.67	317	17.96	328	22.79
305	110.00	334	22.90	344	18.92
320	63.33	351	5.07	362	40.57
333	76.67	365	0.00	380	42.90
347	73.33	384	21.17	396	13.96
360	76.67	398	12.25	414	35.63
373	90.00	410	10.47	430	8.37
387	123.33	422	3.62	444	6.20
400	66.67	435	27.50	457	9.80
414	93.33	448	13.17	471	6.23
427	90.00	461	20.36	486	5.94
440	90.00	474	9.74	500	15.26
454	56.67	488	6.46	515	14.58
467	106.67	502	-3.10	530	14.62
481	73.33	514	6.89	543	-3.18

Table A.2.3 Long column effluent concentration data (FS-7% slow 1, FS-9%, FS-12%)

Time	Concentration(mg/L)
61	13.08
120	6.81
178	10.35
238	3.34
295	3.46
354	10.33
411	10.39
470	44.46
527	190.63
585	111.40
643	90.25
695	64.43
754	50.74
812	27.96
869	38.26
927	24.41
984	24.33
1067	19.28
1124	17.69
1181	27.84
1235	33.33
1292	10.62
1350	27.58
1410	16.63
1461	23.51
1522	29.45
1578	35.46
1638	26.75
1693	14.47
1749	25.12
1814	18.55
1878	21.76
1941	15.98
2002	32.57
2065	22.14
2141	7.96

Time	Concentration(mg/L)
10	0.00
20	0.00
30	10.00
40	10.00
51	6.67
63	6.67
73	10.00
84	30.00
95	36.67
108	26.67
118	16.67
130	10.00
143	6.67
156	10.00
169	6.67
181	16.67
191	13.33
202	10.00
214	20.00
225	13.33
237	6.67
246	10.00
255	13.33
266	6.67
276	10.00
287	6.67
298	6.67
308	3.33
317	3.33
328	26.67
339	10.00
349	16.67
358	13.33
367	53.33
377	33.33
390	26.67

Time	Concentration(mg/L)
15	33.33
44	50.00
74	30.00
103	26.67
133	20.00
166	16.67
200	30.00
232	26.67
264	33.33
297	26.67
329	33.33
360	40.00
395	23.33
431	13.33
468	13.33
502	13.33
531	13.33
561	10.00
595	10.00
627	3.33
657	33.33
690	23.33
724	3.33
757	10.00
792	10.00
826	26.67
856	43.33
889	20.00
923	30.00
953	30.00
982	10.00
1012	10.00
1041	16.67
1072	23.33
1104	30.00
1139	33.33

Table A.2.4: Long columns sediment VS concentrations**.**

(a): FS-7% #1

Segment # from inlet	2	3	4	5	6	7
Volatile solids retained (mg/g)	6.58	3.59	1.01	1.04	2.32	1.06

(b): FS-7% #2

Segment # from inlet	2	3	4	5	6	7
Volatile solids retained (mg/g)	8.00	2.88	3.07	2.67	4.58	3.98

(c): FS-7% #3

Segment # from inlet	2	3	4	5	6	7
Volatile solids retained (mg/g)	0.74	2.71	3.08	2.94	3.22	1.03

(d): FS-7% Slow

Segment # from inlet	2	3	4	5	6	7
Volatile solids retained (mg/g)	3.76	3.88	3.89	2.52	1.65	0.00

(a): FS-9%

Segment # from inlet	2	3	4	5	6	7
Volatile solids retained (mg/g)	5.91	5.28	6.16	4.55	3.14	1.06

(a): FS-12%

Segment # from inlet	2	3	4	5	6	7
Volatile solids retained (mg/g)	4.65	7.66	9.53	5.22	1.62	0.55

APPENDIX A3.1 – HOMOGENEOUS SAND BOX TEST

Table A3.1 Sample/Monitor Tube Locations for Homogeneous Sandbox

Layer 1 intakes are 75 cm from top of tank						
Sample Port No.	A1	A4	A7	B1	B4	B7
Radial Distance from Injection Well (cm)	26.6	46.3	73.4	62.3	71.7	90.5
Layer 2 intakes are 50 cm from top of tank						
Sample Port No.	A2	A5	A8	B2	B5	B8
Radial Distance from Injection Well (cm)	31.4	55.0	82.9	64.0	77.2	98.1
Layer 3 intakes are 25 cm from top of tank						
Sample Port No.	A3	A6	A9	B3	B6	B9
Radial Distance from Injection Well (cm)	38.3	64.1	92.4	67.2	83.5	106.0

Appendix A3.1.1 – Hydraulic and Tracer Test Results

Prior to the start of emulsion injection, the variation in head with radial distance from injection well is shown in Figure A3.1. As expected, head decreases with radial distance. Head difference between the top, middle and bottom layers is not significant with suggesting reasonably uniform flow through the tank. Calculated head distribution using Theim equation is shown with the variation in head.

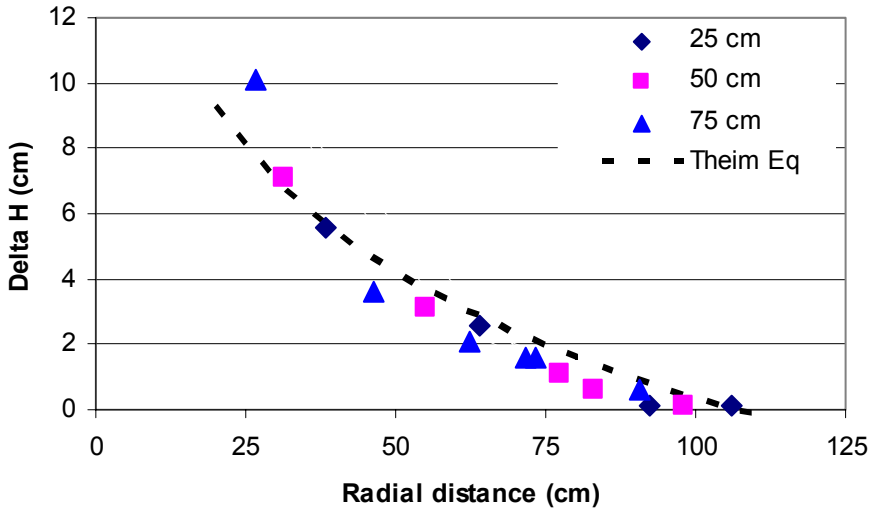

Figure A3.1 Variation in head with radial distance from injection point prior to emulsion injection**.**

Appendix A3.1.2 – Emulsion Injection Test Results

Figure A3.2 shows the variation in fluid injection rate versus time during the emulsion injection test. Emulsion and chase water were injected over a 97 hour period with time = 0 as the start of emulsion injection. By recording the time required to inject 30 L of fluid (emulsion or water) flow rate was measured. Throughout the emulsion injection test, the head in the injection well was maintained 18 cm head above the level in the constant head boundaries. Based on a 5-day non-reactive tracer test conducted prior to emulsion injection, the pre-injection flow rate was 0.13 m^3 /d. As McAuliffe (1973) reported, during the emulsion injection, there was only a small reduction in flow rate, presumably due to the somewhat higher viscosity of the emulsion (1.44 centipoises) and lower density (0.99 g/cm^3). Whereas flow rate was recovered to that of the pre-injection

right after finishing the emulsion injection suggesting there was no significant permeability loss during the test. The piezometer reading over the course of the test indicates there is no measurable change in water levels (data not shown).

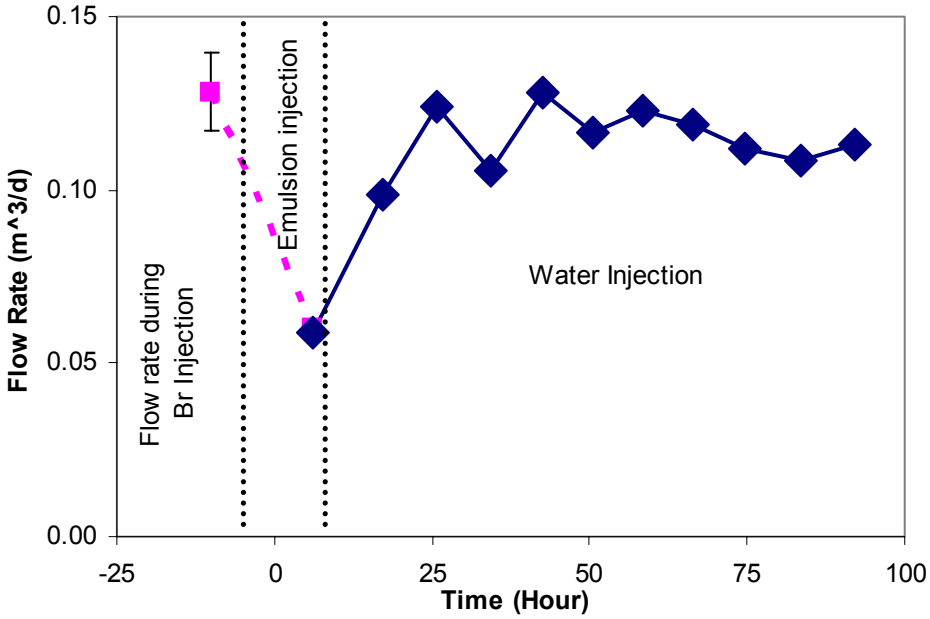

Figure A3.2 Variation in injection flow rate with time during the homogenous injection test.

APPENDIX A3.1 – HETEROGENEOUS SAND BOX TEST

Table A3.2 Sample/Monitor Tube Locations for heterogeneous sandbox

Layer 1 (FS-12% layer) intakes are 90 cm from top of tank						
Sample Port No.	A1	A4	A7	B1	B4	B7
Radial Distance from Injection Well (cm)	35.7	53.3	78.7	67.9	78.5	97.6
Layer 2 (FS-7% layer) intakes are 50 cm from top of tank						
Sample Port No.	A2	A5	A8	B2	B5	B8
Radial Distance from Injection Well (cm)	40.0	61.3	87.8	70.2	84.2	105.1
Layer 3 (FS-9%) intakes are 20 cm from top of tank						
Sample Port No.	A3	A6	A9	B3	B6	B9
Radial Distance from Injection Well (cm)	46.0	69.8	97.1	73.8	90.6	113.0

Appendix A3.2.1 – Hydraulic and Tracer Test Results

Before the emulsion injection, tap water was passed through the heterogeneous sandboxat a constant flow rate (q_t= 0.598 m^3/d) for several weeks to establish steady state conditions. Figure A3.3 shows the variation of head distribution with radial distance. There are slightly different heads between layer 1 (FS-9%) and layer 2 (FS-7%) except layer 3 (FS-7%). Hydraulic heads in Layer 1 and 2 are well matched and the measurement using ASTM d 2434 for permeability of granular soils (constant head) also indicates permeability of those two layers has no significant different (Data not shown). The dashed lines show the head calculated using the Theim equation.

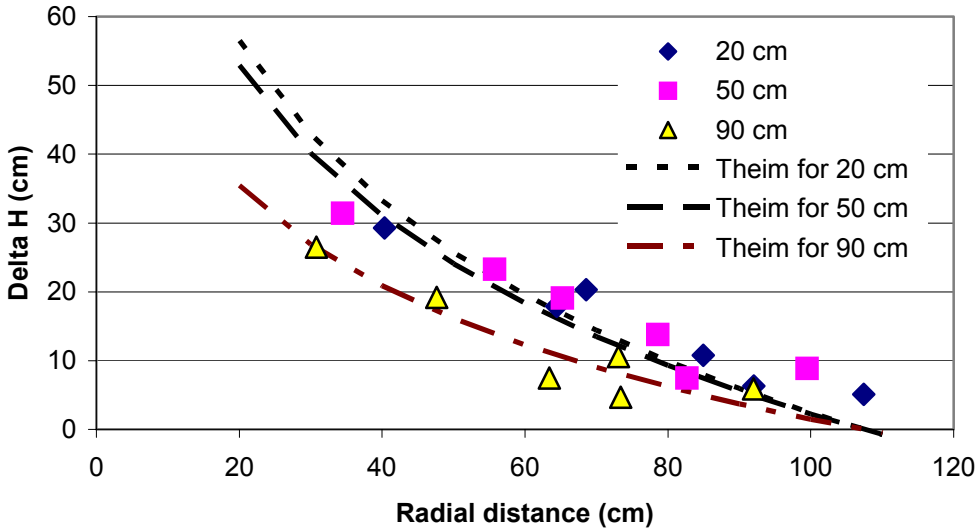

Figure A3.3 Variation in head with radial distance from injection point prior to emulsion injection for heterogeneous sandbox.

Appendix A3.2.2 – Emulsion Injection Test Results

Figure A3.4 shows the variation in injection flowrate with time. Emulsion was injected from 0 to 10 hours followed by tap water injection for 70 hours or approximately 5.0 PV. The head difference between water supply reservoir and constant head reservoir was held constant at 58 cm which is higher than the 18 cm used during the homogeneous injection test. During emulsion injection, the flow rate dropped from 25 L/h (flow rate before emulsion injection) to 10~15 L/h and then the flow rate was recovered to the pre-injection flow rate. However, after 40 hours flow rate was gradually decreased to 8 L/h. We hypothesize that kaolinite added to the upper and lower layers (FS-9 % clay and FS-7%) was mobilized by the surfactant used to form the emulsion, causing clogging of the

non-woven geotextile that formed the constant head boundary. Clay mobilization by surfactants (Ryan et al., 1994) can also effective the aquifer permeability (Konikow et al., 2001)

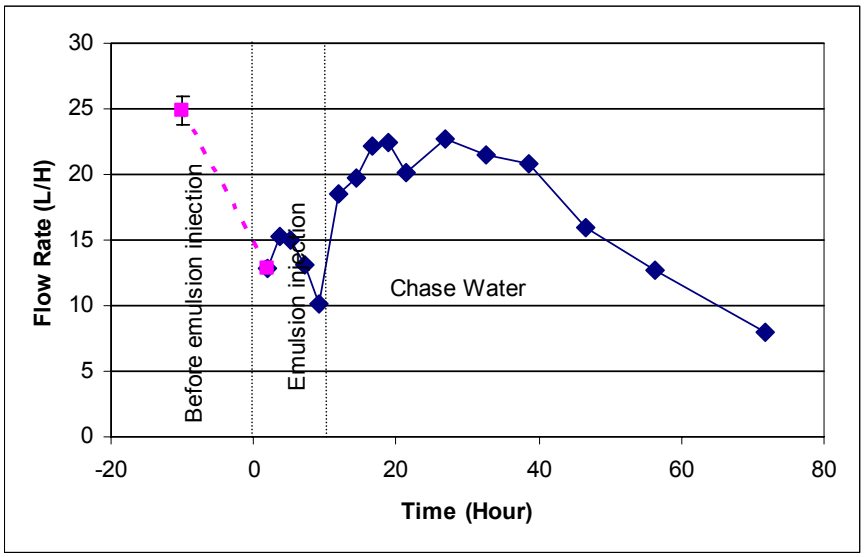

Figure A3.4 Variation in injection flow rate with time during the emulsion injection for heterogeneous sandbox